

Dissertation zur Erlangung des Doktorgrades
der Fakultät für Chemie und Pharmazie
der Ludwig-Maximilians-Universität München



**Anticancer effects and antiangiogenic mechanisms
of the marine compound spongistatin 1**

Andrea Silvia Rothmeier

aus München

2008

Erklärung

Diese Dissertation wurde im Sinne von § 13 Abs. 3 der Promotionsordnung vom 29. Januar 1998 von Herrn PD Dr. Stefan Zahler am Lehrstuhl von Frau Prof. Dr. Angelika M. Vollmar betreut.

Ehrenwörtliche Versicherung

Diese Dissertation wurde selbständig und ohne unerlaubte Hilfe erarbeitet.

München, den 09. Oktober 2008

Andrea Rothmeier

Dissertation eingereicht am: 09. Oktober 2008

1. Gutachter: Herr PD Dr. Stefan Zahler

2. Gutachter: Herr Prof. Dr. Christian Wahl-Schott

Mündliche Prüfung am: 12. November 2008

Meinen Lieben

I. CONTENT

I.	CONTENT	I
II.	ABBREVIATIONS.....	1
III.	INTRODUCTION.....	4
1	BACKGROUND Marine Compounds	5
2	Spongistatin 1	6
3	Microtubule-Inhibiting Drugs in Cancer Therapy.....	7
3.1	Chemotherapy and the War on Cancer.....	7
3.2	Inhibition of Tumor Angiogenesis as an Anticancer Approach.....	8
4	Microtubules	9
4.1	The Structure of Microtubules	10
4.1.1	The Tubulins	10
4.1.2	Protofilaments	10
4.2	Organization of Microtubules.....	11
4.2.1	The MTOC	11
4.2.2	The Dynamics of Microtubules.....	12
4.3	Functions of Microtubules	13
4.3.1	The Mitotic Spindle.....	13
4.3.2	Cellular Transport.....	14
5	Microtubule-Binding Compounds	15
6	Tumor Angiogenesis	16
6.1	Initiation of Angiogenesis: Endothelial Proliferation	17
6.1.1	Hypoxia-Induced Expression of VEGF.....	17
6.1.2	The AKT and the ERK Pathways	18
6.1.3	The PKC pathway	20
6.2	Endothelial Migration.....	21
6.2.1	Matrix metalloproteinases	21
6.2.2	Tip Cells and Stalk Cells	21
6.2.3	Molecular Processes during Migration	22

6.3	Vessel Formation	24
7	Aims of the Work	25
IV.	MATERIALS AND METHODS.....	26
1	Materials	27
1.1	Compounds	27
1.2	Biochemicals, Inhibitors, Dyes, and Cell Culture Reagents	27
1.3	Technical Equipment.....	28
2	Cell Culture.....	29
2.1	HUVEC Isolation and Cultivation.....	29
2.2	L3.6pl Cultivation.....	29
3	Flow Cytometry	30
3.1	Stimulation and Harvest	30
3.2	Cell Cycle Analysis.....	30
4	Cell Viability Measurements	31
5	Microscopy	31
5.1	Immunohistochemistry	31
5.2	Live-Cell Imaging.....	32
5.2.1	Mitochondria Staining.....	32
5.2.2	Visualization of Membrane Traffic.....	32
5.2.3	Expression of Recombinant Proteins	32
6	Protein Sample Preparations.....	33
6.1	Total Cell Lysates.....	33
6.2	Microtubule Fractionation	34
6.3	Membrane Fractionation	35
6.4	Protein Isolation of Tissue Sections	35
7	Western Blot Transfer	36
7.1	Protein Quantification	36
7.2	SDS-PAGE.....	36
7.3	Tank-Blotting	37
7.4	Detection	38

7.4.1	Enhanced Chemiluminescence.....	38
7.4.2	LI-COR.....	38
7.5	Staining Gels and Membranes.....	40
8	Kinome Array (PepChip)	40
9	PKC <i>In Vitro</i> Assay	41
10	Angiogenic <i>In Vitro</i> Assays	41
10.1	Proliferation Assay	41
10.2	Migration Assay.....	41
10.3	Chemotaxis Assay.....	42
10.4	Tube Formation Assay	43
11	Angiogenic <i>Ex/In Vivo</i> Assays.....	43
11.1	Mice.....	43
11.2	Mouse Aortic Ring Assay	44
11.3	Mouse Cornea Pocket Assay.....	44
12	The Orthotopic Pancreas Tumor Model.....	45
12.1	Mice and Cell Line.....	45
12.2	Procedures.....	45
12.3	Necroscopy	46
13	Quantitative Real-Time PCR	46
13.1	RNA-Isolation from Tissue Sections.....	46
13.2	Reverse Transcription.....	47
13.3	Quantitative Real-Time PCR.....	47
14	Zymography	47
15	Electrophoretic Mobility Shift Assay.....	49
15.1	Extraction of Nuclear Proteins.....	49
15.2	Electrophoretic Mobility Shift Assay	49
16	Statistical Analysis	50

V. RESULTS	51
A Spongistatin 1 Exerts Strong Impact on Pancreatic Tumor Progression and Metastasis <i>In Vivo</i>	
1 Orthotopic Tumor Model	52
1.1 Spongistatin 1 Inhibits Pancreatic Tumor Progression.....	52
1.2 Necropsy Reveals Strong Efficacy of Spongistatin 1 on Pancreatic Tumor	53
1.3 Metastasis is Significantly Reduced by Spongistatin 1	53
2 The Influence of Spongistatin 1 on Hypoxia inducible Factor 1α.....	54
2.1 Stabilization of HIF-1 α Is Strongly Reduced by Spongistatin 1 <i>In Vitro</i>	54
2.2 Spongistatin 1 Has No Influence on HIF-1 α Activity <i>In Vivo</i>	54
3 Matrix Metalloproteinase 9 Is Reduced by Spongistatin 1 <i>In Vivo</i>	55
3.1 Reduction of MMP-9 mRNA and Protein Levels by Spongistatin 1.....	55
3.2 Zymography Reveals Reduced MMP-9 Activity in Spongistatin 1-Treated Mice ...	56
B Effects of Spongistatin 1 in Angiogenesis <i>In Vitro</i> and <i>In Vivo</i>	
4 Disassembly of Microtubules	58
4.1 Spongistatin 1 Disassembles Microtubules in Endothelial Cells	58
4.2 Spongistatin 1 Influences the Morphology, the Arrangement of Mitochondria, and Membrane Trafficking of Endothelial Cells.....	59
5 Cytotoxicity, Cell Cycle, and Apoptosis	60
5.1 Cytotoxicity of Spongistatin 1 in Endothelial Cells.....	60
5.2 Spongistatin 1 Induces Cell Cycle Arrest and Apoptosis	61
6 Effects of Spongistatin 1 on Endothelial Proliferation	63
6.1 Spongistatin 1 Strongly Inhibits Endothelial Proliferation <i>In Vitro</i>	63
6.2 Proliferative Signaling: Spongistatin 1 Inhibits AKT-Phosphorylation	64
7 The Impact of Spongistatin 1 on Endothelial Migration	65
7.1 Migration of HUVECs Is Inhibited by Spongistatin 1	65
7.2 Spongistatin 1 Deregulates the Arrangement of F-Actin in HUVECs.....	65
7.3 The Chemotaxis of Endothelial Cells is Inhibited by Spongistatin 1.....	67
7.4 Spongistatin 1 Seems to Have No Influence on MTOC Re-Orientation.....	68

8	Tube Formation Is Inhibited by Spongistatin 1	69
9	Effects of Spongistatin 1 in Angiogenic <i>Ex/In Vivo</i> Assays.....	70
9.1	Spongistatin 1 Inhibits Endothelial Sprouting	70
9.2	Neovascularization <i>In Vivo</i> Is Reduced by Spongistatin 1	71
10	The Influence of Spongistatin 1 on Endothelial Signaling	72
10.1	Kinome Array (PepChip)	72
10.2	The Influence of Spongistatin 1 on PKC-Activity.....	73
10.2.1	Spongistatin 1 Inhibits the Phosphorylation of Distinct PKC Substrates.....	73
10.2.2	Spongistatin 1 Has no Impact on PKC Activity <i>In Vitro</i>	74
10.3	The Influence of Spongistatin 1 on PKC-Translocation.....	75
10.3.1	PKC Expression in HUVECs.....	75
10.3.2	The Translocation of PKC α is reduced by Spongistatin 1-Treatment.....	76
VI.	DISCUSSION.....	78
1	Spongistatin 1 is a Powerful Experimental Compound against Pancreatic Tumor Progression and Metastasis.....	79
2	The Impact of Spongistatin 1 on Hypoxia Signaling.....	79
3	Reduction of MMP-9 Levels by Spongistatin 1 <i>in Vivo</i>.....	80
3.1.1	The Significance of MMP-9 in Pancreatic Cancer.....	80
3.1.2	Reduction of MMP-9 mRNA Levels by Spongistatin 1	80
4	Antiangiogenic Action of Spongistatin 1 and the Underlying Mechanisms	81
4.1	Spongistatin 1 Exerts strong Antiangiogenic Action <i>In Vitro</i> and <i>In Vivo</i>	81
4.2	Inhibition of Endothelial Proliferation	82
4.2.1	Spongistatin Particularly Affects Endothelial Proliferation.....	82
4.2.2	Mitotic and Non-Mitotic Actions of Spongistatin 1 on Proliferation.....	82
4.3	Directed Migration	83
4.3.1	Microtubules Do Not Contribute to the Migration Force in Endothelial Cells ..	83
4.3.2	Microtubules and the Intracellular Polarization	83
4.4	How Microtubules May Control Polarization.....	84
4.4.1	The Small RhoGTPases	84
4.4.2	Effects on PI3K	85

5	Microtubules in Endothelial Signaling	85
5.1	Tubulin Antagonists Inhibit AKT, CK2, and PKC isoforms	85
5.2	PKC α Translocation Depends on Functional Microtubules in Endothelial Cells	86
5.3	Microtubule-Inhibiting Drugs Disrupt Translocation Processes.....	87
6	Conclusions	87
6.1	Anticancer Activities of Spongistatin 1	87
6.2	Non-Mitotic Action of Tubulin Antagonist on Angiogenesis.....	88
6.2.1	The Importance of Cellular Polarization in Vessel Formation	88
6.2.2	Microtubule-Inhibiting Drugs Affect Multiple Signaling Pathways	88
VII.	SUMMARY	90
VIII.	REFERENCES	93
IX.	APPENDIX	105
1	PUBLICATIONS	106
1.1	Abstracts	106
1.2	Original Publications.....	107
2	Grants and Awards	107
3	Curriculum Vitae	108
4	Acknowledgements	109

INDEX of FIGURES

FIGURE III.1: CHEMICAL STRUCTURE OF SPONGISTATIN 1.....	6
FIGURE III.2 THE CYTOSKELETON IS PERVADING THE CELL.	9
FIGURE III.3 THE STRUCTURE OF MICROTUBULES.	11
FIGURE III.4 THE CENTROSOME NUCLEATES MICROTUBULE-ASSEMBLY IN THE CELL.	12
FIGURE III.5 GTP BINDING TO TUBULIN IS CRUCIAL FOR THE MICROTUBULE STABILITY.	13
FIGURE III.6 THE MITOTIC SPINDLE.	14
FIGURE III.7 ANGIOGENESIS.....	17
FIGURE III.8 DOMAIN STRUCTURE OF AKT.....	18
FIGURE III.9 VEGFR2 ACTIVATES AKT AND ERK SIGNALING.	19
FIGURE III.10 ACTIVATION OF PKC.	20
FIGURE III.11 CELL MIGRATION IS DIVIDED INTO THREE DISTINCT STEPS.	23
FIGURE III.12 VESSEL FORMATION COMPLETES ANGIOGENESIS.	24
FIGURE IV.1 CONVERSION OF RESAZURIN TO RESORUFIN.	31
FIGURE IV.2 TANK BLOT ASSEMBLY.....	37
FIGURE IV.3 THE CHEMOTAXIS ASSAY ON μ -SLIDES.....	43
FIGURE IV.4 THE PANCREATIC TUMOR MODEL.....	46
FIGURE IV.5 LINEARITY OF ZYMOGRAPHIC QUANTIFICATION OF MMP-9 ACTIVITY.....	48
FIGURE V.1 SPONGISTATIN 1 INHIBITS PANCREATIC TUMOR PROGRESSION.....	52
FIGURE V.2 NECROPSY DATA.....	53
FIGURE V.3 SPONGISTATIN INHIBITS HIF-1 α ACTIVITY <i>IN VITRO</i> , BUT NOT <i>IN VIVO</i>	55
FIGURE V.4 SPONGISTATIN 1 REDUCES MMP-9 mRNA AND PROTEIN LEVEL.....	56
FIGURE V.5 MMP-9 GELATINASE ACTIVITY IS REDUCED IN SPONGISTATIN 1-TREATED MICE.....	57
FIGURE V.6 SPONGISTATIN 1 CAUSES TIME AND DOES-DEPENDENT DISASSEMBLY OF MICROTUBULES.	58
FIGURE V.7 SPONGISTATIN 1 INFLUENCES THE MORPHOLOGY OF HUVECS.	60
FIGURE V.8 DETERMINATION OF THE CYTOTOXICITY OF SPONGISTATIN 1.....	61
FIGURE V.9 FLOW CYTOMETRIC CELL CYCLE MEASUREMENTS.....	62
FIGURE V.10 <i>IN VITRO</i> PROLIFERATION ASSAY.....	63
FIGURE V.11 SPONGISTATIN 1 INHIBITS THE PHOSPHORYLATION OF AKT.	64
FIGURE V.12 SPONGISTATIN 1 INHIBITS MIGRATION OF HUVECS.	66
FIGURE V.13 SPONGISTATIN 1 REDUCES DIRTECTIONAL MIGRATION IN HUVECS.	67
FIGURE V.14 SPONGISTATIN 1 HAS NO INFLUENCE ON MTOC RE-ORIENTATION.....	68
FIGURE V.15 SPONGISTATIN 1 INHIBITS ENDOTHELIAL TUBE FORMATION.	69
FIGURE V.16 ENDOTHELIAL SPROUTING IS INHIBITED BY SPONGISTATIN 1.....	70
FIGURE V.17 SPONGISTATIN 1 INHIBITS THE NEOVASCULARIZATION OF MOUSE CORNEAS.....	71

FIGURE V.18 SPONGISTATIN 1 INHIBITS PHOSPHORYLATION OF DISTINCT PKC SUBSTRATES.....	74
FIGURE V.19 SPONGISTATIN 1 DOES NOT INFLUENCE PKC ACTIVITY <i>IN VITRO</i>	75
FIGURE V.20 EXPRESSION OF PKC ISOFORMS IN ENDOTHELIAL CELLS.....	76
FIGURE V.21 SPONGISTATIN 1 SPECIFICALLY INHIBITS THE TRANSLOCATION OF PKC α	77

INDEX of TABLES

TABLE III.1: MARINE COMPOUNDS AND ANALOGUES IN CLINICAL TRIALS (DATE 2006)	5
TABLE III.2 ANTIMITOTIC DRUGS, THEIR DIVERSE BINDING SITE ON TUBULIN AND THEIR STAGES OF CLINICAL DEVELOPMENT.	8
TABLE IV.1: PRIMARY ANTIBODIES	39
TABLE IV.2: SECONDARY ANTIBODIES.....	39
TABLE V.1 TREATMENT WITH SPONGISTATIN 1 DECREASED THE INCIDENCES OF METASTASES IN THE PANCREATIC TUMOR MODEL.	54
TABLE V.2 RESULTS OF PEPCHIP WITH SPONGISTATIN 1, VINBLASTINE, AND CA4P.	73

II. ABBREVIATIONS

ABBREVIATIONS

ANOVA	Analysis of variance between groups
Ap1	Activated protein 1
APS	Ammonium persulfate
BSA	Bovine serum albumin
CA4P	Combretastatin A4 phosphate
DMEM	Dulbecco's Modified Eagle Medium
DNA	Deoxyribonucleic acid
DTT	Dithiothreitol
(e)GFP	(enhanced) green fluorescent protein
ECL	Enhanced chemiluminescence
EDTA	Ethylenediaminetetraacetic acid
EGTA	Ethylene glycol-bis(2-aminoethylether) tetraacetic acid
ELISA	Enzyme-linked immunosorbent assay
ER	Endoplasmatic reticulum
ERK1/2	Extracellular signalin-regulated kinase 1 and 2
FACS	Fluorescence-activated cell sorter
FAK	Focal adhesion kinase
FC(B)S	Fetal calf (bovine) serum
FGF	Fibroblast growth factor
FL	Fluorescence
GAPDH	Glycerin aldehyde 3 phosphate dehydrogenase
GTP/GDP	Guanosine-5'-tri/diphosphate
HEPES	N-(2-hydroxyethyl)piperazine-N'-(2-ethanesulfonic acid)
HFS	Hypotonic fluorochrome solution
HIF-1 α	Hypoxia inducible factor 1 α
HRP	Horseradish peroxidase
HUVEC	Human umbilical vein endothelial cells
i.p.	intraperitoneal
kDa	Kilo Dalton
KSR	Kinase suppressor of Ras
MAP	Mirotubules-associated protein
MAPK	Mitogen-activated protein kinase
MMP	Matrix metalloproteinase

mRNA	Messenger ribonucleic acid
MTOC	Microtubules organization center
NCI	National Cancer Institute
NF- κ B	Nuclear factor kappa B
NSCLC	Non-small cell lung carcinoma
p-	Phospho-
PAA	Polyacrylamide
PBS	Phosphate buffered saline
PCR	Polymerase chain reaction
PH	Pleckstrin homology
PI3K	Phosphoinositide 3-kinase
PIPES	Piperazine-1,4-bis(2-ethanesulfonic acid)
PKB	Protein kinase B (AKT)
PKC	Protein kinase C
PLC γ	Phospholipase C γ
PMA	Phorbol myristate acetate
PMSF	Phenylmethanesulphonyl fluoride
PTEN	Phosphatase and tensin homolog
qRT-PCR	Quantitative real-time polymerase chain reaction
RIPA	Radio Immuno Precipitation Assay
RTK	Receptor-associated tyrosine kinase
SDS	Sodium dodecyl sulfate
SDS-PAGE	Sodium dodecyl sulfate polyacrylamide gel electrophoresis
SEM	Standard error of mean
Sp1	Specific protein 1
T/E	Trypsine/EDTA
TBE	Tris/Borate/EDTA
TBS-T	Tris buffered saline with tween
TEMED	N,N, N' N' tetramethylethylene diamine
VEGF	Vascular endothelial growth factor
VEGFR2	Vascular endothelial growth factor receptor 2

III. INTRODUCTION

1 BACKGROUND Marine Compounds

High diversity and limited resources generate a relentless competition among marine habitants. As most sessile marine invertebrates contain only a primitive immune system to defend them, these organisms developed an impressive arsenal of chemical weapons through millions of years in their everyday fight for survival. These bioactive compounds are necessarily highly potent substances, since they become immediately diluted by large volumes of sea water. In the last decades, huge efforts were made by both pharmaceutical companies and academic institutions, to screen marine biotopes for new compounds that may help to battle medical challenges like cancer. This systematic investigation of marine environments is reflected in the large number of novel compounds reported in the literature. Over 16,000 new marine compounds have been described, patents for the biological activity of more than 300 substances were applied for, and over a dozen marine anticancer molecules are in different phases of clinical trials (Table III.1). Although, the development of marine compounds as therapeutic agents is still in its infancy, as in contrast to terrestrial natural products, marine compounds lack an ethno-medical history of several thousand years. Thus, marine ecosystems potentially stock new compounds of a non-estimable extent which may become clinical relevant (1-4).

Table III.1: Marine Compounds and Analogues in Clinical Trials (3,4)

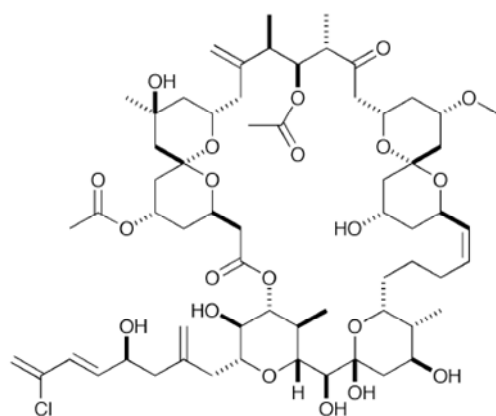
Compound	Source	Target	Clinical Phase	Company
Bryostatin	<i>Bugula neritina</i>	Protein kinase C	II solid tumors	Aphiosis
Halichondrin B (E7389)	<i>Halichondria okadai</i>	Microtubules	II metastatic breast cancer	Eisai
Kahalalide F	<i>Bryopsis</i> sp.	unknown	II in prostate cancer	PharmaMar
Hemiasterlin (HTI-286)	<i>Hemiasterella minor</i>	Microtubules	II NSCLC	Wyeth
Soblidotin*	<i>Dolabella auricularia</i>	Microtubules	I NSCLC	Daiichi Pharmaceuticals
Cemadotin*	<i>Dolabella auricularia</i>	Microtubules	II NSCLC, breast, lung, ovarian cancer	Knoll Pharmaceutical Company
Synthadotin*	<i>Dolabella auricularia</i>	Microtubules	II NSCLC, prostate cancer	Genzyme Corporation
Didemnins	<i>Trididemnum solidum</i>	Palmitoyl thioesterase	II non-Hodgkin's lymphoma	PharmaMar
Aplidin	<i>Aplidium albicans</i>	Ornithin decarboxylase	II medullary thyroid	PharmaMar

* Dolastatin analogue

2 Spongistatin 1

In the late 1980's, Pettit *et al.* extracted a macrocyclic lacton polyether from a dark brown sponge of the genus *Spongia sp.* (*Spirastrella spinispirulifera*) retrieved in the East Indian Ocean. According to its source, it was named spongistatin 1 (5). During the same period of time, althoyrtin A was isolated from *Hyrtios altum* by Kobayashi *et al.*, which revealed to have the identical chemical structure (6). Chemists all over the world made notable investments to synthesize the complex structure of the molecule, which can now be done within 46 discrete steps (7).

Spongistatin 1 is a tubulin antagonist that binds to β -tubulin at a specific site, and thereby destabilizes the microtubules (8). Microtubule-targeting compounds are a wide class of strong anticancer compounds. In fact, when spongistatin 1 was tested in NCI (National Cancer Institute) panel against human tumor cell lines, it showed strong effects on twenty cancer cell lines, including highly aggressive forms like colon carcinoma, melanoma, and ovarian carcinoma at remarkably low concentrations (9). In recent studies, spongistatin 1 has been demonstrated to be highly effective against a chemotherapy-resistant leukemia cell line, whereas peripheral mononuclear blood cells were not significantly affected, indicating the therapeutic aptitudes of spongistatin 1 (10). However, besides its initial characterization as a tubulin binding agent, reports about the mechanism of action of spongistatin 1 are rare and demand for further investigation.



Spongia sp.
(Pettit G.R., et al. *J Org Chem*, 1993)



Hyrtios erecta
(Kobajashi M., et al. *Tetrahedon Lett*, 1993)

Figure III.1: Chemical structure of spongistatin 1.

Spongistatin 1 is a macrocyclic lacton (left panel), isolated from the sponges *Spongia sp.* and *Hyrtios erecta* (right panel).

3 Microtubule-Inhibiting Drugs in Cancer Therapy

3.1 Chemotherapy and the War on Cancer

Cancer presents a medical challenge, inflicting the second highest disease-related mortality in the Western world, right after cardiovascular diseases (11). Surgical removal of tumors and radiotherapy has shown benefit in many cancer types and were even able to cure some diseases. But these therapies are restricted to local and regional tumors. Effective treatment of patients with advanced or metastatic cancer needs cytotoxic drugs, capable of reaching every organ in the body. However, chemotherapy with cytotoxic compounds is often accompanied by complications, including severe toxic side effects and the development of resistance of cancer cells to chemotherapeutic agents (12). Further, the formation of metastases impedes the success of the therapy. Thus for instance, currently only about 5% of patients with pancreatic cancer survive 5-years after their initial diagnose (13). At the time of diagnose, pancreatic cancer is inoperable in more than 80% of case, since the primary tumor typically is in an advanced state and metastases have spread to distant organs (14, 15). Chemotherapy with the standard therapeuticum gemcitabine has shown no benefit in the overall survival. Therefore, investigation of new anticancer drugs is required to improve chemotherapy for the inoperable advanced case.

To reduce toxic-side effects and to improve convalescence, it is important to achieve a selectivity of cytotoxic compounds for tumor cells. Cancer cells can be distinguished per definition from normal cells: they are characterized by uncontrolled proliferation. Thus, targeting the proliferation of cells should repress tumor growth without harming healthy, non-proliferating cells. The importance of microtubules in mitosis and cell division makes them a prime target for anticancer drugs. In view of the success of this class of drugs (Table III.2) it has been argued that microtubules represent the best cancer target to be identified so far. However, further development of microtubule-targeting compounds is of urgent need, to overcome their neurotoxicity and the development of resistances by cancer cells, both of which commonly occur with these drugs (16-18).

Table III.2 Antimitotic Drugs and Their Stages of Clinical Development (16)

Binding Site	Drug/Analogue	Therapeutic Use	Clinical Development
<i>Vinca</i> site	Vinblastine	Hodgkin's disease, testicular germ-cell cancer	In clinical use: 22 combination trials in progress
	Vincristine	Leukemia, lymphomas	In clinical use: 108 combination trials in progress
	Vinorelbine	Solid tumors, lymphomas, lung cancer	In clinical use: 29 Phase I-III clinical trials in progress
	Vinfluvine	Bladder, NSCLC, breast cancer	Phase III
	Cryptophycin 52	Solid tumors	Phase II finished
Colchicine site	Combretastatins	Potential vascular-targeting agent	Phase I, II
	Methoxybenzene-sulphonamide	Solid tumors	Phase I, II
Taxane site	Paclitaxel	Ovarian, breast and lung tumors, Kaposi's carcinoma, trials with numerous other tumors	In clinical use: 207 Phase I-III trials in the U.S.
	Docetaxel	Prostate, brain and lung tumors	8 Phase I-III trials in the U.S.
	Epothilone	Paclitaxel-resistant tumors	Phase I-III
Other sites	Estramustine	Prostate cancer	Phase I-III, in numerous combinations with taxanes, epothilones and <i>Vinca</i> alka.

3.2 Inhibition of Tumor Angiogenesis as an Anticancer Approach

Besides the classical chemotherapy which targets tumor growth directly by inhibiting tumor cell proliferation, the inhibition of pathological angiogenesis as therapeutic approach has gained particular importance in cancer treatment (19, 20). As tumors can only grow to a size of 1-2 mm³ without being connected to blood vessels to supply them with oxygen and nutrients, they secrete endothelial growth factors including VEGF (vascular endothelial growth factor) and FGF (fibroblast growth factor) to stimulate vessel growth into the tumor tissue. Tumor angiogenesis allows exceeded growth of the tumor and the formation of metastases. Some cancer types promote angiogenesis to a very high extent, and are extremely difficulty to treat due to their strong vascularization, which optimizes tumor progression and metastasis. The inhibition of vessel growth starves the tumor and suppresses metastasis, and is therefore an excellent contact point for cancer therapy, especially since antiangiogenic therapy targets genetically stable endothelial cells, making the development of resistance mechanisms very unlikely (20-22).

Similar to cancer cells, endothelial cells have to pass multiple proliferation cycles to form new vessels. Thus, it was thought that angiogenesis could be inhibited by the application of cell cycle inhibiting compounds, e.g. microtubule-inhibiting drugs (23, 24). In fact, these drugs turned out to belong to the most potent antiangiogenic compounds (25-27). Importantly, it was reported that the interphase microtubules of endothelial cells are much more sensitive to tubulin-targeting agents, than the mitotic microtubules of the spindle apparatus (28). Consequently, non-mitotic effects of tubulin-targeting drugs seem to be essential in their antiangiogenic action. However, these non-mitotic effects are still poorly characterized, since some functions of interphase microtubules are quite cell type-specific and the complexity of the effects of microtubule-disassembly in endothelial cells is not understood at all (29, 30).

4 Microtubules

A dense network of filaments is an essential component of the eukaryotic cell, providing the cytoplasm structure and stability. These filaments make up the cytoskeleton consisting of three main elements: the microfilaments (actin), the microtubules (tubulin), and the intermediate filaments (various proteins) (Figure III.2). The functions of the cytoskeleton are as multifaceted as its structures are including cellular shaping, scaffolding, cellular movement, transport activities, and many more.

The microtubules are tubes of 24 nm in diameter, and are thereby thicker and more rigid than the other cytoskeletal structures. They act as scaffolding and are crucial in development and maintenance of cell shape, in the transport of vesicles, mitochondria and other components through the cell, in cell signaling and in cell division. However, the relevance of microtubules for some functions depends particularly on species and cell-type (31, 32).

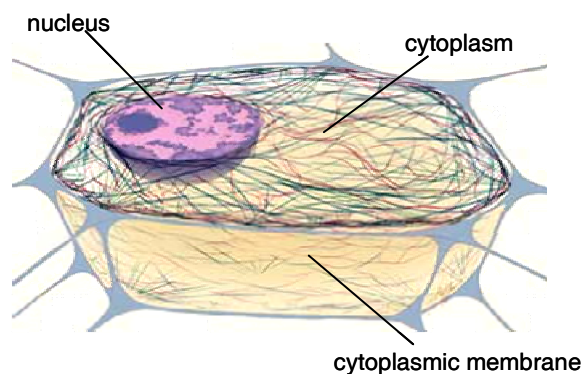


Figure III.2 The cytoskeleton is pervading the cell.

The cytoplasm is pervaded by a network of filamentous structures, the cytoskeleton. (Source: Inside the Cell NIH Pub. No. 05-1051)

4.1 The Structure of Microtubules

4.1.1 The Tubulins

Microtubules are assembled of tubulins, globular proteins, each of ~55 kDa molecular weight and 4 nm length. They exist in several isotypic forms, at least 14 tubulin isotypes that are expressed in a variety of tissue specific manners have been identified (33). The α - and the β -tubulin dimerize into tubulin heterodimers. A third species of tubulins, the γ -tubulin, is only located in centrosomes. The α - and the β -monomers are highly conserved and can be found in every eukaryotic organism. Although not found in prokaryotes, bacteria express the FtsZ-protein, a GTPase which is essential in the cell division, with homology in structure and function to the tubulins in eukaryotes, underlining the fundamental role of these proteins through all phyla (34).

4.1.2 Protofilaments

The interactions between the α - and the β -tubulins are very stable in the heterodimers, and typically the monomers do not dissociate from each other under normal conditions. Thus, the heterodimer is the smallest subunit of microtubules. By head to tail attachment, tubulin-heterodimers are forming the protofilaments, which assemble laterally and generate a tube: the microtubule (Figure III.3). The length of microtubules can vary from nanometers up to several hundred micrometers. The head-tail arrangement of the heterodimers in the protofilaments disposes the polarity of a microtubule: all protofilaments have the same polarity and thus there are only α -tubulins at the minus end and only β -tubulins at the plus end of the microtubule. The exact alignment of the protofilaments in a tube is not clear yet. They appear to be slightly shifted, so that α - and β -tubulin form spirals. The majority of microtubules in a cell have the typical singlet structure consisting of 13 protofilaments (Figure III.3 C), whereas duplet and triplet structures can only be found in specialized microtubule-structures like cilia or centrosomes (31, 32, 34).

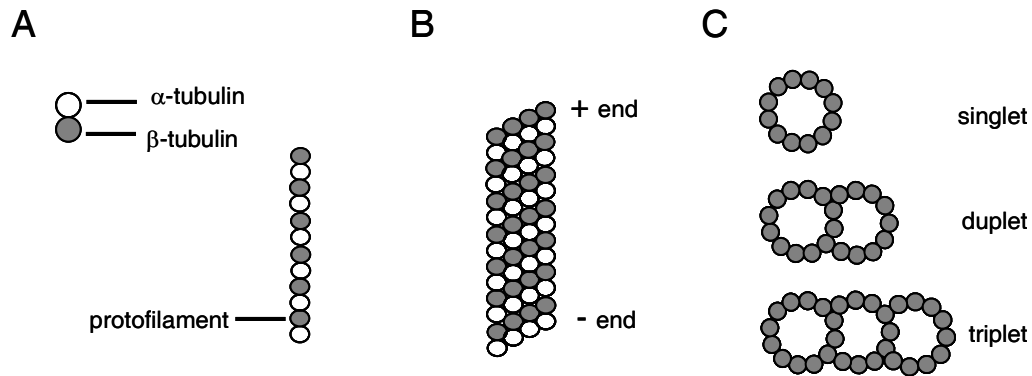


Figure III.3 The structure of microtubules.

(A) α - and β -tubulins dimerize to tubulin heterodimers, which assemble to protofilaments. (B) Protofilaments are forming the microtubule, displaying a polarity with α -tubulins at the plus end (+ end) and β -tubulins at the minus end (- end). (C) Oversight: the typical cytoplasmic microtubule is organized in the singlet structure consisting of 13 protofilaments. Duplet and triplet structures can be only found in the centrosome and the basal body.

4.2 Organization of Microtubules

The regulation of microtubule-assembly in the cell is very complex: growing, shrinking, and stable microtubules can be found in the same cell. Further, a single microtubule can switch between assembly and disassembly. This highly dynamic behavior of microtubule growth and collapse is called 'dynamic instability', and is regulated by the MTOC (microtubule-organizing center) and by MAPs (microtubule-associated proteins).

4.2.1 The MTOC

MTOCs are specialized structures in the cell, which nucleate microtubule polymerization by binding and stabilizing the minus end of microtubules. The MTOC consists of a right angled pair of centriols, which are assembled of microtubule triplets in a windmill-like configuration. The centriols are positioned in the center of a MTOC, but they do not contact the microtubule minus end directly. In contrast, γ -tubulin and pericentrin, two further proteins located in the MTOC, are supposed to interact with the microtubule minus end, since the assembly of microtubules can be completely suppressed by employing inhibitory antibodies against one of these proteins.

MTOCs exert different functions in the cell and have different terms due to their functions. During the interphase, there is only one single MTOC, the centrosome. It is located near the nucleus and organizes all cytoplasm pervading microtubules (Figure III.4). The centrosome doubles in the early phase of mitosis, moves to opposite poles of the nucleus and forms the spindle poles. The spindle poles nucleate the astral and the mitotic microtubules in the

mitotic spindle apparatus. The basal body is a MTOC structure, organizing the microtubules in flagella and cilia. Besides, the basal body and associated motorproteins are generating the driving forces of flagella and cilia movements (35-37).

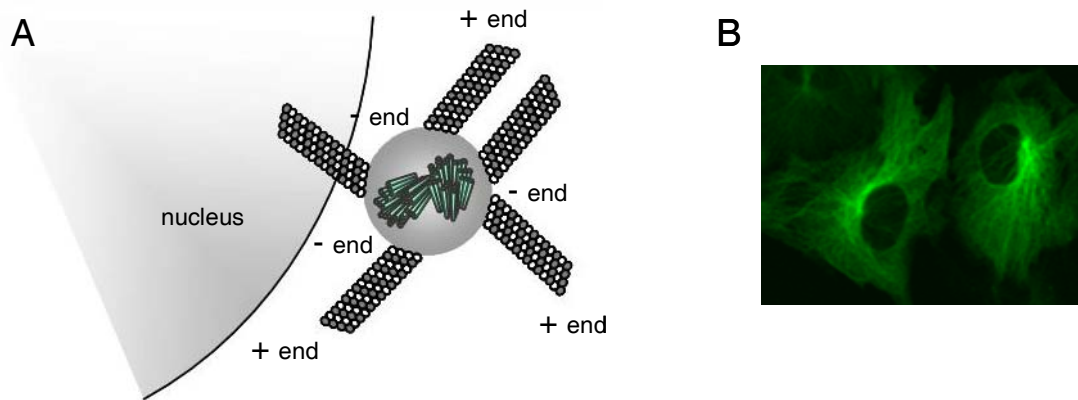


Figure III.4 The centrosome nucleates microtubule-assembly in the cell.

(A) Two pairs of centrioles (in blue-green) are in the center of the centrosome, each consisting of 9 triplet microtubules. During interphase, the centrosome is located near the nucleus and promotes microtubule-assembly by stabilizing their minus ends. (B) In GFP-tubulin transfected endothelial cells, the location of the centrosome can be perceived near the nucleus (bright signal). Outgoing from this point, microtubules (green) extend to the cell periphery.

4.2.2 The Dynamics of Microtubules

Microtubules exert many different functions and microtubule dynamics is critical for them. Permanent microtubules can be found in cilia and flagella, or in the axons of neurons, as microtubules have stabilizing and scaffolding functions. In contrast, microtubule-formation is transient during highly dynamic processes, like the assembly and disassembly of the mitotic spindle in proliferating cells or the microtubule re-organization during migration (31, 32).

A critical factor in microtubule-stability is the GTP-binding status of the tubulins. One molecule GTP is reversibly bound at the molecule surface of the β -subunit of the heterodimer. It can be hydrolyzed to GDP, which in turn can be replaced by GTP. Stabilization of the minus end by the MTOC facilitates microtubule growth, but only heterodimers with a GTP bound to β -tubulin are incorporated into a growing microtubule. During maturation of the microtubule, GTP is hydrolyzed to GDP. Thus a 'GTP cap' is generated at the plus end, which is a major factor for the stability of microtubules: whenever GTP-bound tubulin molecules are added more rapidly than GTP is hydrolyzed, the microtubule will retain the GTP cap at its plus end and growth will continue. When the rate of polymerization decreases, the GTP cap at the plus converts of to a GDP cap, resulting in instability and the disassembly of microtubules (Figure III.5) (35, 37-39).

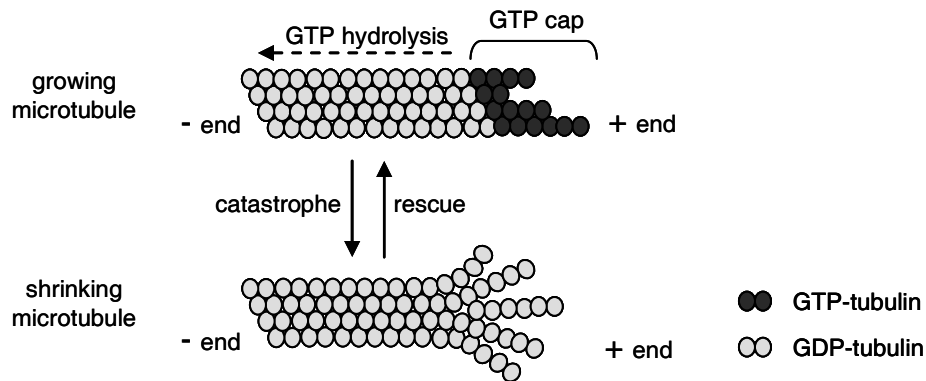


Figure III.5 GTP binding to tubulin is crucial for the microtubule stability.

Growing microtubules incorporate tubulin heterodimers with GTP bound to the β -subunit at the plus end. In the course of time, GTP is hydrolyzed to GDP. If hydrolysis is faster than the incorporation of new GTP-tubulin dimers, the GTP cap is lost and the microtubule disassembles (catastrophe). The shrinkage of the microtubules can be reversed upon increased assembly of GTP tubulin to the plus end (rescue).

Additionally, an ever-increasing number of MAPs regulate the dynamics of microtubules. One class of MAPs binds to more mature sections of microtubules, and mediate both stabilization and destabilization of the microtubule. A second class of microtubule-interacting proteins, including CLIP170, EB1/3, and APC, preferentially binds to the plus end of the microtubule and is therefore called +TIPs. These proteins control microtubule plus end dynamics and anchor microtubules to the cell cortex. The latter function is a crucial factor in vesicle transport and chemotactic migration (37, 40, 41).

4.3 Functions of Microtubules

4.3.1 The Mitotic Spindle

The spindle apparatus assembles during mitosis and separates the chromosomes into the daughter cells. During early prophase, interphase microtubules are disassembled and the centrosom is doubled, forming the spindle poles, which nucleate astral and mitotic microtubules. In the meantime, the chromosomes are arranged in the metaphase plate of the spindle, with the sister chromatids pointing to opposite end of the spindle. Mitotic microtubules extend to the chromosomes and bind to the kinetochore proteins at the centromers (Figure III.6). After kinetochor capture, pole bodies induce microtubule shortening and sister chromatids are pulled apart to the opposite sites of spindle poles (31, 32). However, prior to chromatid-separation, the cell cycle has to pass the spindle assembly checkpoint. Thus, if microtubules are not connected properly to centrosomes, the transition to anaphase is delayed. A prolonged delay in cell cycle progression in turn results in the

initiation of apoptosis. Thus, therapeutic tubulin antagonists are directly interfering with mitotic spindle assembly, and thereby induce apoptosis in proliferating cells (42, 43).

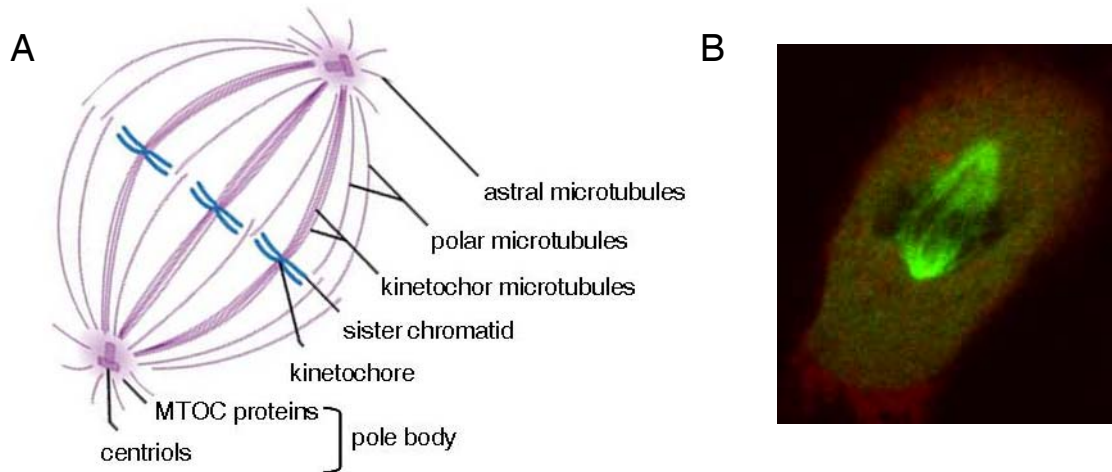


Figure III.6 The mitotic spindle.

(A) The assembly of the mitotic spindle apparatus (adopted from The Mc Graw-Hill Company). (B) Picture of the mitotic spindle in a GFP-tubulin transfected endothelial cell. Interphase microtubules are disassembled and the only polymer microtubule-structures in the cell are the astral and the mitotic (kinetochor and polar) microtubules of the spindle.

4.3.2 Cellular Transport

Cellular transport processes, including the arrangement of organelles and the translocation of endosomal vesicles, are largely microtubule-dependent. Since microtubules are organized into single arrays with their minus ends associated with the MTOC near the nucleus, and with their plus ends located toward the cell's periphery near the plasma membrane (cortical sites), a defined polarity is established. This polarity is utilized by microtubule-associated motor proteins to move cargo along the microtubules. The cell also uses actin filaments as a transport system. Since actin fibers are significantly shorter than microtubules, they have been suggested to bridge the gap between different microtubule arrays at the cell cortex (44).

The microtubule-dependent motor proteins can be divided into two classes: the kinesins and the dyneins. The different properties of the two motors are crucial for the regulation of transports. Kinesins move in plus end direction and are responsible for the main part of exocytosis (secretion) (45), whereas dyneins move predominantly in minus end direction, achieving endocytosis, transcytose, and vesicle transport between the ER (endoplasmic reticulum), cis-Golgi, and trans-Golgi (46). Traffic jams on the microtubules are avoided by the different nature of kinesin and dynein movement. Kinesins are strong, progressive motors, with low tendency for side or back steps. In contrast, dyneins show only poor

processivity and the long and flexible stalks of dyneins allow a certain degree of maneuverability. Thus, strong walking kinesins force dyneins to give right-of way (47).

Not only vesicles, but also organelles, the Golgi and mitochondria, are arranged along microtubules. These organelles express different surface proteins that are recognized and bound by dyneins and kinesins. During migration, the re-arrangement of the Golgi apparatus towards the leading edge is of particular importance, as it keeps lipid and protein supply coming to cell front (40, 44, 48). Besides the arrangement and the transport of organelles and vesicles, microtubules are reported to participate in signaling pathways by translocation of protein complexes. However, these processes are very cell-type specific.

5 Microtubule-Binding Compounds

A large number of chemically diverse compounds bind to soluble tubulin or directly to tubulins in the microtubule, and thereby interfere with microtubule-stability and dynamics. The role of microtubule-binding compounds in cancer therapy was discussed previously (III 3 Microtubule-Inhibiting Drugs in Cancer Therapy).

Three major binding sites on the heterodimers are characterized:

- 1.) the taxane binding site
- 2.) the colchicine binding site
- 3.) the *Vinca* alkaloids binding site.

Tubulin antagonists binding to the taxane-site, like paclitaxel, have only poor affinity for soluble tubulin and are rather binding to β -tubulin on the inside surface of a microtubule. This binding stabilizes the microtubules, interrupts the microtubule-dynamics and increases the polymerization of microtubules at higher concentration of the compound. In contrast, compounds which bind to the colchicine site preferentially bind to soluble tubulins, forming a poorly reversible colchicinoid-tubulin complex. Incorporation of this complex in the microtubule causes the inhibition of its dynamics at low concentration and the disassembly of the microtubule at high concentration, since the colchicinoid-tubulin complex cause the loss of the GTP cap. Interestingly, most compounds which bind to the colchicine site have turned out to be only barely applicable in cancer therapy due to their strong cytotoxic side-effects, which might be a consequence of the irreversibility of the colchicinoid-tubulin complex formation. Most prominent compounds binding to the colchicine-site are CA4P (combretastatin A4 phosphate) and nocodazole. Vinblastine and related compounds bind to

the so called *Vinca*-domain on the β -subunit of the heterodimers. The *Vinca* alkaloids bind rapidly and reversibly to soluble tubulin, as well as to the extreme ends of polymerized microtubules with high affinity. Similar to drugs binding to the colchicine site, the binding of a compound to the *Vinca*-domain inhibits microtubule-dynamics at low concentration and causes the disassembly of microtubules at high concentration. Other than the compounds binding to one of these three tubulin sites, several substances including spongistatin 1 are known to bind to tubulin at neither of the presented sites. Their action on microtubule-stability and dynamics are quite unique and might provide new properties, allocating them for therapeutic approach (49, 50).

6 Tumor Angiogenesis

Angiogenesis is the physiological process of developing new blood vessels from pre-existing ones. The term of angiogenesis must be distinguished from 'vasculogenesis', the spontaneous formation of new blood vessels out of endothelial stem cells (angioblasts), and from 'arteriogenesis', which is characterized by the formation of medium-sized vessels possessing tunica media and tunica adventitia. Angiogenesis in the narrower sense describes the formation of thin-walled vessels that can be associated with smooth muscle cells and pericytes.

The process of angiogenesis can be divided into distinct steps (Figure III.7) (51):

- 1.) endothelial activation and proliferation
- 2.) chemotactic orientation and migration
- 3.) the formation of a new lumen

Angiogenesis can be primarily observed during embryogenesis, whereas in adults, vessel formation is quite inactive and only takes place in wound healing, ovulation or menstruation. In the last decades, it was revealed that pathological angiogenesis plays a key role in a variety of diseases, like diabetes, rheumatoid arthritis, proliferative retinopathies or cancer (20). The process of angiogenesis has been only descriptive for a long time. Only recently, research is revealing the molecular mechanisms underlying angiogenesis. These findings offer new targets for therapeutic tools and furthermore, allow understanding the mechanisms of antiangiogenic compounds that have been well described but not well characterized, e.g. the mechanisms of microtubule-inhibiting drugs (52).

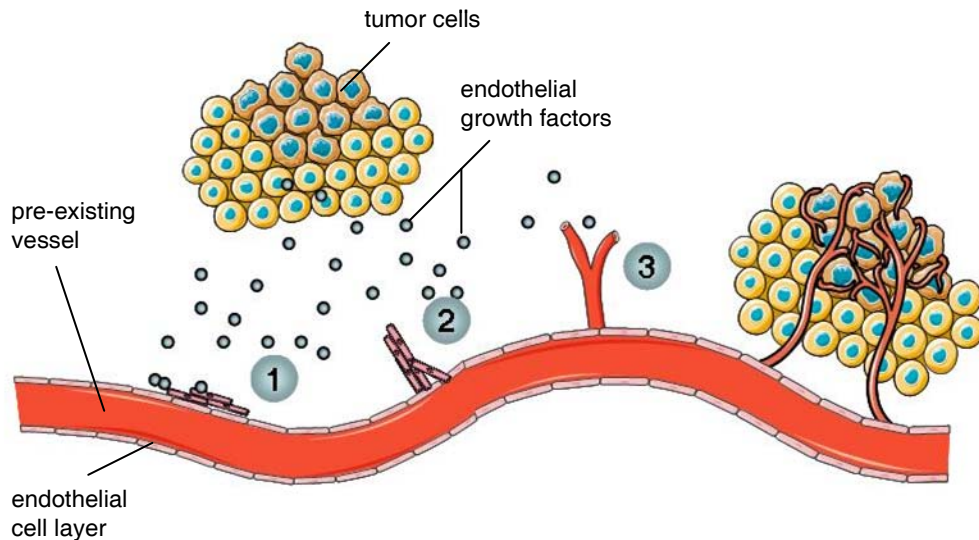


Figure III.7 Angiogenesis.

The physiological process of angiogenesis can be separated into distinct steps. (1) Tumor cells activate and stimulate endothelial proliferation by secretion of endothelial growth factors. (2) Endothelial cells migrate directional to the growth factor gradient and (3) form tubes. Finally, the newly established vessels pervade the tumor tissue and supply tumor cells with oxygen and nutrients.

6.1 Initiation of Angiogenesis: Endothelial Proliferation

6.1.1 Hypoxia-Induced Expression of VEGF

Tumor cells are rapidly proliferating cells with a corresponding demand of nutrients and oxygen. The strong metabolic activity of tumor cells causes a permanently hypoxic environment. The most important transcription factor of cell's response to oxygen availability is HIF-1 (hypoxia inducible factor 1). HIF-1 controls the expression of a variety of proteins, which play crucial roles in the acute and chronic adaptation to oxygen deficiency, including the expression of VEGF. HIF-1 is a heterodimer, consisting of two subunits: HIF-1 α and HIF-1 β . The later is constitutively expressed, whereas the protein level of HIF-1 α is highly regulated in an oxygen-dependent manner. Hypoxic conditions allow the formation of the HIF-1 α /HIF-1 β heterodimer, which induces the expression of VEGF. The growth factor is secreted into the extracellular space, diffuses to neighbored blood vessels and initiate angiogenesis, by binding to the VEGFR2 (VEGF-receptor 2) on endothelial cells (53). Upon binding to its receptor on the endothelium, VEGF induces signaling cascades, which promote survival, proliferation, and directional migration. The most prominent cellular pathways transducing VEGFR2-activation are AKT, MAPK (ERK) and PKC signaling pathways.

In fact, there are several growth factors expressed by tumor cells, binding to a plurality of endothelial receptors, regulating angiogenesis in many different ways. However, VEGF and

its binding to VEGFR2 on endothelial cells are the most important factors promoting tumor angiogenesis.

6.1.2 The AKT and the ERK Pathways

AKT, also known as Protein kinase B, is a 57 kDa serine/threonine kinase and represents a central node in proliferation and survival signaling. AKT has three domains: the PH - domain (pleckstrin-homology domain), the kinase domain, and the C-terminal tail.



Figure III.8 Domain structure of AKT.

The PH-Domain binds to PIP3 at the cytoplasm membrane. PDK1 interacts with the C-tail and phosphorylates T308. The S-residues at position 473 is phosphorylated by PDK2. Phosphorylation at both sites recovers full kinase activity of the AKT kinase domain.

Only when the threonine-residue at position 308 (T308) and the serine-residue at position 473 (S473) are both phosphorylated, AKT is activated. These phosphorylation events depend on VEGFR2-activation. After binding to a growth factor, the receptor induces activation of the receptor-associated PI3K (Phosphoinositide 3-kinases), which in turn phosphorylates the second messenger PI(3,4)P₂ to PI(3,4,5)P₃. PI(3,4,5)P₃ is the binding substrate for PH-domains, and binding to PI(3,4,5)P₃ recruits AKT to the close neighborhood of the membrane-associated kinases PDK1 and PDK2, which then can phosphorylate AKT at T308 and S473 (Figure III.9). Being phosphorylated, AKT is released to the cytoplasm, where it activates a large number of substrates by phosphorylation (54, 55). Most of AKT substrates are involved in survival, cell cycle progression, glucose metabolism, and protein synthesis, which are essential processes in proliferation (56). Further, activation of AKT is involved in generation and maintenance of cell polarity and migration (57). In this context, AKT knock-out cells have been shown to be decreased in proliferation, and impaired in migratory and extracellular matrix response (58).

MAPKs (Mitogen-activated protein kinases) are serine/threonine-specific kinases that respond to extracellular stimuli and regulate various cellular activities, such as gene expression, mitosis, differentiation, and cell survival. Proteins of the MAPK-cascade are organized in multi-protein complexes that are scaffolded by specific proteins with binding domains for multiple proteins. The proteins in those complexes can be composed in different constellations, depending on the scaffolding protein. The most important MAPK during angiogenesis is ERK1/2 (extracellular-signal regulated kinase 1/2), also known as MAPK p42/p44. Activation of VEGFR2 triggers a cascade that converts Ras-GDP to Ras-GTP and results in ERK activation by the phosphorylation of two critical residues in the activation loop. Activated ERK is released from the multi protein complex, scaffold by KSR (kinase suppressor of Ras), and phosphorylates more than 70 substrates, both nuclear and non-nuclear proteins, which promote cell proliferation and migration (Figure III.9) (59-61).

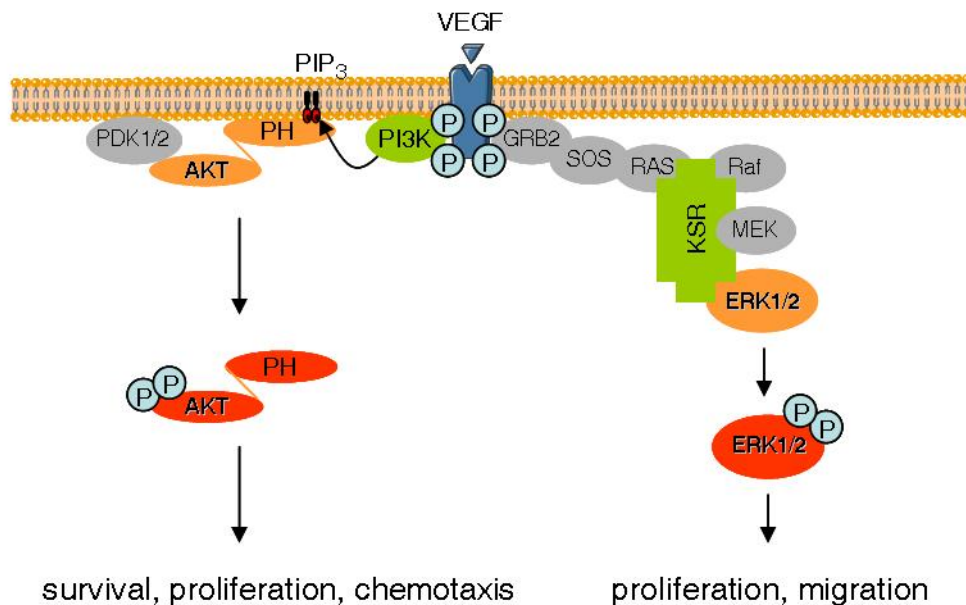


Figure III.9 VEGFR2 activates AKT and ERK signaling.

The binding of VEGF induces autophosphorylation of the cytoplasmic domain of VEGFR2. This phosphorylation promotes the activation of the AKT and the ERK pathway. AKT is phosphorylated and activated by PDK1/2 in a PIP₃-dependent manner. The activation of ERK is taking place after VEGFR2-mediated activation of Raf. Raf phosphorylates MEK, which in turn phosphorylates ERK1/2. The ERK phosphorylation chain is facilitated by the scaffold protein KSR.

6.1.3 The PKC pathway

The Protein Kinase C-family is a family of serine/threonine protein kinases, consisting of at least 10 members, which are divided into three groups: the conventional PKCs (cPKC) α , β_1 , β_{II} , and γ , the novel PKCs (nPKC) δ , ϵ , η/L , θ and the atypical PKCs (aPKC) ι/λ , and ζ . The cPKC and the nPKC are both activated by translocation to the membrane, where they bind DAG (diacylglycerol) and undergo conformational changes. In addition, cPKC-activation depends both on the release of Ca^{2+} and on translocation to the membrane (62, 63). PKC α , δ , and ϵ , are known to be involved especially in angiogenic processes (64-66). The binding of growth factors to their receptors can activate PLC γ (Phospholipase C γ), which is a central enzyme in cellular signaling, since it generates the second messengers PI $_3$ and DAG by hydrolysis of PI(3,4)P $_2$. The binding of PI $_3$ to Ca $^{2+}$ -channels results in a Ca $^{2+}$ -influx, thus both activators of cPKCs, Ca $^{2+}$ and DAG, are present upon PLC activation, initiating PKC-signaling cascades.

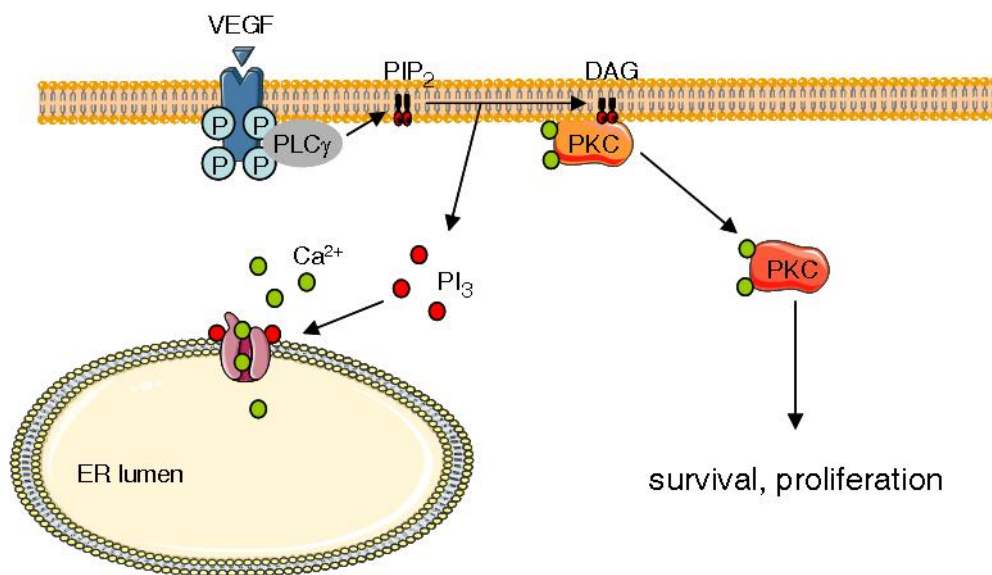


Figure III.10 Activation of PKC.

The VEGF-induced activation and autophosphorylation of VEGFR2 activate PLC γ , which cleaves the second messenger PI(3,4)P $_2$ into DAG and PI $_3$. PKCs bind to DAG in the membrane and take conformational changes. Additionally, PI $_3$ promote Ca $^{2+}$ release from the ER (endoplasmic reticulum). Binding of Ca $^{2+}$ to PKC is necessary for full activation.

6.2 Endothelial Migration

6.2.1 Matrix metalloproteinases

During angiogenesis, proteolytic activities are required to degrade the basement membrane of endothelial cells allowing the invasion into the tissue. Moreover, this process includes the removal of obstructing matrix proteins and the creation of space in the matrix for the generation of endothelial cell tubes. MMPs (matrix metalloproteinases) are the most prominent proteases involved in the remodeling of the extracellular matrix. Especially MMP-2 and MMP-9 are important during invasive processes, since these proteases are basal lamina-degrading enzymes and thus, are able to degrade the basement membrane. The promoter regions of MMP genes are very complex, containing multiple consensus sequences for different transcription factors. Thus, it could be shown that endothelial growth factors VEGF and FGF both induce the expression of MMPs, but the responsible signaling cascades remain to be elucidated (67-69).

6.2.2 Tip Cells and Stalk Cells

In sprouting vessels, two types of endothelial cells can be identified. Upon a pro-angiogenic stimulus (e.g. VEGF), the so-called tip cell is the first cell to emerge from the parent vessel and to lead the sprout into the tissue. A tip cell is characterized by distinct properties: it does not proliferate, but it is highly migratory, expressing numerous filopodia and lamellopodia that search the surrounding tissue for growth factors. Thus, the tip cell functions as motile guide that dynamically extends filopodia to explore attractive or repulsive signals that are present in the tissue environment. The tip cell is tailing the stalk cells, which have fewer filopodia and lamellopodia but undergo cell divisions. These cells form the new vessel lumen. It was recently found that the signaling of Notch/Dll4 regulates this differentiation of endothelial cells (51, 70, 71).

6.2.3 Molecular Processes during Migration

The process of endothelial migration can be divided into three basic steps:

- 1.) polarization of the cell
- 2.) formation of protrusion and adhesions
- 3.) the retraction of the rear.

The polarization of the endothelial cell is the key step of migration. Cell polarity and its maintenance depend on interlinked positive feedback loops, involving small Rho GTPases, PI3K, microtubules and vesicular transport. Upon a growth factor stimulus, PI3K rapidly accumulates at the leading edge, generating the second messenger PI(3,4,5)P₃. PI(3,4,5)P₃ can be dephosphorylated and thus inactivated by the phosphatase PTEN. However, PI3K-dependent activation of the small Rho GTPase Cdc42 at the leading edge restricts the localization of PTEN to the sides and the rear, thereby generating a polarized accumulation of second messengers at the front of the cell. Further, Cdc42 regulates the reorientation of the MTOC towards the leading edge. In the course, the Golgi apparatus is brought in position, keeping supply for the protrusion coming.

The second messenger PI(3,4,5)P₃ activates signaling pathways, including the AKT-pathway, which induce the formation of protrusion by activation of the small Rho GTPase Rac1 with restriction to the leading edge. Rac1 and microtubules polymerization activate each other in a reciprocal manner, resulting in F-actin polymerization in the leading edge. Accumulation of F-actin at the front generates protrusions that are stabilized by the formation of new focal adhesions.

At the rear, adhesions are disassembled in dependency on FAK/Src/ERK-pathway and RhoA. Besides, RhoA regulates the activity of myosin II and therewith the generation of tractional forces by F-actin in concert with myosin II motor proteins, which are driving the cell forward (for review see (72, 73)).

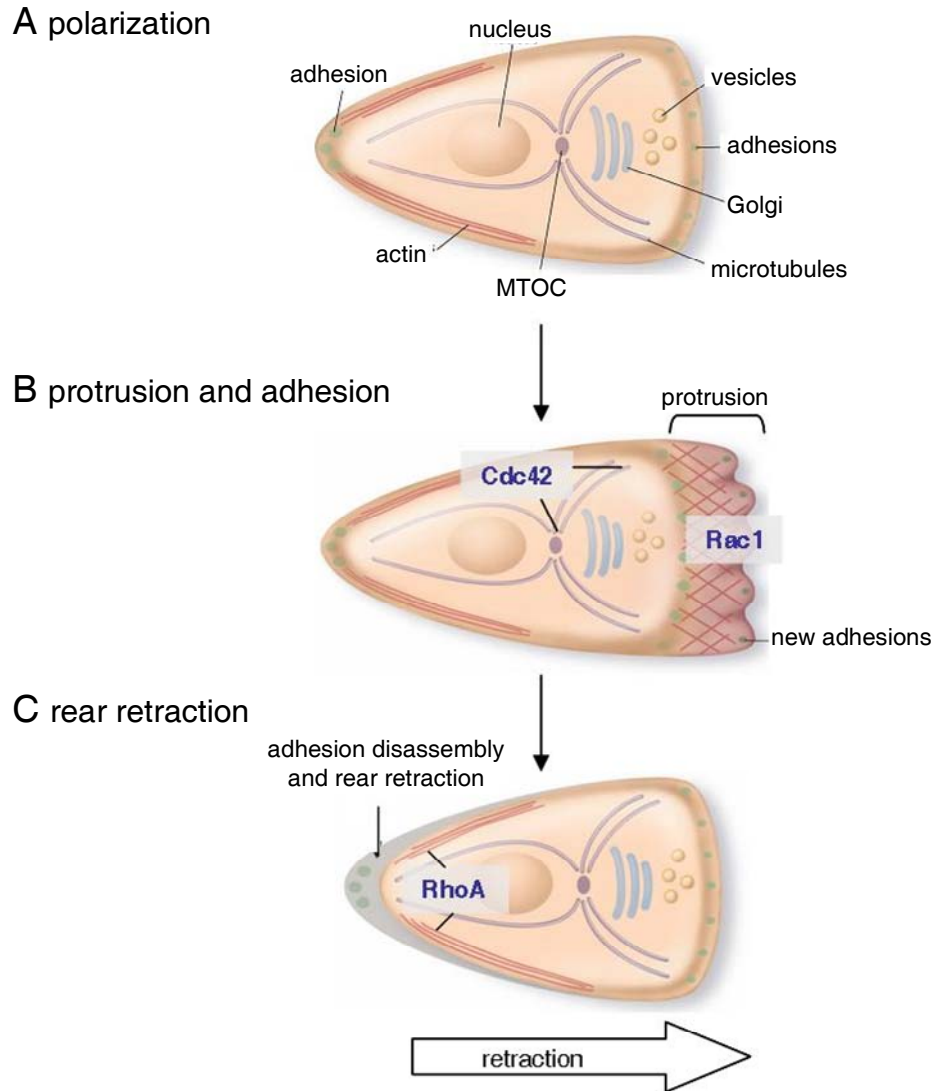


Figure III.11 Cell migration is divided into three distinct steps.

(A) Cell polarization (B) Formation of protrusions and adhesions (C) Disassembly of adhesions and retraction of the rear. Cdc42 mediates polarization by capturing microtubules at the leading edge and re-orientating the MTOC. Rac1 promotes actin polymerization in the leading edge and therewith the formation of the protrusion. RhoA mediates the disassembly of the adhesions in the rear. Further, the contraction of the actin fibers at the sides is regulated by RhoA (adapted from A.J. Ridley *et al.* (72))

6.3 Vessel Formation

In advanced angiogenesis, endothelial cells assemble as solid cords that subsequently acquire a lumen. However, angiogenesis is not completed until smooth muscle cells and pericytes are sheathing the newly developed vessel, providing stability and protection. Moreover, smooth muscle cells, pericytes, and the basal membrane of the intima mediate survival signals that prevent endothelial cells to undergo apoptosis. Once assembled in new vessels, endothelial cells become quiescent and survive for years (52, 53).

However, the physiology of pathological angiogenesis shows differences from normal vessel sprouting by formation of a deregulated, chaotic vessel system with enlarged, leaky vessels that are only restricted capable in meeting oxygen supplying demands. Moreover, endothelial cells are multilayered, and protrude extensions bridging and splitting vessels, contain inter- and intracellular holes, show uncontrolled permeability and undergo constant remodeling. This seems to be a consequence of uncontrolled and spatially uncoordinated release of endothelial growth factors by the tumor cells (52, 53).

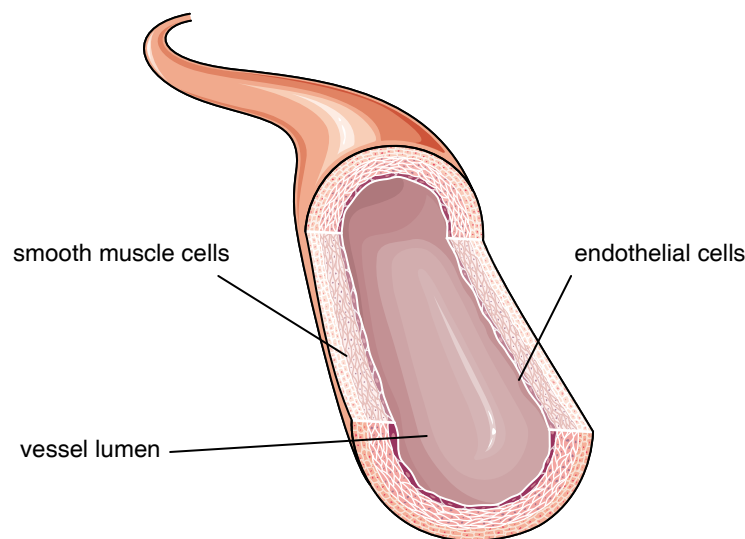


Figure III.12 Vessel formation completes angiogenesis.

The formation of new vessels is not complete until smooth muscle cells and pericytes are assembled around the endothelium, providing stability, protection and pro-survival signalings.

7 Aims of the Work

Based on the pronounced efficacy of the marine compound spongistatin 1 against some cancer cell lines *in vitro*, it was aim of the present work to investigate its anticancer activity on pancreatic tumor progression and metastasis *in vivo*. Besides this classical anticancer approach, it was also the aim to elaborate the antiangiogenic profile of spongistatin 1. In this context, investigation of the underlying mechanisms of the antiangiogenic action of spongistatin 1 was supposed to give information not only about spongistatin 1 effects, but also about the general action of tubulin antagonism in angiogenesis.

IV. MATERIALS AND METHODS

1 Materials

1.1 Compounds

Spongistatin 1 and CA4P were donated by George R. Pettit (Cancer Research Institute, Tempe, AZ, USA). Paclitaxel was purchased from Sigma (Taufkirchen, Germany), vinblastine from HEXAL (Holzkirchen, Germany), and staurosporine from Cayman Chemicals (Ann Arbor, MI, USA).

1.2 Biochemicals, Inhibitors, Dyes, and Cell Culture Reagents

Accustain [®] formaldehyde	Sigma-Aldrich, Taufkirchen, Germany
Bradford Reagent [™]	Bio-Rad, Munich, Germany
CellTiter Blue [™]	Promega, Madison, WI, USA
Collagen A	Biochrome AG, Berlin, Germany
Collagen G	Biochrome AG, Berlin, Germany
Collagenase G	Biochrome AG, Berlin, Germany
Complete [®]	Roche diagnostics, Penzberg, Germany
DMEM	PAN Biotech, Aidenbach, Germany
Endothelial Growth Medium	Provitro, Berlin, Germany
FCS gold	PAN Biotech, Aidenbach, Germany
M199 Medium	PAN Biotech, Aidenbach, Germany
Matrigel [™]	BD Discovery Labware, Bedford, MA, USA
MitoTracker Mitochondrion-Selective Probes	Invitrogen, Karlsruhe, Germany
Non-essential amino acids	PAA Laboratories, Cölbe, Germany
Page Ruler [™] Prestained Protein Ladder	Fermentas, St. Leon-Rot, Germany
Penicillin	PAN Biotech, Aidenbach, Germany
Propidium iodide	Sigma-Aldrich, Taufkirchen, Germany
PermaFluor mounting medium	Beckman Coulter, Krefeld, Germany
PMA	Sigma, Taufkirchen, Germany
Pyruvate	Merck, Darmstadt, Germany
Rhodamin-phalloidin	Invitrogen, Karlsruhe, Germany
RNAlater	Ambion, Austin, TX, USA
Streptomycin	PAN Biotech, Aidenbach, Germany
Triton X-100	Merck, Darmstadt, Germany
Vybrant Cell-Labeling Solution	Invitrogen, Karlsruhe, Germany

Trypsin/EDTA (T/E)		PBS (+)	
Trypsin	0.50 g	NaCl	7.20 g
EDTA	0.20 g	Na ₂ HPO ₄	1.48 g
PBS	ad 1.0 l	KH ₂ PO ₄	0.43 g
H ₂ O	ad 1.0 l, pH 7.4	(MgCl ₂ x 6 H ₂ O)	0.10 g)
		(CaCl ₂ x 2 H ₂ O)	0.10 g)
		H ₂ O	ad 1.0 l, pH 7.4

1.3 Technical Equipment

Name	Device	Producer
AB7300 RT-PCR	Real-time PCR system	Applied Biosystems, Fosterer City, CA, USA
Axiovert 200	Inverted microscope	Zeiss, Jena, Germany
Curix 60	Tabletop film processor	Agfa, Cologne, Germany
Custom-made climate chamber	Life-cell observation on LSM 510 Meta	EMBLEM, Heidelberg, Germany
Cyclone	Storage Phosphor Screens	Canberra-Packard, Schwadorf, Austria
FACSCalibur	Flow cytometer	Becton Dickinson, Heidelberg, Germany
FastPrep	Homogenizer	MP Bio, Illkirch, France
LSM 510 Meta	Confocal laser scanning microscope	Zeiss, Jena, Germany
Mikro 22R	Table centrifuge	Hettich
Nucleofector II	Electroporation device	Amaza, Cologne, Gemrany
Odyssey 2.1	Infrared Imaging System	LI-COR Biosciences, Lincoln, NE, USA
Optima TLX™	Ultracentrifuge	Beckman Coulter Krefeld, Germany
Polytron PT1200	Ultrax homogenizer	Kinematica AG, Lucerne, Switzerland
Potter S	Homogenizer	Braun Biotech GmbH, Mesungen, Germany
SpectraFluor Plus™	Microplate multifunction reader	Tecan, Männedorf, Switzerland
Sunrise™	Microplate absorbance reader	Tecan, Männedorf, Switzerland

2 Cell Culture

2.1 HUVEC Isolation and Cultivation

Primary HUVECs were isolated by collagenase treatment of umbilical cords (74) and used at third passage. Cells were cultivated on 0.001% Collagen G-coated flasks or plates in Endothelial Growth Medium, containing 10% inactivated FCS and growth factors (FGF 1.0 ng/ml, Heparin 0.004 ml/ml, and EGF 0.1 ng/ml). M199 medium was used as starvation medium, and M199 medium supplemented with 10% FCS as stopping medium.

For splitting and seeding (1:3), cells were washed once with pre-warmed PBS, which was removed completely with a sterile pipette. 3 ml T/E was added (75 cm² flask), and cells were incubated for 1-2 minutes at 37°C. The digest was terminated by adding approximately 20 ml stopping medium. Next, cells were centrifuged for 5 minutes at 1,000 rpm to remove the T/E. The supernatant was discarded and the cells were resuspended in pre-warmed Endothelial Growth Medium and seeded into flasks or well plates (coated with Collagen G).

2.2 L3.6pl Cultivation

For *in vitro* analysis of spongistatin 1 effects on pancreatic cancer, the human pancreatic cancer cell line L3.6pl was kindly provided by Christiane J. Bruns (Department of Surgery, Klinikum Großhadern, LMU Munich, Germany). The cells were cultivated on 0,001% Collagen G-coated culture flasks and stimulation plates in DMEM (Dulbecco's Modified Eagle Medium), supplemented with 10% FCS, 1x non-essential amino acids, and 1 mM pyruvate.

For splitting and stimulation, cells were treated according to the treatment of HUVECs. In contrast to HUVECs, L3.6pl needed approximately 5 minutes of incubation in T/E to detach from the flask, and the reaction was stopped by adding about 20 ml of L3.6pl culture medium. Then cells were centrifuged, resuspended in fresh culture medium, and seeded for further cultivation or experiments. As L3.6pl cells are extremely rapid growing cells, they were diluted 1:10 upon splitting.

3 Flow Cytometry

HFS Buffer

Na ₃ -citrate	0.1%
Triton-X 100	0.1%
PBS	ad 1 ml

FACS Buffer

NaCl	8.12 g
KH ₂ PO ₄	0.26 g
Na ₂ HPO ₄	2.35 g
KCl	0.28 g
Na ₂ EDTA	0.36 g
LiCl	0.43 g
Na-azide	0.20 g
H ₂ O	ad 1.0 l, pH 7.37

3.1 Stimulation and Harvest

75,000 HUVECs per well were seeded into 12-well-plates, allowed to incubate over night at 37°C, followed by stimulation for 24 hours with various concentrations of spongistatin 1, vinblastine, CA4P, and paclitaxel. Cells were washed, trypsinized, resuspended in the supernatant, and centrifuged 10 minutes 600x g at 4°C. After another wash with PBS, cells were resuspended in HFS-buffer containing 2 mg/ml propidium iodide, and incubated protected from light at least 30 minutes at 4°C. The fluorescence of propidium iodide was detected by flow cytometry.

3.2 Cell Cycle Analysis

The fluorescence intensity was measured in the logarithmic mode of the fluorescence channel 2 (FL2, λ_{em} 585 nm) using a flow cytometer. Intercalating into the DNA-helix, propidium iodide-fluorescence depends on the status of cellular chromatin. Under control conditions, most cells are in the G₀/G₁ cell cycle phase with 2n chromosome set, lacking the sister chromatids. Cells in the G₂/M-phase are in the process of cell division, meaning they possess the normal 2n chromosome set as well as the duplicate sister chromatids. This

duplication allows the G₂/M-phase to be differentiated from the G₀/G₁-phase due to the higher fluorescence peak from the increased amount of propidium iodide intercalation. HUVECs in the S-phase are in the synthesis-phase, in which the cytosol is accreted and chromatids become duplicated. Hence, the fluorescence peak of S-phase cells is located between the fluorescence peaks of G₀/G₁- and G₂/M-phase. In contrast, the DNA is fragmented in apoptotic cells and apoptotic bodies, generating a peak which is located left of the G₀/G₁ fluorescence. Regions were set on each fluorescence peak of the four enumerated chromatin states, and cells of each region were quantified and set into relation of the total cell number.

4 Cell Viability Measurements

Cell viability under spongistatin 1-treatment was measured via reduction of resazurin to resorufin (CellTiter-Blue™) by endothelial cells. 5,000 (proliferating) and 15,000 (confluent) HUVEC per 96-well were seeded and stimulated with spongistatin 1 for 24 hours. The assay was performed as described in the provided protocol of CellTiter-Blue™ Cell Viability Assay. Fluorescence (excitation 530 nm, emission 595 nm) was measured with SpectraFluor Plus plate reader.

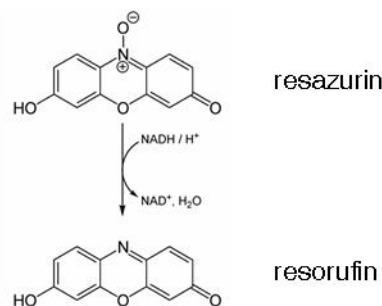


Figure IV.1 Conversion of resazurin to resorufin.

5 Microscopy

5.1 Immunohistochemistry

Cells were seeded either on collagen A-coated glass slides, or on ibi-Treat μ -slides (IBIDI, Martinsried, Germany). After stimulation, cells were washed once with ice-cold PBS+ and fixed in 4% formaldehyde (Accustain®, Sigma-Aldrich, Taufkirchen, Germany) for

10-15 minutes. After one PBS washing step, cells were permeabilized by incubating cells in 0.2% Triton X-100 in PBS for exactly 2 minutes. Then, cells were washed three times for 5 minutes with PBS, blocked for 15 minutes in 0.2% BSA in PBS, and incubated with the primary antibody against Cdc42 (Santa-Cruz Biotechnology Inc., 1:200 in 0.2% BSA/PBS) for 45-60 minutes. After three washes with PBS for 5 minutes, cells were incubated with light-protection for 30-60 minutes with the Alexa Fluor 546-conjugated secondary antibody (Invitrogen, 1:400 in 0.2% BSA/PBS). Afterwards, cells were washed again three times with PBS, and covered with PermaFluor mounting medium for confocal microscopy.

5.2 Live-Cell Imaging

5.2.1 Mitochondria Staining

Mitochondrion staining was performed by adding 50 nM MitoTracker Red Cmx Ros to the medium. After 15 minutes of dye-uptake, 1.0 nM spongistatin 1 was added (MitoTracker remained in the medium) and mitochondria arrangement was documented by live-cell imaging (Axiovert 200).

5.2.2 Visualization of Membrane Traffic

Documentation of membrane trafficking was done by staining HUVECs with the membrane-staining dye VYBRANT Cell-Labeling solution. Cells were either left untreated, or pre-incubated with 2.0 nM spongistatin 1 for 3 hours, then the dye was added to the medium (15 minutes, 5 μ l/ml). Cells were washed and live cell-imaging (LSM 510 Meta) was done in endothelial growth medium over a period of 5 hours.

5.2.3 Expression of Recombinant Proteins

Plasmids were amplified in the *E.coli* strain DH5 α and purified by using the EndoFree Plasmid Maxi Kit (Qiagen GmbH, Hilden, Germany). Procedures were done according to the provided protocol. HUVECs were transfected with 7 μ g endotoxin-free purified pEGFP-C1-tubulin (kindly given by Stefan Linder). Transfection was done by electroporation in the Nucleofector II, according to the protocol given with the HUVEC Nucleofector Kit (Amaxa). At days 2 and 3 after transfection, cells were stimulated with 2.0 nM spongistatin 1 and placed into a customized live-cell observation chamber mounted to the confocal microscope. A time series was collected with images taken every 5 minutes for 16 hours. Images were analyzed by the LSM Image Browser (Zeiss).

6 Protein Sample Preparations

6.1 Total Cell Lysates

RIPA Buffer (store at 4°C)

Tris/HCl	0.79 g
NaCl	0.87 g
Nonidet NP 40	1.0 ml
Deoxycholic acid	0.25 g
SDS	0.10 g
Complete [®]	1:25
PMSF	1.0 mM
Na ₃ VO ₄	1.0 mM
NaF	1.0 mM
H ₂ O	ad 100 ml

5x SDS-Sample Buffer (store at -20° C)

Tris/HCl	3.125 M, pH 6.8
Glycerol	10 ml
SDS	5%
DTT	2%
Prionin Y	0.025%
H ₂ O	ad 20 ml

For Western blot analysis, cells were washed with ice-cold PBS after stimulation. The PBS was removed completely and cells were lysed by adding RIPA buffer and freezing at -80° C. Cells were thawed on ice, scratched from the plate/dish and transferred to 1.5 ml reaction tubes. Cellular debris was removed by centrifugation for 10 minutes at 10.000x g and 4° C. Supernatants were transferred to a new reaction tube, and aliquots were taken for protein quantification (IV 7.1 Protein Quantification). 5x SDS-sample buffer was added to the lysates, and lysates were boiled for 5 minutes at 95° C for inactivation. Protein samples were stored at -20°C until use.

6.2 Microtubule Fractionation

PIPES Buffer

PIPES	0.1 M, pH 6.9
Glycerol	2.0 M
Triton X-100	0.5%
MgCl ₂	2.0 mM
K-EGTA	2.0 mM
Paclitaxel	5.0 μM
GTP	1.0 mM
PMSF	1.0 mM
Complete	1:25

Ca²⁺ Buffer

Tris/HCl	0.1 M, pH 6.8
MgCl ₂	1.0 mM
CaCl ₂	10 mM
PMSF	1.0 mM
Complete	

HUVECs were stimulated with spongistatin 1 or paclitaxel, washed twice with ice cold PBS and lysed 20 minutes at room-temperature in PIPES buffer. Lysates were centrifuged 45 minutes at 100,000x g, 4° C. The supernatants were collected (fraction of soluble tubulin), while the sediments were incubated one hour at 4° C with 40 μl of Ca²⁺ buffer. Insoluble debris was removed by centrifugation, 10,000x g for 10 minutes at 4° C, to obtain a clear fraction of PIPES-insoluble tubulin. Both fractions were boiled 5 minutes in 5x SDS-sample buffer (IV 6.1 Total Cell Lysates) for immunoblotting.

6.3 Membrane Fractionation

Membrane Lysing Buffer

Tris/HCl	0.05 M, pH 7.5
EDTA	0.5 mM
EGTA	0.5 mM
DTT	2.0 mM
Glutathione	7.0 mM
Glycerol	10%
Complete [®]	1:25
PMSF	1.0 mM

To investigate PKC translocation, HUVEC lysates were separated into a soluble (cytosolic) and a particulate (membranous) fraction, as described previously by Li H *et al.* (75). HUVECs were either pre-incubated with 5.0 nM spongistatin 1 prior to stimulation with 10 nM PMA, or stimulated with 10 nM PMA alone, washed twice with ice-cold PBS, and homogenized in lysing buffer. Lysates were centrifuged at 100.000x g for 1 hour. The supernatant (cytosolic fraction) was collected, the pellet washed in lysing buffer containing 1.0 M NaCl, and centrifuged at 100.000x g for 30 minutes. The supernatant was discarded, and the pellet was solubilized with lysing buffer containing 20 mM CHAPS at 4° C for 30 minutes. After centrifugation at 100.000x g for 1 hour, the supernatant was kept as membranous fraction. Both fractions were used for Western blotting.

6.4 Protein Isolation of Tissue Sections

60-80 mg of RNAlater-stored tissue was homogenized 15 seconds in 600 µl RIPA-buffer (IV 6.1 Total Cell Lysates) using the Potter S homogenizer. Lysates were centrifuged at 14.000 rpm and 4° C for 15 minutes. The clear supernatants were boiled in 5x SDS-sample buffer (IV 6.1 Total Cell Lysates). Protein concentration was determined using the Bradford assay (IV 7.1 Protein Quantification).

7 Western Blot Transfer

7.1 Protein Quantification

Protein samples were quantified according to Bradford (76). The calibration curve was generated by using samples containing defined concentrations of BSA in H₂O (50 µg/ml – 500 µg/ml). 190 µl Bradford reagents (diluted 1:5 in H₂O) were added to each 10 µl aliquot of 1:10 (in H₂O) diluted protein samples and calibration samples in an ELISA-plate. All measurements were performed in duplicate. Probes were incubated for 5-10 minutes and the absorbance was measured in the Sunrise™ ELISA reader.

7.2 SDS-PAGE

Electrophoresis Buffer

Tris base	3.0 g
Glycine	14.4 g
SDS	1.0 g
H ₂ O	ad 1.0 l

Stacking Gel		Separating Gel (10%)	
PAA solution 30%	1.275 ml	PAA solution 30%	5.0 ml
1.25 M Tris/HCl, pH 6.8	0.75 ml	1.5 M Tris/HCl, pH 8.8	3.75 ml
10% SDS	75 µl	10% SDS	150 µl
H ₂ O	5.25 ml	H ₂ O	6.1 ml
APS	75 µl	APS	75 µl
TEMED	20 µl	TEMED	20 µl

SDS-PAGE according to Laemmli (77) was performed by using the Mini Protean III system from Bio-Rad (Munich, Germany). Prior to loading the samples, the apparatus was assembled as described by the producer, and the chamber was filled with ice-cold electrophoresis buffer.

Protein concentrations of the probes were unified, by adding required volume of 1x SDS-sample buffer. Then probes were boiled for 5 minutes at 95° C before loading the samples on the SDS-Gel. Empty slots were filled with an appropriate volume of 1x SDS-sample buffer. To estimate the molecular weights of the separated proteins, 2 µl of the marker Page Ruler™ Prestained Protein Ladder was additionally loaded on the gel.

Proteins were separated in a discontinuous electrophoresis: proteins were focused by running the probes through the stacking gel, pH 6.8, (100 V, 20 minutes), and then separated in the separating gel, pH 8.8 (200 V, 45 minutes).

7.3 Tank-Blotting

5x Tank Buffer		1x Tank Buffer	
Tris base	15.2 g	5x Tank buffer	200 ml
Glycin	72.9 g	Methanol	200 ml
H ₂ O	ad 1.0 l	H ₂ O	ad 1.0 l

After separating in the SDS-PAGE, proteins were transferred to a nitrocellulose membrane (Hybond-ECL™, Amersham Bioscience, Freiburg, Germany) via tank blotting. A blotting sandwich was prepared in a box filled with 1x Tank Buffer to avoid bubbles as follows: cathode – pad – blotting paper – separating gel (from SDS-PAGE) – nitrocellulose membrane – blotting paper – pad – anode (Figure IV.2). Pads, papers, and membrane were equilibrated with 1x Tank buffer 15 minutes prior to running the tank blot. Sandwiches were mounted in the Mini Trans-Blot® system (Bio-Rad, Munich, Germany), ice-cold 1x Tank buffer filled the chamber and a cooling pack was inserted to avoid excessive heat. Transfers were carried out at 4° C, either at 100 V for 90 minutes or at 23 V overnight (especially for high-molecular weight proteins).

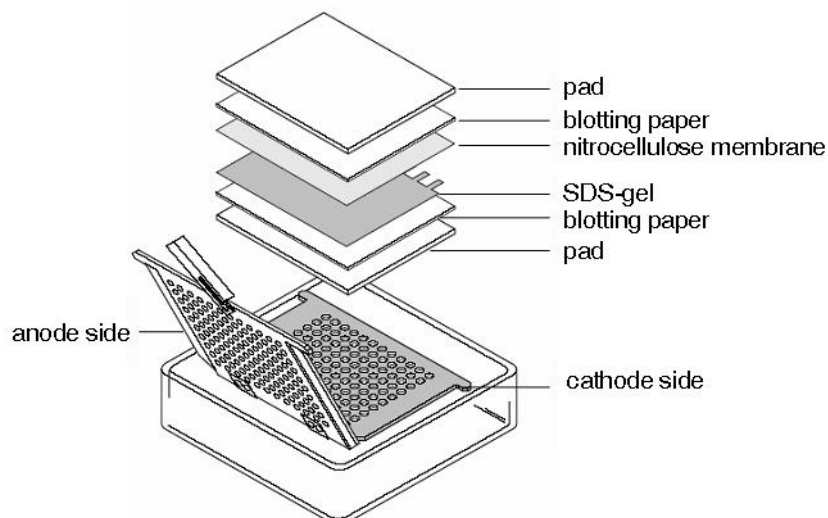


Figure IV.2 Tank blot assembly.

(Adopted from Bio-Rad, Munich, Germany)

7.4 Detection

TBS-T

Tris base	3.0 g
NaCl	11.1 g
Tween 20	1.0 ml
H ₂ O	ad 1.0 l

After the transfer, sandwiches were disassembled, gels were stained in Coomassie (I 7.5 Staining Gels and Membranes), and membranes were washed in 1x TBS-T. Unspecific binding reactions were blocked by incubating membranes for at least 2 hours in 5% BSA or 5% Blotto, each in PBS. After one washing step with 1x TBS-T, membranes were incubated with the primary antibody dilution over night at 4° C. The next day, membranes were washed 3-times with 1x TBS-T, prior to incubation with the secondary antibody. Secondary antibodies were incubated protected from light for 1 hour at room-temperature (infrared dye-conjugated antibodies) and 2 hours at room-temperature (peroxidase-conjugated antibodies), respectively.

7.4.1 Enhanced Chemiluminescence

Proteins were detected with ECL (enhanced chemiluminescence) when the secondary antibody was conjugated to HRP (horseradish peroxidase). Membranes were washed three times for 5 minutes with TBS-T after incubation with the secondary antibody. Then the membrane was shaken protected from light in ECL Plus™ Western Blotting detection reagent (Amersham Bioscience) for 1 minute, and layered between two plastic sheets afterwards. Chemiluminescence was detected by exposing the membranes to an X-ray film for the appropriate time period in a darkroom. X-ray films were developed in a table processor.

7.4.2 LI-COR

The detection of protein levels was performed with the Odyssey Infrared Imaging System version 2.1 when the secondary antibody was conjugated to an infrared dye (AlexaFluor 680 or IR-Dye 800). Membranes were washed three times with TBS-T after incubation with the secondary antibody and one time with PBS to remove the interfering Tween 20. After washing, membranes were scanned and analyzed, and proteins were quantified using the Odyssey system software.

Table IV.1: Primary Antibodies

Antigen	Isotype	Dilution	Provider	Detection
β -Actin	goat	1:1,000	Santa Cruz	LI-COR
AKT	rabbit	1:1,000	Cell Signaling	LI-COR
p-AKT T308	rabbit	1:500	Cell Signaling	ECL
p-AKT S473	mouse	1:1,000	Cell Signaling	LI-COR
ERK 1/2	rabbit	1:1,000	Cell Signaling	LI-COR
p-ERK 1/2 T202/Y204	mouse	1:1,000	Cell Signaling	LI-COR
HIF-1 α	mouse	1:250	BD Transduction	ECL
MMP-2	rabbit	1:1,000	Cell Signaling	LI-COR /ECL
MMP-9	rabbit	1:1,000	Sigma	LI-COR
PKC α	rabbit	1:1,000	Santa Cruz	LI-COR
PKC β	mouse	1:500	BD Transduction	ECL
PKC δ	rabbit	1:1,000	Santa Cruz	LI-COR
PKC ϵ	rabbit	1:1,000	Santa Cruz	LI-COR
PKC η	rabbit	1:1,000	Santa Cruz	LI-COR
PKC θ	rabbit	1:1,000	Santa Cruz	LI-COR
PKC ζ	rabbit	1:1,000	Santa Cruz	LI-COR
p-serine PKC substrates	rabbit	1:1,000	Cell Signaling	ECL
β -Tubulin	mouse	1:500	Santa Cruz	LI-COR
VE-Cadherin	rabbit	1:1,000	Cell Signaling	LI-COR

Table IV.2: Secondary Antibodies

Antigen	Conjugate	Dilution	Provider
Goat anti:rabbit	HRP	1:1,000	Dianova
Goat anti:mouse	HRP	1:1,000	Santa Cruz
Goat anti:mouse	AlexaFluor 680	1: 10,000	Invitrogen
Donkey anti:goat	AlexaFluor 680	1: 10,000	Invitrogen
Goat anti:rabbit	IR-Dye 800	1: 10,000	Rockland

7.5 Staining Gels and Membranes

Coomassie Staining Solution		Coomassie Destaining Solution	
Coomassie blue	3.0 g		
Glacial acetic acid	100 ml	Glacial acetic acid	100 ml
Ethanol	450 ml	Ethanol	333 ml
H ₂ O	ad 1.0 l	H ₂ O	ad 1.0 l

To control equal loading of the gel and the performance of the transfer, polyacrylamide gels were stained for 30 minutes with Coomassie-blue, and destained with destaining solution. After protein detection, membranes were stained with Ponceau S (0.2% Ponceau S in 5% acetic acid) for 5 minutes, and destained with distilled water.

8 Kinome Array (PepChip)

To address the question, which effects tubulin-inhibiting drugs have on overall signaling in endothelial cell, a kinome array (PepChip) was performed. The array was done in collaboration with Dr. Jos Joore from Pepscan System BV, Lelystad, The Netherlands.

HUVECs in 4x 100 mm dishes for each treatment group were grown to confluency. Untreated cells and cells stimulated with spongistatin 1 (5.0 nM, 30 minutes), vinblastine (10.0 nM, 30 minutes), or CA4P (20.0 nM, 30 minutes) were washed twice with ice-cold PBS, and lysed with M-PER Mammalian Protein Extraction Reagent (Pierce, Rockford, IL), containing 2.5 mM Na₄-pyrophosphate, 2 mM Na₂-β-glycerophosphate, 1 mM Na₃VO₄, and 1 mM NaF. Lysates were centrifuged for 10 minutes at 13,000 rpm, 4° C, and supernatants were frozen immediately in liquid nitrogen. PepChip performance and analysis of the results were done by Pepscan Presto BV (Lelystad, The Netherlands). On the chip 1,152 different peptides with best possible specific phosphorylation motifs for upstream kinases were spotted in triplicates (78). Native protein lysates of HUVECs incubated on PepChip with [γ -³³P] ATP. A radiosensitive screen determined and quantified the phosphorylation status of peptides (\cong kinase substrates), which gave information about the activity of the associated upstream kinase.

9 PKC *In Vitro* Assay

Potential inhibition of PKC isozymes *in vitro* by spongistatin 1 was assessed using a micellar based assay. 150 ng recombinant GST-tagged PKC isozymes α , β I, β II, δ , ϵ or ζ (kindly provided by Dr. M. Kubbutat, ProKinase Ltd, Freiburg, Germany) were incubated in a buffer containing 20 mM Tris-HCl, pH 7.5 and 20 mM $MgCl_2$, with 50 μ M PKC- α -19-31/Ser25 substrate peptide (NeoMPS, Strasbourg, France), 1 mM $CaCl_2$, 10 μ M phosphatidylserine (Sigma), 1 μ M 12-O-tetradecanoylphorbol-13-acetate (Sigma), 40 μ M ATP and 1 μ Ci γ - 33 ATP (PerkinElmer, Fremont, CA; 3000 Ci/mM) per 100 μ l as previously described (79). In the assays for PKC δ and ϵ $CaCl_2$, and for PKC ζ $CaCl_2$, phosphatidylserine and 12-O-tetradecanoylphorbol-13-acetate were omitted. Samples containing 50-100 nM of spongistatin 1 were compared to controls. The samples were incubated for 10 min. at 30°C and subsequently loaded onto phosphocellulose filter disks (Whatman, Dassel, Germany). The membranes were washed three times with 1.5% phosphoric acid and twice with distilled water. 2 ml of scintillation fluid (Ultima Gold, PerkinElmer) was added to each filter disk and radioactivity was counted with a liquid scintillation counter. Two independent experiments in which triplicate samples were taken within each experiment were performed.

10 Angiogenic *In Vitro* Assays

10.1 Proliferation Assay

1,500 HUVECs were seeded in 96-well-plates and stimulated the next day. Control cells were fixed to determine the initial cell number. After 72 hours of stimulation, cells were fixed and stained with crystal-violet solution (0.5% crystal violet in 20% methanol) for 10 minutes, washed, and air dried. Crystal violet was eluted with 0.1 M sodium citrate in 50% ethanol, and the absorbance was measured at 550 nm with the SUNRISE™ plate reader.

10.2 Migration Assay

HUVECs were seeded in 24-well-plates and grown to confluency. The cell monolayer was scratched with a pipette-tip (generating a wound of approximately 1 mm), washed and incubated over night. Analysis of the wound closure was done by light microscopy using the Axiovert 200 microscope and Imago-QE camera system (Till Photonics, Graefelfing, Germany). For quantification, the migration tool of S.CORE online imaging analysis (S.CO LifeScience, Munich, Germany) was used.

For actin staining, HUVECs were seeded on 0.1% Collagen A-coated glass coverslips. The confluent monolayer was wounded again with a pipette-tip, washed and stimulated for 6 hours. Cells were washed with PBS, fixed in 4% formaldehyde for 15 minutes, and permeabilized with 0.2% Triton X-100 in PBS. After three washes with PBS, cells were stained with rhodamine-conjugated phalloidin for 45 minutes. Another three washes later, coverslips were mounted in PermaFluor mounting medium. Visualization and imaging was done using the confocal microscope LSM 510 Meta.

10.3 Chemotaxis Assay

Measurement of the chemotaxis of spongistatin 1-stimulated HUVECs were done using 'μ-slides Chemotaxis' (IBIDI, Martinsried, Germany). A HUVEC suspension of 5×10^6 cells per ml was seeded as described in the 'μ-slide Chemotaxis' protocol provided. The upper reservoir of the slides contained Endothelial Growth Medium with 10% FCS; the lower reservoir contained medium M199 without FCS, generating a FCS-gradient from 0 to 10% FCS over the seeded HUVECs (Figure IV.3 A). Chemotaxis was observed over 24 hours by live-cell imaging. A time series was collected containing 1 picture every 10 minutes. Cell tracking and analysis was done using the manual tracking plug-in (Fabrice Cordelieres) and the 'Chemotaxis and Migration Tool' (IBIDI) for ImageJ (NIH, Bethesda, MD), as described in μ-slide Chemotaxis protocol (Figure IV.3 B).

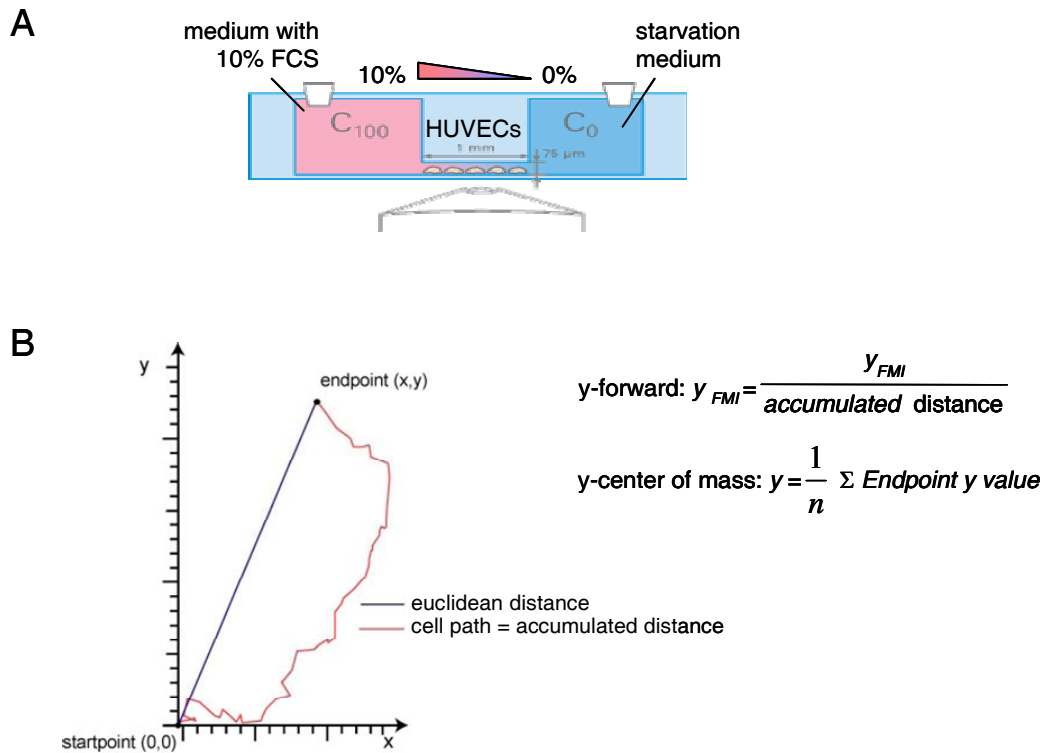


Figure IV.3 The chemotaxis assay on μ -slides.

(A) Design of the chemotaxis slides. (B) Calculation of endothelial cell movement and directionality.

10.4 Tube Formation Assay

MatrigelTM was filled into the lower chambers of 'μ-slide Angiogenesis' wells (IBIDI), and allowed to harden for 30 minutes at 37° C. 12,000 HUVECs/well were seeded on the MatrigelTM and stimulated in triplicates overnight. The level of tube formation was determined by light microscopy and analyzed with the tube formation module of S.CORE analysis (S.CO LifeScience).

11 Angiogenic *Ex/In Vivo* Assays

11.1 Mice

NMRI mice and male C57BL6 mice were purchased from Charles River Laboratories (Sulzfeld, Germany).

11.2 Mouse Aortic Ring Assay

Blocking Solution

BSA	1.0%
Tween 20	0.1%
Triton X-100	0.01%

The abdominal arteries of NMRI mice were prepared, cut into rings and placed on the Matrigel™. Aortic rings were incubated for two days in Endothelial Growth medium prior to stimulation with spongistatin 1. Endothelial cell sprouting was analyzed two days after all untreated rings sprouted.

Additionally, CD31-staining was performed to ensure that sprouted cells are endothelial cells. Therefore, rings were washed one time with PBS and fixed in 1% formaldehyde for 25 minutes at 37° C. Afterwards, rings were shaken overnight at 4° C in PBS, before they were incubated for at least 2 hours in blocking solution at 4° C. Then, rings were incubated for 6 hours with the primary antibody against mouse CD31 (BD Biosciences, San Jose, CA, USA) 1:200 in 1% BSA at 4°C. Next, rings were washed once with PBS before incubating them overnight with the secondary antibody, conjugated to AlexaFluor 488 (1:400 in 1% BSA, Invitrogen) at 4° C. Prior to microscopic observation (LSM 510 Meta), rings were washed at least 3 times with PBS, each for 1 hour at 4°C.

11.3 Mouse Cornea Pocket Assay

The mouse cornea pocket assay was performed in collaboration with Dr. Ivan Ischenko and PD Dr. Christiane J. Bruns from the Department of Surgery, Klinikum Großhadern at the Ludwig-Maximilians-University Munich.

Corneal micropockets were created in C57BL6 mice with a modified von Graefe cataract knife. A micropellet (0.35×0.35 mm) of sucrose aluminium sulfate (Sigma-Aldrich, Steinheim, Germany) coated with Hydron polymer (Sigma-Aldrich, Steinheim, Germany) (10 µl of 12% Hydron in ethanol) containing approximately 80 ng of recombinant human FGF (R&D Systems, Wiesbaden, Germany) was implanted into each corneal pocket, as described (80). Control animals were implanted with pellets containing no growth factor only PBS. The pellet was positioned 1.2-1.4 mm from the corneal limbus. After implantation, erythromycin/ophthalmic ointment was applied to each eye. Spongistatin 1 (in 2% DMSO, 0.9% NaCl) was administered intraperitoneally at a dose of 10 µg/kg daily for 5 days beginning from the first postoperative day (n = 5). The controls received vehicle only (n = 5). The maximal vessel length and clock hours of circumferential neovascularization were measured on the sixth day

after corneal implantation. The length of new vessels in the cornea was measured from the inside margin of vessels around the limbus to the tip of the longest neovascular sprout. The contiguous circumferential zone of neovascularization was measured as clock hours (length of the limbal vessel showing sprouts) with a 360° reticule (where 30° of arc equals 1 clock hour and 1 clock hour further corresponds to 1 mm limbal vessel length).

12 The Orthotopic Pancreas Tumor Model

The orthotopic tumor experiment was performed in collaboration with Dr. Ivan Ischenko and PD Dr. Christiane J. Bruns from the Department of Surgery, Klinikum Großhadern at the Ludwig-Maximilians-University Munich.

12.1 Mice and Cell Line

Female immunodeficient Balb/c nu/nu mice were purchased from Charles River Laboratories (Sulzfeld, Germany). Animal procedures were approved by the regional authorities. The human pancreatic cancer cell line L3.6pl was maintained in Dulbecco's Minimal Essential Medium (Gibco, Invitrogen, Germany), supplemented with 10% fetal bovine serum (Biochrom AG, Berlin, Germany).

12.2 Procedures

L3.6pl human pancreatic cancer cells were injected orthotopically as described previously (81). Briefly, a small left abdominal flank incision was made and the spleen was exteriorized. Tumor cells (8×10^5 in 40 μ L PBS) were injected into the subcapsular region of the pancreas just beneath the spleen. A 30-gauge needle, a 1 ml disposable syringe, and a calibrated pushbutton-controlled dispensing device were used to inject the tumor cell suspension. A successful subcapsular intrapancreatic injection of tumor cells was identified by the appearance of a fluid bleb without intraperitoneal leakage. To prevent such leakage, a cotton swab was held for 1 min over the site of injection. One layer of abdominal wound was closed by suture.

Pancreatic tumors were allowed to become established for 6 days before initiation of treatment. Six days after implantation of tumor cells, mice were randomly assigned to one of the following groups of 10 mice each: 1) daily intraperitoneal administration of spongistatin 1 at a dose of 10 μ g/kg (in 2% DMSO, 0.9% NaCl); 2) daily intraperitoneal administration of vehicle solution for only (in 2% DMSO, 0.9% NaCl).

12.3 Necroscopy

The animals were sacrificed 21 days after the initiation of treatment, when > 50% of the control animals had become moribund. At the time of necropsy, all control and treated mice had developed primary pancreatic tumors. Primary pancreatic tumor size, liver and lymph node metastasis, and local peritoneal carcinosis were assessed. The tumor volume was then calculated using the formula $V = \pi/6 \times a \times b \times c$, where a, b and c represent the length, width, and height of the mass. Tumor lesions were harvested, some were embedded in optimum cutting temperature (OCT) compound (Miles, Inc., Elkhart, IN, USA), snap-frozen in liquid nitrogen, and stored at -80°C , and some were stored in RNAlater at -80°C .

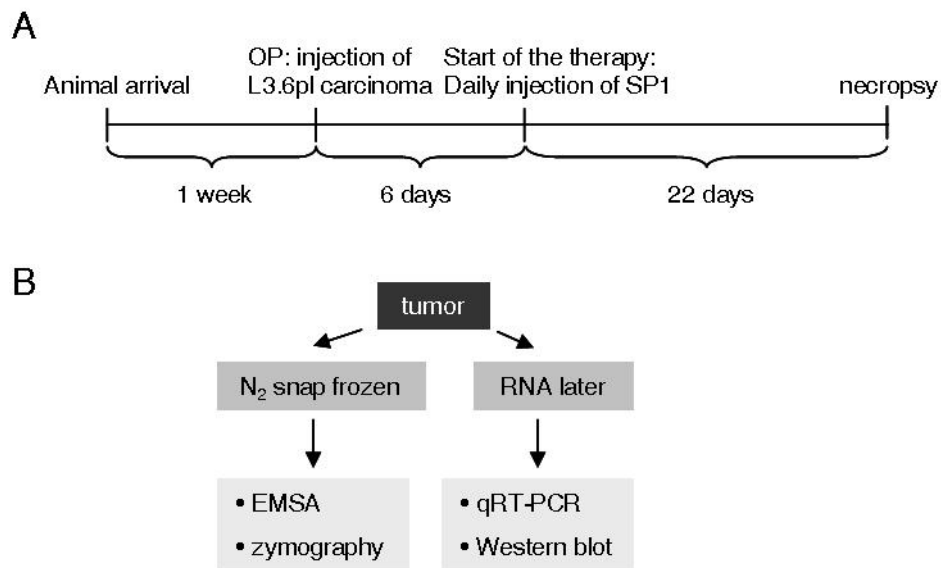


Figure IV.4 The Pancreatic tumor model.

(A) Schematic of the procedures of the orthotopic tumor experiment. SP1, spongistatin 1. (B) In necropsy, tumors were split and sections were either snap-frozen in liquid nitrogen (for EMSA and zymography) or stored in RNA later (for qRT-PCR and Western blot).

13 Quantitative Real-Time PCR

13.1 RNA-Isolation from Tissue Sections

RNA was isolated from RNAlater-stored tumor lesions using the RNeasy Mini Kit (Qiagen, Hilden, Germany). The tissues were homogenized, each about 25 mg in 600 μl RTL buffer (provided with the RNeasy Mini Kit) using the ultraturax homogenizer. Then procedures were followed as default by the RNeasy Mini Kit protocol. Finally, RNA was eluted with RNase-free water, amounts were quantified with the NanoDrop, and integrity of the RNA was controlled on an agarose-gel (18s and 28s rRNA subunits).

13.2 Reverse Transcription

2 µg of total RNA were re-transcribed with random primers and the high capacity cDNA Reverse Transcription Kit (Applied Biosystems, Foster City, CA, USA) for 2 hours at 37°C. The cDNA was stored at -20° C until qRT-PCR.

13.3 Quantitative Real-Time PCR

Quantitative real-time PCR was performed on AB 7300 RealTime PCR system, using TaqMan Universal PCR Mastermix (Applied Biosystems). Probe and primers were from TaqMan gene expression assay (MMP-9: Hs00234579_m1; VEGF: Hs00900054_m1). PCR on GAPDH was used as reference, and serial dilution of cDNA served as standard curves. GAPDH primers were designed using the Primer Express® 2.0 software program (Applied Biosystems). GAPDH forward primer: 5'-GGG AAG GTG AAG GTC GGA GT-3'; reverse primer: 5'-TCC ACT TTA CCA GAG TTA AAA GCA G-3'; probe: 5'-ACC AGG CGC CCA ATA CGA CCA A-3'. Fluorescence-development was analyzed using the AB 7300 system software, and calculation of relative mRNA amount was done according to Pfaffel (82).

14 Zymography

5x Sample Buffer (store at -20° C)

Tris/HCl	312.5 mM, pH 6.8
Glycerol	50%
SDS	5%
Bromphenolblue	1.25%

Developing Buffer

Tris/HCl	50 mM, pH 6.8
NaCl	200 mM
CaCl ₂	5.0 mM
Brij35	0.02%

Protein samples for zymograms were prepared by homogenizing 40 mg of snap-frozen tissue in 400 µl RIPA-buffer without proteinase-inhibitors (IV 6.1 Total Cell Lysates), using the FastPrep homogenizator (2x 20 seconds, 4 m/s) and shredder columns, containing

Lysing Matrix D (MP Biomedicals, Illkirch, France). After centrifugation (14,000 rpm, 15 minutes, 4°C), supernatants were collected and stored in 5x sample buffer at -80° C. Protein concentrations were determined by Bradford analysis and adjusted to equal amounts.

Prior to loading on 10% SDS-Polyacrylamide gels containing 1% gelatin as substrate for MMPs, samples were not boiled, but incubated at room-temperature for 10 minutes. After running, the gel was incubated 30 minutes in 2.5% Triton X-100 to renature gelatinases. Subsequently, gels were equilibrated 30 minutes in developing buffer at room-temperature, before they were incubated in fresh developing buffer at 37° overnight. For quantification, gels were stained 45 minutes in Coomassie staining solution (IV 7.5 Staining Gels and Membranes), and afterwards destained with distilled water. Zymograms were scanned using the Odyssey Infrared Imaging System. Gelatin degradation was quantified with Odyssey scanning software 2.1. The linear range of the measurements was determined by preparing dilution series of the samples. Quantification of gelatinase activity has proven to be linear: $m=1.0098$.

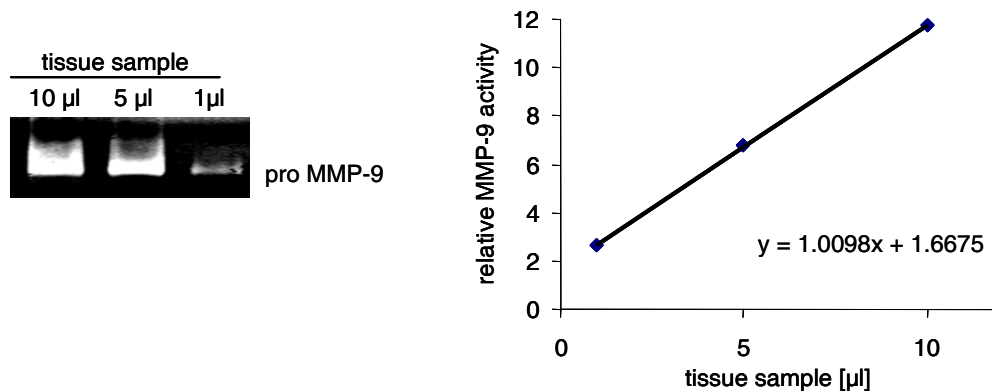


Figure IV.5 Linearity of zymographic quantification of MMP-9 activity.

A dilution series of a tissue sample was run on zymography and quantified by Licor Image Analysis. The linearity of MMP-9 measurements was proven since the slope of the calibration curve was $m=1.0098$.

15 Electrophoretic Mobility Shift Assay

15.1 Extraction of Nuclear Proteins

Extraction Buffer A		Extraction Buffer B	
HEPES, pH 7.9	10 mM	HEPES, pH 7.9	20 mM
KCl	10 mM	NaCl	0.4 mM
EDTA	0.1 mM	EDTA	0.1 mM
EGTA	0.1 mM	EGTA	0.1 mM
DTT	1.0 mM	DTT	1.0 mM
PMSF	0.5 mM	PMSF	0.5 mM
		Glycerol	25%

For nuclear preparation, 40 mg of snap-frozen tissue was homogenized in 400 μ l nuclear extraction buffer A using FastPrep homogenization system. Tissues and buffer A were filled into tubes containing Lysing Matrix D and homogenized 20 seconds with 4m/s speed in FastPrep. After centrifugation (1,500 rpm, 5 minutes, 4° C) supernatants were discarded and sediments were incubated in fresh buffer A containing 0.625% Nonidet NP-40 for 15 minutes. Probes were centrifuged (14,000 rpm, 1 minute, 4° C), supernatants removed, and pellets incubated for 30 minutes under shaking at 4° C in 40 μ l nuclear extraction buffer B. After centrifugation (14,000 rpm, 5 minutes, 4° C), supernatants were collected and frozen at -80° C. Protein concentrations were determined by Bradford assay (IV 6.1 Protein Quantification).

15.2 Electrophoretic Mobility Shift Assay

5x Binding Buffer		Loading Buffer	
Tris/HCl	50 mM	Tris/HCl	250 mM
NaCl	250 mM	Glycerol	40%
MgCl ₂	5.0 mM	Bromphenolblue	0.2%
EDTA	2.5 mM		
Glycerol	20%		

Transcription factor-specific oligonucleotides were 5' end-labeled with [γ ³²P]-ATP using the T4 polynucleotide kinase. Oligonucleotides for HIF-1 α with the consensus sequence 5'-TCT GTA CGT GAC CAC ACT CAC CTC-3' were purchased from Santa Cruz Biotechnology, Inc. 20 μ g protein were incubated with 2 μ g poly(dIdC) and 3 μ l of freshly prepared reaction buffer for 10 minutes at room temperature. The reaction buffer consisted of 450 μ l of 5x binding buffer, 50 μ l Gel loading buffer, and 1 mM DTT. The binding-reaction was started by adding 1 μ l of the radioactive oligonucleotide and carried out for 30 minutes at room-temperature. The protein-oligonucleotide complexes were separated by gel electrophoresis (Mini-Protean III, BioRad) with 0.25 x TBE buffer at 100 V for 60 minutes using non-denaturing polyacrylamide gels (5% PAA, 20% glycerol). After electrophoresis, gels were exposed to Cyclone Storage Phosphor Screens (Canberra-Packard, Schwadorf, Austria) for 24 hours, followed by analysis with a phosphor imager station (Cyclone Storage Phosphor System, Canberra-Packard).

16 Statistical Analysis

Statistic analyses were performed with SigmaStat version 3.5 statistic software (Systat Software Inc., Richmond, CA). Data were expressed as mean value \pm S.E.M., and analyzed using One Way ANOVA, Student's *t*-test, or Rank On Sum-test. $P < 0.05$ was considered as statistical significant *, $p < 0.05$; **, $p < 0.01$; ***, $p < 0.001$.

V. RESULTS

A Spongistatin 1 Exerts Strong Impact on Pancreatic Tumor Progression and Metastasis *In Vivo*

1 Orthotopic Tumor Model

The orthotopic tumor experiment was performed in collaboration with Dr. Ivan Ischenko and PD Dr. Christiane J. Bruns from the Department of Surgery, Klinikum Großhadern at the Ludwig-Maximilians-University Munich.

1.1 Spongistatin 1 Inhibits Pancreatic Tumor Progression

In the orthotopic nude mouse model, the efficacy of spongistatin 1 on L3.6pl pancreatic tumor *in vivo* was demonstrated. Six days after tumor implantation, mice were treated daily with spongistatin 1 or solvent i.p. for 22 days. During this time, tumor size was calculated by palpation through the skin. 15 days after tumor implantation, tumor growth strongly increased in the control animals. This tumor progression was significantly reduced by treatment with spongistatin 1 (Figure V.1).

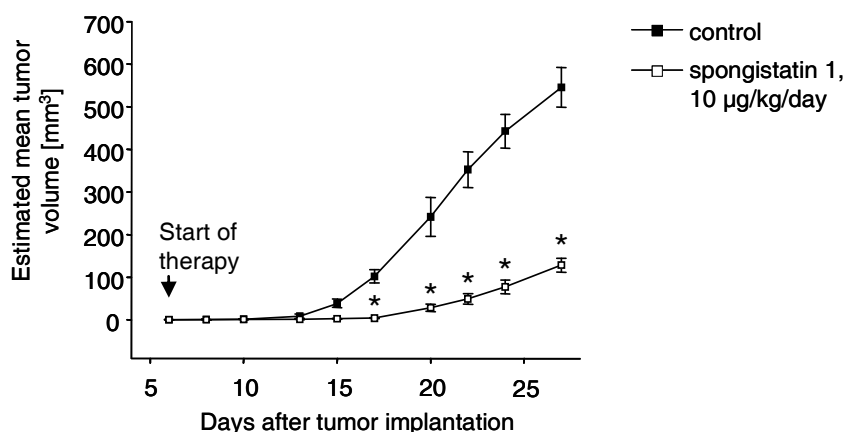


Figure V.1 Spongistatin 1 inhibits pancreatic tumor progression.

L3.6pl human pancreatic cancer cells were injected into the pancreas of nude mice. Six days after implantation of tumor cells, mice were either treated (i.p., daily) with spongistatin 1 (10 µg/kg; n=10) or vehicle (2% DMSO, in NaCl, control; n=10). Progression of tumor volume was estimated by palpation through the skin. The diagram shows time course of tumor growth in vehicle (control) and spongistatin 1-treated animals. Data are shown as mean \pm S.E.M., *p<0.05, student's t-test.

1.2 Necropsy Reveals Strong Efficacy of Spongistatin 1 on Pancreatic Tumor

At the day of necropsy, mice were finally weighed, and tumor volume and weight were assessed. Treatment with spongistatin 1 significantly reduced tumor volume, as well as tumor weight compared to animals that have received vehicle treatment only (Figure V.2). Moreover, spongistatin 1 did not cause a reduction of body weight (vehicle treated group $18.6 \text{ g} \pm 2.46$; spongistatin 1 treated group $19.0 \text{ g} \pm 2.18$ at time of necropsy).

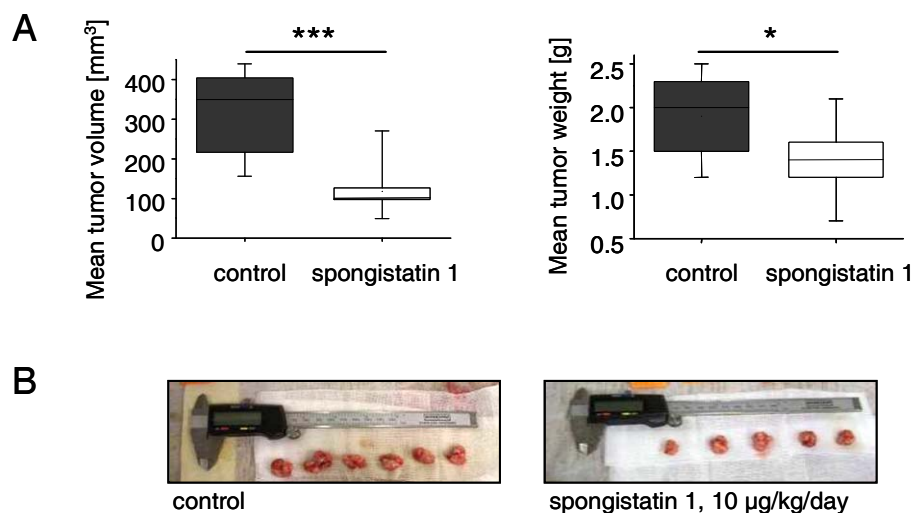


Figure V.2 Necropsy data.

(A) Tumor volume and tumor weight were quantified at time of necropsy (day 22 after initiation of the therapy), as described in 'Material and Methods'. Treatment with spongistatin 1 i.p. strongly reduced both tumor volume and tumor weight. Bars, the mean \pm S.E.M. of all pancreases, *** $p < 0.001$, * $p < 0.05$, student's t-test. (B) Representative photos of pancreatic tumors at time of necropsy (day 22 after initiation of the therapy).

1.3 Metastasis is Significantly Reduced by Spongistatin 1

The primary tumors were removed, and the liver and the surrounding tissue were visually scanned for metastases and peritoneal carcinosis (nodules $\geq 1 \text{ mm}$ in diameter). Spongistatin 1-treatment significantly reduced the incidence of metastases: all control animals, but only three of the spongistatin 1-treated mice had incidences of metastases in lymph nodes. Likewise, two of nine spongistatin 1-treated mice developed liver metastases compared to nine of ten mice in the control group. Additionally, peritoneal carcinosis was reduced to half, when mice were treated with spongistatin 1 (Table V.1).

Table V.1 Treatment with spongistatin 1 decreased the incidences of metastases.

In necropsy, regional lymph nodes and liver were visually examined for metastases (visible nodules ≥ 1 mm in diameter). In addition, incidence of peritoneal carcinosis was determined. Incidences are presented as number of animals with metastases per total number of animals.

Treatment	Metastases		
	Lymph nodes	Liver	Peritoneal carcinosis
control	10/10	9/10	9/10
10 $\mu\text{g}/\text{kg}/\text{day}$ spongistatin 1	3/9	2/9	5/9

2 The Influence of Spongistatin 1 on Hypoxia Inducible Factor 1 α

2.1 Stabilization of HIF-1 α Is Strongly Reduced by Spongistatin 1 *In Vitro*

Hypoxia-induced signaling *via* stabilization of the transcription factor HIF-1 α is strongly associated with tumor growth and the formation of metastases. Further, the inhibition of HIF-1 α was shown to reduce tumor progression (83). Since it was previously demonstrated that tubulin-binding drugs inhibit HIF-1 α signaling *in vitro*, the impact of spongistatin 1 on HIF-1 α stability was investigated in pancreatic L3.6pl cells.

Stimulation with CoCl_2 mimics hypoxia, by stabilizing the transcription factor HIF-1 α (84). In Western blot analysis, incubation of L3.6pl cells with 100 nM CoCl_2 resulted in increased amounts of HIF-1 α in comparison to control cells. Co-stimulation with 1.0 nM spongistatin 1 inhibited clearly CoCl_2 -induced stabilization of HIF-1 α (Figure V.3 A).

2.2 Spongistatin 1 Has No Influence on HIF-1 α Activity *In Vivo*

Due to the importance of hypoxia-mediated signaling in tumor progression, pancreatic tumor sections were investigated for effects of spongistatin 1 on HIF-1 α activity *in vivo*. From all tissue samples, nuclei were isolated in order to investigate the DNA-binding activity of HIF-1 α to its consensus sequence by EMSA. Quantification of EMSA-studies revealed no significant difference in HIF-1 α -binding activity between the control group and the spongistatin 1 group (Figure V.3 B). Further, the mRNA levels of VEGF were quantified as indicator for HIF-1 α activity, since VEGF is the most important angiogenic factor regulated by HIF-1 α . However, there were no significant differences in both treatment-groups on VEGF mRNA levels (Figure V.3 C).

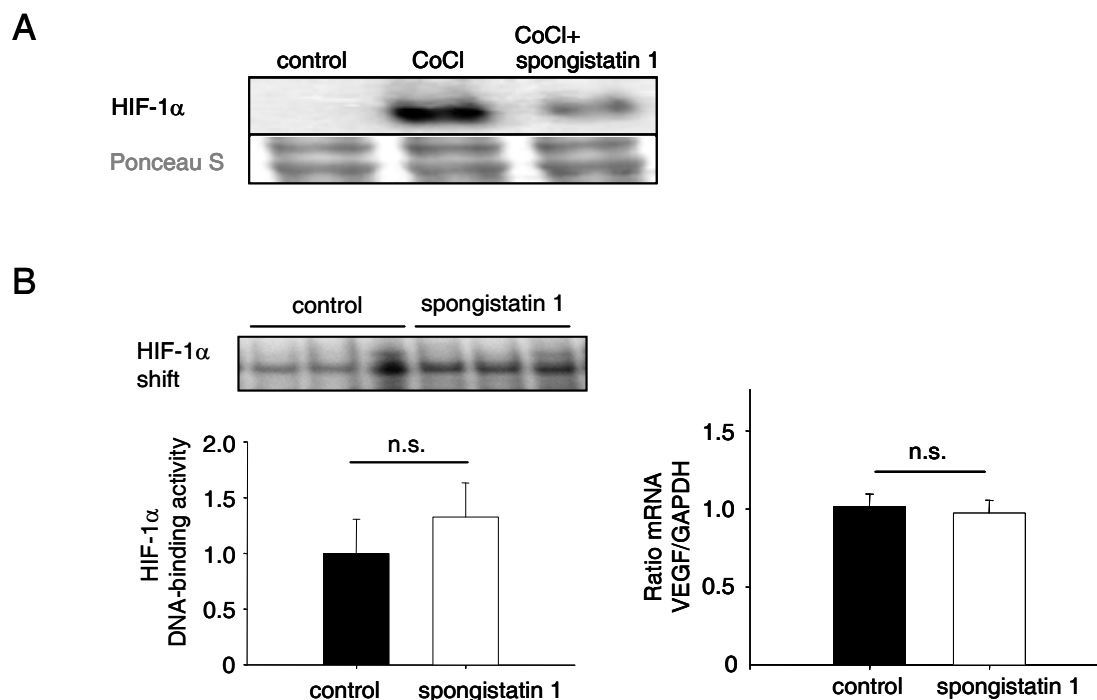


Figure V.3 Spongistatin inhibits HIF-1 α activity *in vitro*, but not *in vivo*.

(A) Stimulation of pancreatic L3.6pl cells with 100 nM CoCl₂ for 4 hours resulted in stabilization of HIF-1 α . Co-stimulation of spongistatin 1 (1.0 nM) reduced CoCl₂-induced stabilization of HIF-1 α . Ponceau S-staining proved equal protein loading. (B) EMSA of tumor tissue sections revealed that spongistatin 1 had no significant impact on the DNA-binding activity of HIF-1 α (left panel). Analysis of HIF-1 α transcription product VEGF mRNA in tumor tissue sections (right panel) has shown no influence of spongistatin 1 on HIF-1 α activity *in vivo*. Bars, the mean \pm S.E.M. of all pancreases, $p > 0.05$, n.s., not significant, student's *t*-test.

3 Matrix Metalloproteinase 9 Is Reduced by Spongistatin 1 *In Vivo*

3.1 Reduction of MMP-9 mRNA and Protein Levels by Spongistatin 1

In many tumors, including pancreatic cancer, the overexpression of MMPs is correlated with metastasis. Quantitative real-time PCR-analysis of tissue samples from the pancreatic *in vivo* experiment revealed that the amount of MMP-9 mRNA was significantly reduced in animals treated with spongistatin 1, which is well in line with the reduced incidences of metastases (Figure V.4 A).

A reduction of MMP-9 mRNA-level is supposed to result in reduced protein-levels of MMP-9. Thus, MMP-9 protein was quantified by Western blot analysis and normalized to β -actin (Figure V.4B). Level of MMP-9 protein were clearly reduced (31.52% vs. control animals), in the tissues of spongistatin 1-treated mice. The expression of MMP-2 was very low, and even balancing up-regulation of MMP-2 in spongistatin 1-animals could not be detected.

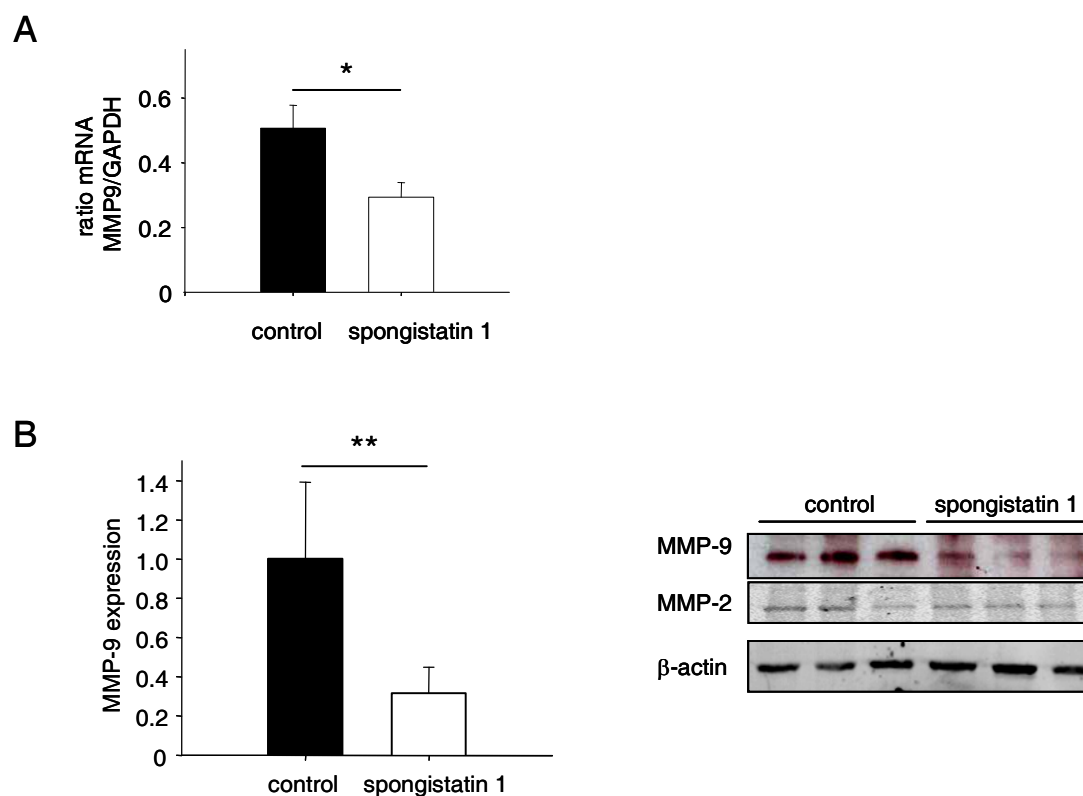


Figure V.4 Spongistatin 1 reduces MMP-9 mRNA and protein level.

(A) Quantitative real-time PCR analysis of tumor tissues showed significant reduced MMP-9 mRNA level in tissues of spongistatin 1-treated animals as compared to vehicle-treated (control) animals. (B) Quantification of MMP-9 protein level via Western blot analysis of all animals confirmed reduced amounts of MMP-9 in spongistatin 1-treated mice. MMP-9-protein was normalized to β -actin, and MMP-9 expression in control animals was set as 1.0. The blot shows a representative experiment based on $n=3$ tissue samples, respectively. Bars, the mean \pm S.E.M. of all pancreases, * $p<0.05$, ** $p<0.01$, student's t -test.

3.2 Zymography Reveals Reduced MMP-9 Activity in Spongistatin 1-Treated Mice

The clinically relevant factor of MMP-9 quantification in tumor tissues is not the level of MMP-9 mRNA or protein, but the amount of enzymatic active MMP-9. Thus, gelatinase-activity of MMP-9 in the tumor sections was determined by zymography. MMPs exert their enzymatic activity in extracellular space, degrading gelatin and collagen elements of the extracellular matrix, and are therefore quite stable in their activity. In zymography, MMPs can be separated under non-denaturing conditions in a modified SDS-PAGE. After refolding, the MMPs degrade the gelatin cast in the separation gel. Coomassie-staining of the gels reveals the sites of gelatinase-activity by means of unstained areas.

Comparing an MMP-marker (kindly donated by Dr. Christian Ries) with a tissue sample identified MMP-9 to be the most prominent MMP in the pancreatic tumor, whereas detection of MMP-2 was marginal (Figure V.5 A). Molecular weights of MMPs can vary, since they are cell type- and stimulus-specific posttranslational modified (85). Zymography of tumor tissue

showed a reduction of MMP-9 gelatinase-activity to 71.1% in the tumors of spongistatin 1-treated mice as compared to untreated mice (Figure V.5 B).

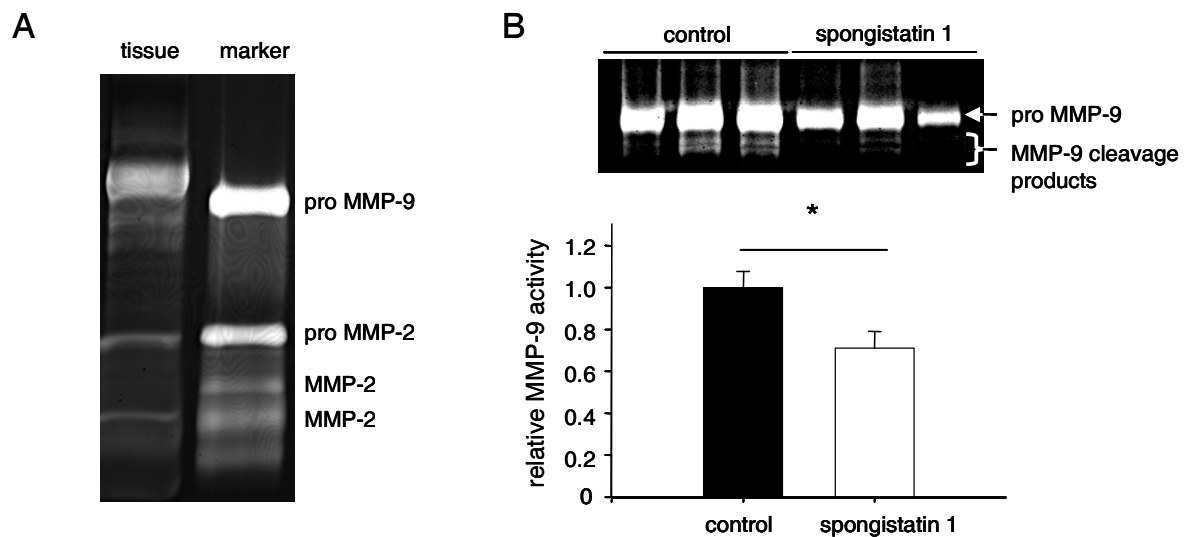


Figure V.5 MMP-9 gelatinase activity is reduced in spongistatin 1-treated mice.

(A) Zymogram of a tissue sample (tissue) and a well-characterized MMP-marker. Posttranslational modifications results in a higher molecular weight of the MMP-9 band in the tissue sample compared to pro-MMP-9 in the marker. Also small amounts of proMMP-2 and MMP-2 could be detected in the tissue sample. (B) The zymogram shows one representative analysis of tumor tissue sections (n=3) of both control and spongistatin 1-treated mice. Bars (mean ± S.E.M.) represent the densitometric analysis of MMP-9 activity of all control (n=10) or spongistatin1-treated tumor tissues (n=9). MMP-9 activity of tissue samples of untreated mice was set as 1. Bars, the mean ± S.E.M. of tissue sections of all animals. * $p < 0.05$, student's *t*-test.

B Effects of Spongistatin 1 on Angiogenesis *In Vitro* and *In Vivo*

4 Disassembly of Microtubules

4.1 Spongistatin 1 Disassembles Microtubules in Endothelial Cells

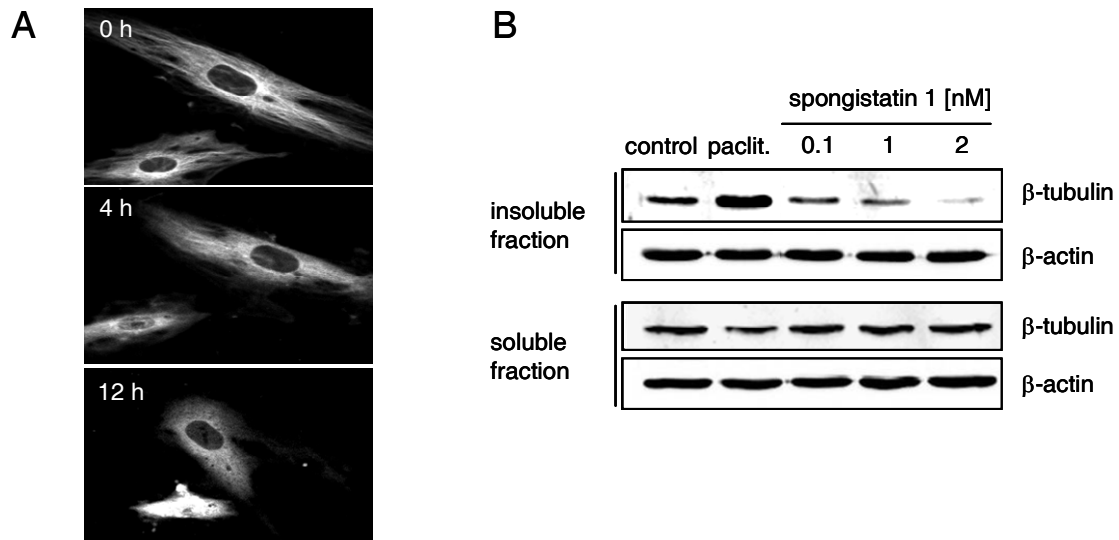


Figure V.6 Spongistatin 1 causes time and dose-dependent disassembly of microtubules. (A) Live cell imaging: GFP-tubulin transfected HUVECs were stimulated with 2.0 nM spongistatin 1 for 16 hours. The clear structures of microtubules at the beginning of the record (0h) slowly dispersed with prolonged spongistatin 1-incubation (4h and 12h). (B) Cell lysates of paclitaxel (paclit.) and spongistatin 1-stimulated HUVECs were separated in PIPES buffer-soluble and -insoluble fractions. Using an antibody against β -tubulin, tubulin heterodimers were detected in the soluble fraction and polymerized microtubules in the insoluble fraction. Incubation with spongistatin 1 reduced polymerized microtubules dose-dependently as judged by the decreasing amounts of β -tubulin in the PIPES-insoluble fraction, whereas paclitaxel (1 μ M) increased microtubules polymerization. The equality of protein loading was controlled by detection of β -actin.

To verify microtubule-depolymerizing properties of spongistatin 1 in endothelial cells, two different approaches were pursued to characterize the impact of spongistatin 1 on the tubulin cytoskeleton of HUVECs. First, live cell imaging of GFP-tubulin transfected HUVECs, incubated with 2.0 nM spongistatin 1, was performed. Time-lapse microscopy of these cells documented the disassembly of the microtubules by spongistatin 1 over 16 hours. The GFP-signal showed clearly structured microtubules in the beginning of the record. With increased period of spongistatin 1-stimulation, microtubules collapsed and only diffuse GFP-signals all over the cell were detectable (Figure V.6 A).

Since the expression of recombinant proteins like GFP-tubulin is likely to evoke artifacts, the disassembly of the microtubules by spongistatin 1 was also investigated in non-transfected HUVECs. Therefore, endothelial cells were incubated for 4 hours with different

concentrations of spongistatin 1 (0.1 nM, 1.0 nM, and 2.0 nM) and paclitaxel (1.0 μ M, serving as crosscheck), respectively. After incubation, cells were fractionated in two fractions: one containing soluble tubulin heterodimers (PIPES-soluble fraction), and one containing polymerized microtubules (PIPES-insoluble fraction). Paclitaxel, which is a microtubule-stabilizing drug, caused an increase of tubulin in the fraction of polymerized microtubules, as expected. In contrast, incubation with spongistatin 1 induced a dose-dependent decrease of tubulin in this fraction as a result of microtubules disassembly (Figure V.6 B).

4.2 Spongistatin 1 Influences the Morphology, the Arrangement of Mitochondria, and Membrane Trafficking of Endothelial Cells

The inhibition of microtubules - a central element of the cytoskeleton - by spongistatin 1 is supposed to entail structural and functional changes in the endothelial cell. Under control conditions, endothelial cells are spindle shaped. After incubating a confluent HUVEC-monolayer with spongistatin 1 (1.0 nM, 8 hours), endothelial cells rounded up and added the appearance of a cobblestone pavement to the monolayer (see Figure V.7 A).

Microtubules are essential for the intracellular arrangement of organelles. Mitochondria arrangement in spongistatin 1-stimulated cells was investigated by live cell imaging. In the beginning of the record, mitochondria were distributed over the whole cell. Prolonged incubation with spongistatin 1 (1.0 nM, 3 hours) induced translocation of the mitochondria near the nucleus (Figure V.7 B).

Besides the arrangement of mitochondria, also membrane trafficking and vesicle transport are microtubule-dependent. To investigate the influence of spongistatin 1 on the membrane flow of endothelial cells, HUVECs were incubated with a membrane-integrating dye. Under control conditions, HUVECs took up the dye within 15 minutes, and the dye could be detected in vesicular compartments in the cell. In spongistatin 1 pre-incubated HUVECs (1.0 nM, 3 hours) the membrane-dye remained distributed over the cytoplasmic membranes. Thus, cells were no longer able to incorporate the dye, indicating that the membrane trafficking was discontinued upon spongistatin 1-treatment (Figure V.7 C).

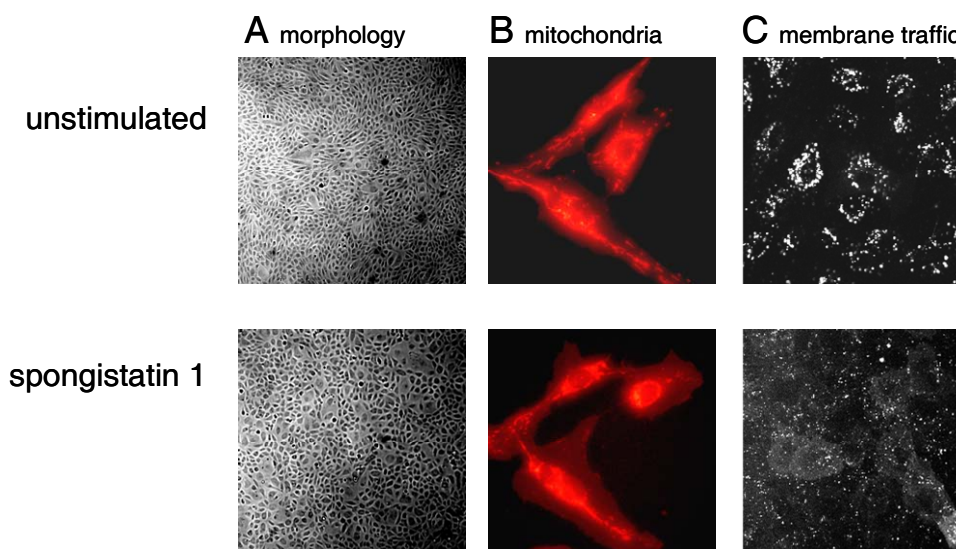


Figure V.7 Spongistatin 1 influences the morphology of HUVECs.

(A) In a confluent monolayer, HUVECs were spindle-shaped under control conditions. After spongistatin 1-treatment (1.0 nM, 8 hours), cells round up and the monolayer became a cobblestone structure. (B) In the beginning of spongistatin 1-treatment of HUVECs (1.0 nM, 0 hours), mitochondria were distributed in the whole cytoplasm, whereas prolonged stimulation (1.0 nM, 3 hours) caused a perinuclear localization of mitochondria. (C) Membrane trafficking in non-stimulated HUVECs was determined by accumulation of an externally applied membrane dye in intracellular vesicles. Spongistatin 1 (1.0 nM, 3 hours) reduced membrane trafficking, since most of the membrane dye remained on the cell surface.

5 Cytotoxicity, Cell Cycle, and Apoptosis

5.1 Cytotoxicity of Spongistatin 1 in Endothelial Cells

The cytotoxicity of spongistatin 1 was measured in a cell viability assay. Functional intact cells are able to reduce metabolically the chromophore resazurin to resorufin. Resorufin emits fluorescence at 590 nm, and thus can be quantified fluorometrically. Confluent and proliferating HUVECs were stimulated with increasing concentrations of spongistatin 1 for 24 hours. Resazurin was added to the medium and after 4 hours of incubation the conversion of resazurin to resorufin was determined. Proliferating cells showed a significant reduction of metabolic activity at a concentration as low as 5.0 nM spongistatin 1, indicating an acute cytotoxicity of spongistatin 1. In confluent HUVEC, metabolic activity was significantly reduced starting from 50.0 nM spongistatin 1. Thus, confluent HUVECs can tolerate a 10-fold higher concentration of spongistatin 1 than proliferating cells (Figure V.8).

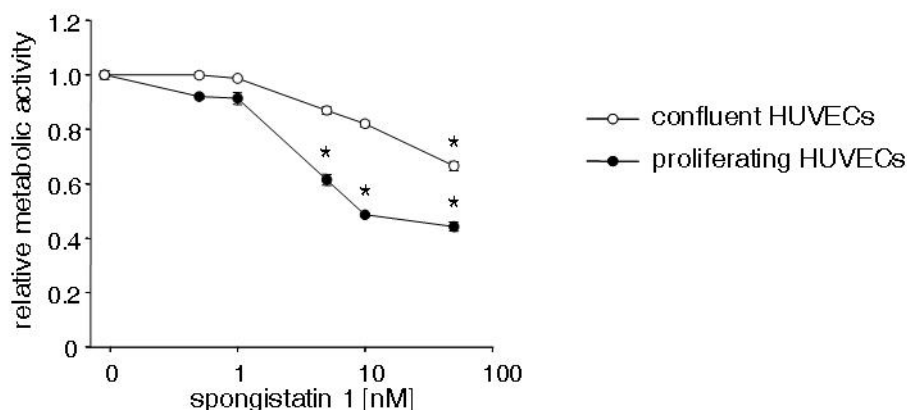


Figure V.8 Determination of the cytotoxicity of spongistatin 1.

The conversion of resazurin to resorufin is an indicator of the metabolic activity and therefore the viability of cells. HUVECs showed a dose-dependent inhibition of metabolic activity upon spongistatin 1-treatment. Apparently, proliferating HUVECs are more sensitive towards cytotoxic effects of spongistatin 1 than confluent cells. Data are expressed as the mean \pm S.E.M., * $p < 0.05$, One Way ANOVA.

5.2 Spongistatin 1 Induces Cell Cycle Arrest and Apoptosis

Tubulin antagonists disrupt the mitotic spindle of dividing cells, and thereby cause cell cycle arrest in the G_2 to M phase transition, which sooner or later results in apoptosis (III 4.3.1 The Mitotic Spindle). By staining the chromatin of endothelial cells with the intercalating agent propidium iodide, cell cycle phases and DNA-fragmentation can be determined in flow cytometry, since the fluorescence of propidium iodide depends on DNA-condensation, DNA-fragmentation, and the state of chromosome replication. Thus, in flow cytometric measurements, each cell cycle phase generates a characteristic peak which can be quantified. (Figure V.9 A).

Incubation with spongistatin 1 caused a G_2 to M-phase arrest in HUVECs, as expected. Starting from a concentration of 1.0 nM spongistatin 1, significantly more cells were in G_2/M phase (Figure V.9 B, left panel). The sub- G_1 peak presents apoptotic cells. Quantification of this peak revealed a significant increase of apoptotic cells at a concentration as low as 2.0 nM spongistatin 1 (Figure V.9 B, right panel). Compared to the established tubulin-binding drugs vinblastine, paclitaxel, or CA4P, which caused G_2/M -phase arrest and apoptosis, too, effects of spongistatin 1 occurred at concentrations well below (Figure V.9 C).

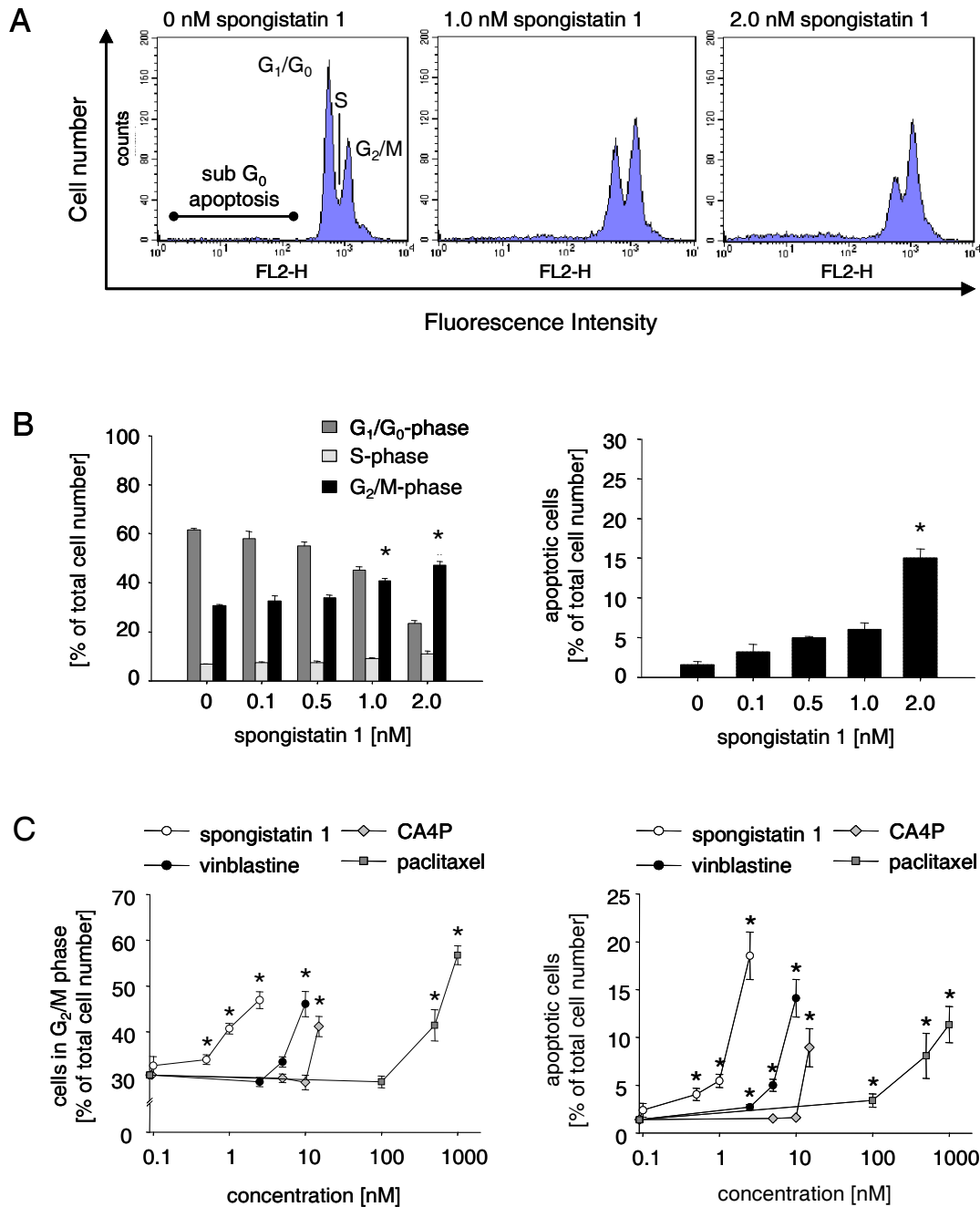


Figure V.9 Flow Cytometric Cell Cycle Measurements.

(A) FACS data files of different spongistatin 1-treatment groups. Cell cycle phases are determined and quantified by characteristic fluorescence peaks of the DNA intercalating compound propidium iodide. (B) Spongistatin 1-stimulated HUVECs revealed a dose-dependent G₂/M phase arrest starting from 1.0 nM spongistatin 1. Apoptosis was significantly increased at a concentration of 2.0 nM spongistatin 1. (C) Comparison of spongistatin 1 with the established tubulin antagonists vinblastine, CA4P, and paclitaxel revealed spongistatin 1 to induce G₂/M arrest and apoptosis most effectively. Data are expressed as the mean \pm S.E.M., * p <0.05, One Way ANOVA.

6 Effects of Spongistatin 1 on Endothelial Proliferation

6.1 Spongistatin 1 Strongly Inhibits Endothelial Proliferation *In Vitro*

In the angiogenic *in vitro* proliferation assay, endothelial cells were seeded in low density at day -1, stimulated with the respective compound at day 0, and proliferation was evaluated at day 3 (72 hours) by staining the cells with crystal-violet (Figure V.10 A). The staining intensity of crystal-violet is proportional to cell proliferation. Relative proliferation was related to the number of cells at day 0. Proliferation of control cells without stimulus was set as 100% proliferation.

Astonishingly, proliferation of HUVECs was already strongly inhibited at the very low concentration of 100 pM spongistatin 1, whereas more than 25 to 500-time higher concentrations of vinblastine (2.5 nM), CA4P (7.5 nM), or paclitaxel (50.0 nM) were needed to inhibit endothelial proliferation (Figure V.10 B).

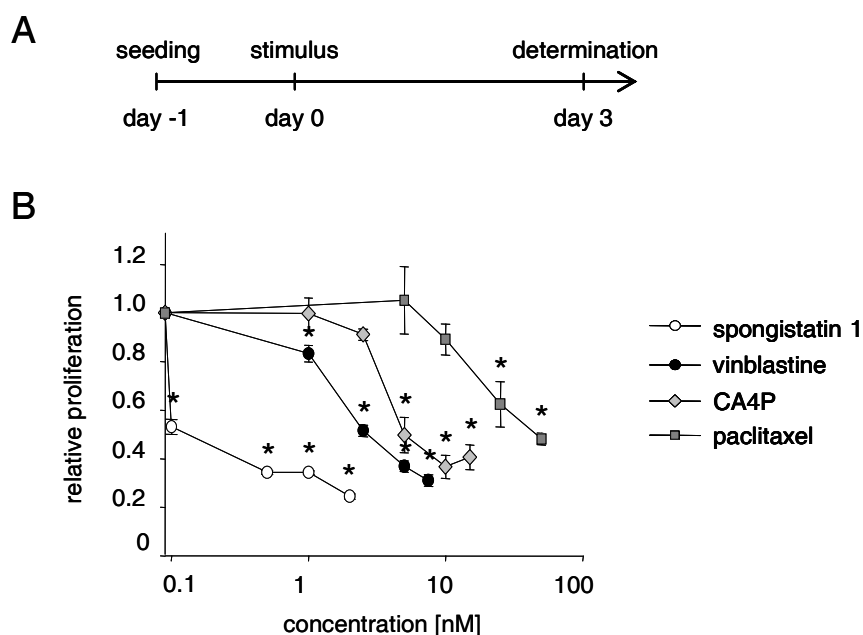


Figure V.10 *In Vitro* Proliferation Assay.

(A) In the proliferation assay, HUVECs were stimulated for 3 days (72 hours) with increasing concentrations of spongistatin 1, vinblastine, CA4P, and paclitaxel. (B) Spongistatin 1 strongly inhibited proliferation at a concentration of 100 pM, whereas 25-500-time higher concentrations of the other investigated tubulin antagonists were needed. Data are expressed as the mean \pm S.E.M., * $p < 0.05$, One Way ANOVA.

reduced the FCS-induced phosphorylation of AKT at T308 and S473. Thus, activation of AKT seems to be inhibited by spongistatin 1-treatment.

7 The Impact of Spongistatin 1 on Endothelial Migration

7.1 Migration of HUVECs Is Inhibited by Spongistatin 1

The influence of spongistatin 1 on endothelial cell migration was investigated in a scratch assay. Due to their function as vascular barrier, endothelial cells have the natural impulse to close gaps in the united cell structure. Thus, wounding an endothelial monolayer with a pipette-tip stimulates the cells to migrate into cell-free area and to close the wound.

Endothelial cells in culture medium closed the inflicted scratch overnight (positive control, 100% migration), whereas wound closure was completely abolished, when cells were incubated in starvation medium (negative control, 0% migration). The addition of spongistatin 1 to the culture medium effectively inhibited wound closure in a dose-dependent manner with an IC_{50} of approximately 1.0 nM, and was therewith again more potent than the established tubulin-antagonists vinblastine (7.5 nM), C4AP (10.0 nM), or paclitaxel (25.0 nM) (Figure V.12 A). The degree of wound closure was quantified by using a migration software tool, which detects and quantifies the cell-free area (Figure V.12 B).

7.2 Spongistatin 1 Deregulates the Arrangement of F-Actin in HUVECs

The actin cytoskeleton is essential in generating cellular protrusions. Hence, alterations in F-actin organization could be expected in cells that are inhibited in migration. F-actin in growth factor deprived cells (starvation medium) was organized in cortical rings and lamellipodia only barely existed (Figure V.12 C, left panel). In contrast, F-actin in migrating HUVECs (culture medium) was arranged in fibers in the cell body and lamellipodia at the leading edge. Both were directed towards the wound (Figure V.12 C, middle panel). Spongistatin 1-treated cells exhibited the characteristics of F-actin arrangement in both migrating and non-migrating cells. Actin fibers in the cell body and cortical rings were formed. Furthermore, the appearance of lamellipodia was reduced upon spongistatin 1-treatment (Figure V.12 C, right panel).

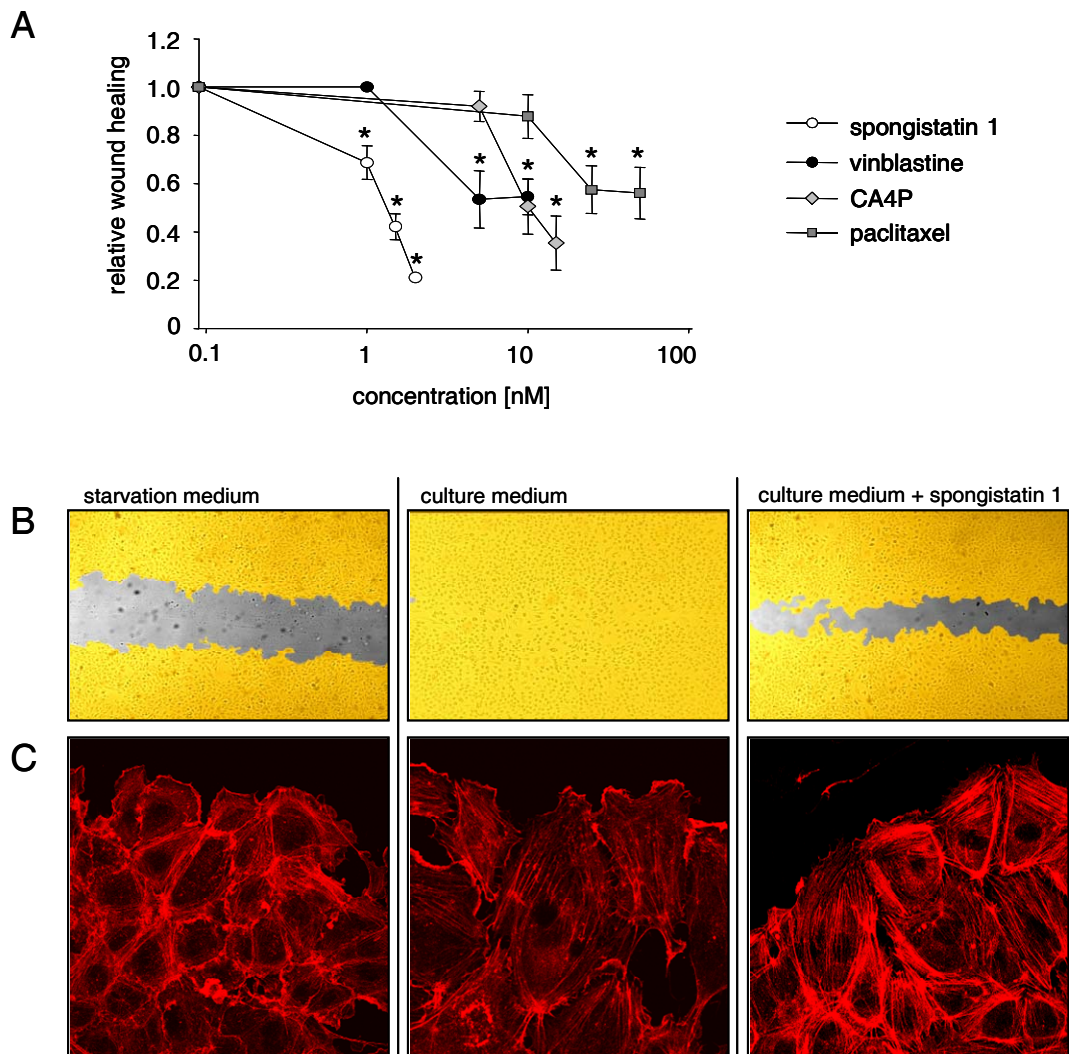


Figure V.12 Spongistatin 1 inhibits migration of HUVECs.

(A) Spongistatin 1, vinblastine, CA4P, and paclitaxel inhibited wound closure of a scratched HUVEC monolayer in a dose-dependent manner. Data are expressed as the mean \pm S.E.M., $*p < 0.05$, One Way ANOVA. (B) Representative images of the quantification of wound healing (S.CORE image analysis). Endothelial cells are colored in yellow; the cell-free area is marked in grey. (C) Actin-cytoskeleton (red) in migrating HUVECs: under spongistatin 1-treatment, the formation of lamellipodia is reduced, and the formation of cortical rings is increased, compared to control cells in culture medium without spongistatin 1.

7.3 The Chemotaxis of Endothelial Cells is Inhibited by Spongistatin 1

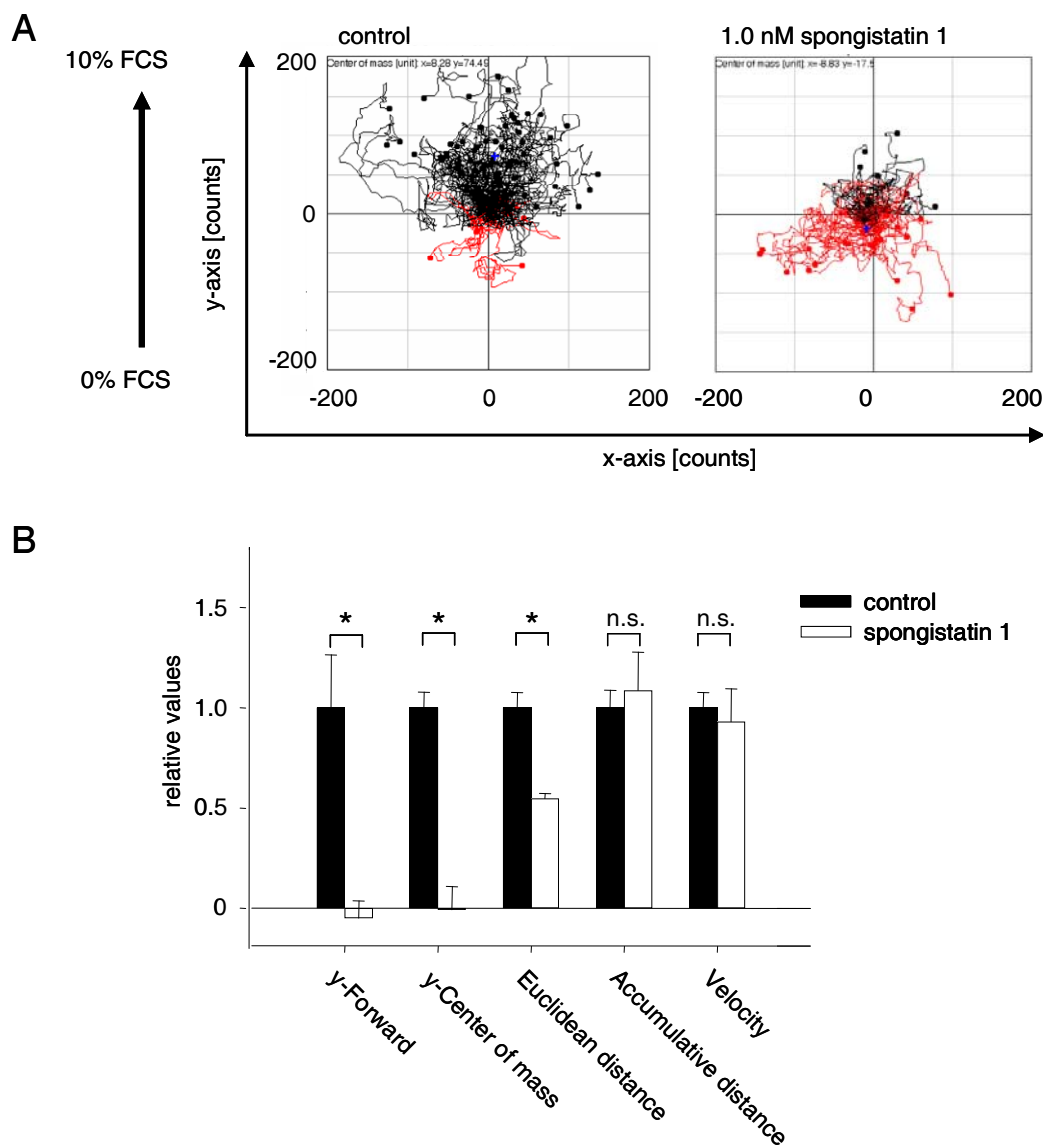


Figure V.13 Spongistatin 1 reduces directional migration in HUVECs.

(A) Track plots of control cells and spongistatin 1-treated cells of representative chemotaxis experiments are shown. The starting point of each single cell is placed in the center of the diagram. Tracks of cells, moving towards FCS are displayed in black, the tracks of cells without attraction to FCS in red. The blue point symbolizes the y-center of mass. (B) Analysis of y-forward (y-forward migration index of each cell), y-center of mass (y-value center of mass of all tracking endpoints), Euclidean distance (direct distance between starting point and endpoint), accumulated distance, and velocity (pixel/slide), means of control cells were set as 1.0. Accumulative distance and velocity were not significantly affected by spongistatin 1, indicating that not migration itself, but directionality was inhibited. Bars, the mean \pm S.E.M, * p <0.05, n.s., not significant, student's t -test.

The influence of spongistatin 1 on directed migration of endothelial cells was investigated in a chemotaxis assay. In this assay, HUVECs were exposed to a serum-gradient ranging from 0% FCS to 10% FCS. Untreated HUVECs were attracted by FCS and moved along a serum-

gradient. Their directionality to the serum was expressed in y -values, since the gradient was set up along the y -axis of the chemotaxis-chamber (Figure IV.3 and Figure V.13 A). The values of control HUVECs were set as 1.0. Thus, the migration index of each single cell in FCS gradient referred as 'y-forward' was 1.00 ± 0.264 and center of mass of all tracking endpoints in FCS gradient referred as 'y-center of mass' was 1.00 ± 0.078 in untreated HUVECs. In contrast, spongistatin 1-treated cells were reduced in their directionality for the FCS gradient, which is reflected in their values for y -forward (-0.049 ± 0.087) and y -center of mass ($-7.344 \cdot 10^{-3} \pm 0.117$).

Besides the directionality for the FCS-gradient, single parameters of chemotactic migration were evaluated. The Euclidean distance is the direct distance between starting point and endpoint of a cell-track and was reduced to half (0.548 ± 0.024) by treatment with 1.0 nM spongistatin 1. This finding is well corresponding to spongistatin 1 IC_{50} -values in the wound-healing assay (Figure V.12 A). Astonishingly, accumulative distance and velocity were not reduced upon treatment with spongistatin 1, indicating that spongistatin 1 does not disrupt cellular movement itself (chemokinesis), but the ability of HUVECs for directional migration (Figure V.13 B).

7.4 Spongistatin 1 Seems to Have No Influence on MTOC-Orientation

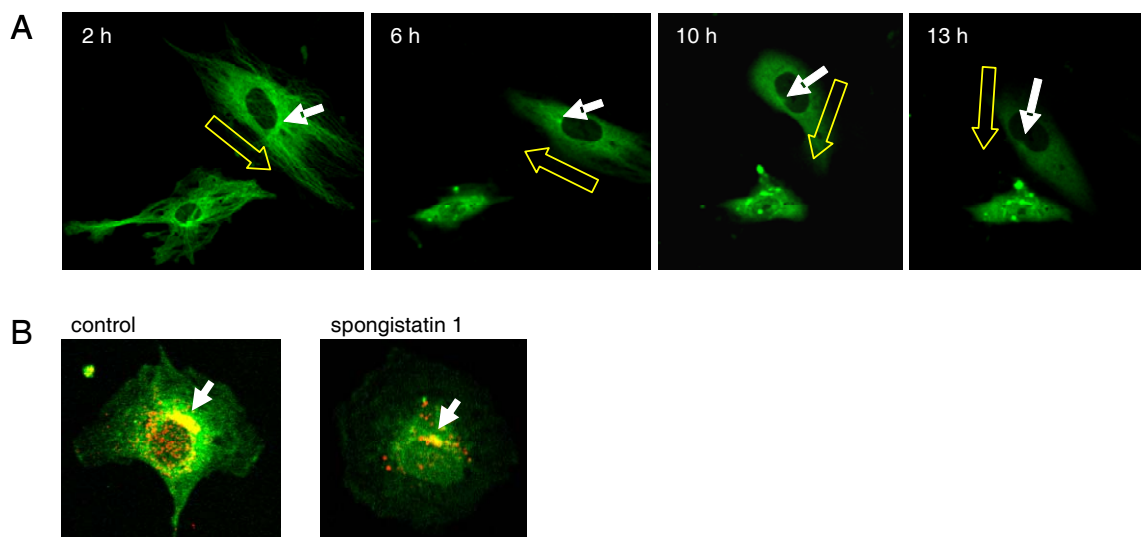


Figure V.14 Spongistatin 1 has no influence on MTOC-orientation.

(A) Life cell imaging of GFP-Tubulin transfected cells incubated with 2.0 nM spongistatin 1. The MTOC is visible as bright point near the nucleus (white arrows), even after the disassembly of interphase microtubules. The yellow arrows indicate the direction of HUVEC migration, which is also traceable by the localization of the upper and the lower cell. (B) Cdc42 staining (red) in GFP-tubulin transfected cells. The merge of both signals (yellow) shows the co-localization of Cdc42 and the MTOC in control and spongistatin 1-treated cells (5.0 nM, 30 minutes).

The re-orientation of the MTOC is essential for directed migration, and is regulated by the small RhoGTPase Cdc42. Time-lapse microscopy of GFP-tubulin transfected cells show the disassembly of microtubules. Furthermore, GFP-tubulin expression in the cell allows tracking the orientation of the MTOC, which is visible as bright structure in close neighborhood to the nucleus. Treatment with spongistatin 1 did neither disassemble the MTOC structure nor had it any influence on its orientation (Figure V.14 A). Cdc42, the master regulator of MTOC re-orientation, seemed to be associated with the centrosome structure, also under spongistatin 1 treatment (Figure V.14 B).

8 Tube Formation Is Inhibited by Spongistatin 1

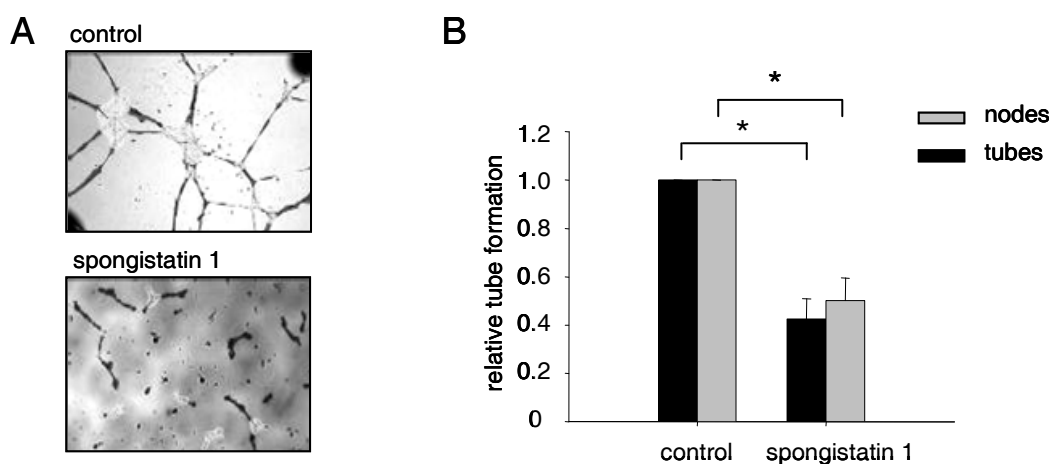


Figure V.15 Spongistatin 1 Inhibits Endothelial Tube Formation.

(A) Representative images of the tube formation assay. Quantification was done by S.CORE image analysis. Tubes are marked in dark grey, nodes in light grey. (B) The formation of endothelial tubes on Matrigel™ was reduced to half by 1.0 nM spongistatin 1. Bars, the mean \pm S.E.M, * p <0.05, One Way ANOVA.

The inhibition of endothelial tube formation on Matrigel™ is a characteristic attribute of antiangiogenic agents. In time-lapse microscopy, freshly seeded HUVECs formed a tubular network on Matrigel™ within only 4-7 hours. However, upon addition of 1.0 nM spongistatin 1 to the seeding medium, cells seemed to be no longer able to adhere properly to Matrigel™, and therefore were not able to form tubes (data not shown). Quantification of tube formation by S.CORE tube formation software showed about 50% reduction in tube length and number of nodes by 1.0 nM spongistatin 1 (Figure V.15).

9 Effects of Spongistatin 1 in Angiogenic *Ex/In Vivo* Assays

9.1 Spongistatin 1 Inhibits Endothelial Sprouting

In the *ex vivo* mouse aortic ring model, slices of mouse aortas were incubated on Matrigel™ for several days. Without spongistatin 1 (control), endothelial cells sprouted out of the aortic ring and spanned the Matrigel™ within 3-5 days. Stimulation of the aortic rings with 0.5 nM spongistatin 1 yielded reduced sprout formation, which was completely suppressed by treatment with 1.0 nM spongistatin 1 (Figure V.16 A).

CD31 is an endothelium-specific surface antigen. Staining the aorta slices and the sprouted cells with CD31-specific antibody verified that in fact endothelial cells have sprouted and not for instance smooth muscle cells (Figure V.16 B).

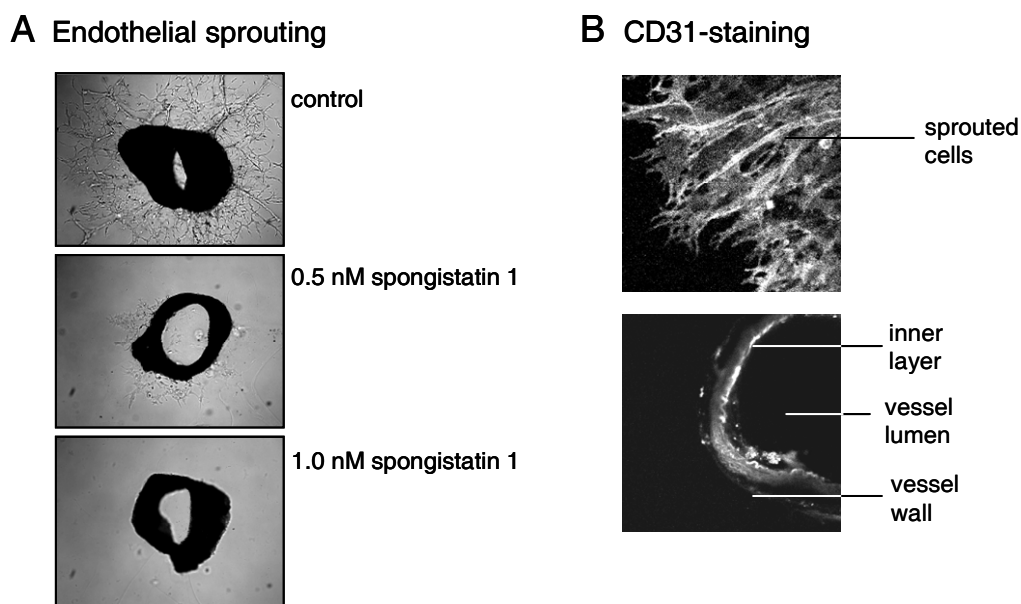


Figure V.16 Endothelial sprouting is inhibited by spongistatin 1.

(A) Representative pictures of the aortic ring assay show vessels of the three different treatment groups control, 0.5, and 1.0 nM spongistatin 1. In control, endothelial cells have spread out of the aorta solices, and cover the Matrigel™. The sprouting was dose-dependently inhibited by spongistatin 1. (B) CD31-staining proved that sprouted cells were endothelial cells.

9.2 Neovascularization *In Vivo* Is Reduced by Spongistatin 1

Antiangiogenic properties of spongistatin 1 *in vivo* were determined in the mouse corneal micropocket assay. This experiment was performed in collaboration with Dr. Ivan Ischenko and PD Dr. Christiane J. Bruns from the Department of Surgery, Klinikum Großhadern at the Ludwig-Maximilians-University Munich. Spongistatin 1 was administered intraperitoneally to investigate its impact on neovascularization after 6 days of stimulation with FGF.

Pellets containing sucrose aluminium sulfate alone without growth factors did not induce corneal neovascularization (data not shown). Corneal neovascularization induced by FGF in spongistatin 1-treated animals was markedly reduced compared to vehicle-treated control animals. Quantitative comparison showed that all parameters relevant for measuring the extent of corneal neovascularization were significantly lower in spongistatin 1-treated animals: the circumference of neovascularization and the vessel length in the corneas from spongistatin 1-treated mice were reduced by 37% and 53% respectively, compared to controls (Figure V.17).

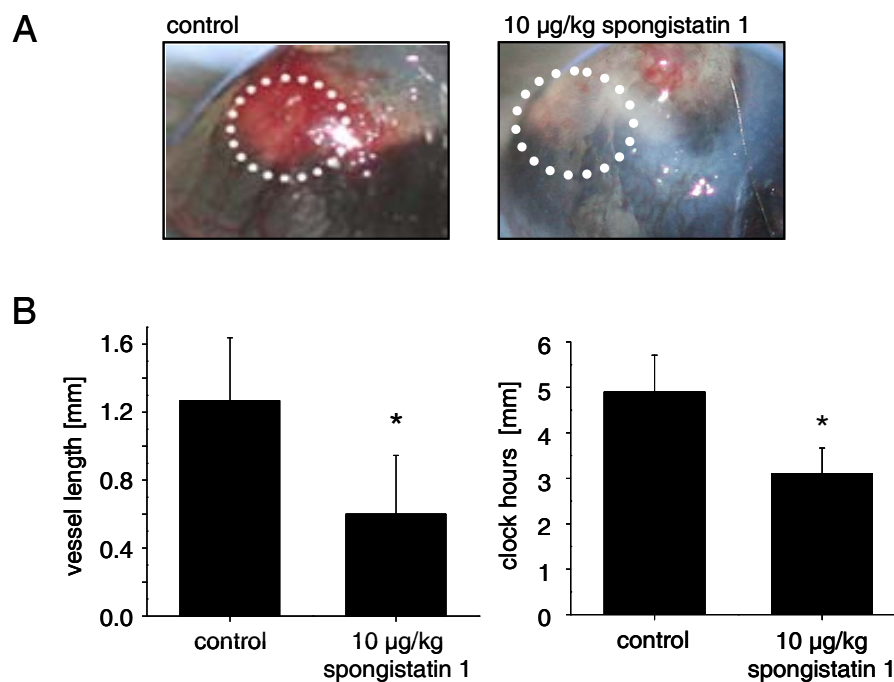


Figure V.17 Spongistatin 1 inhibits the neovascularization of mouse corneas.

(A) The corneal neovascularization was examined and photographed on day 6 after pellet implantation (~ 20× magnification of the mouse eye; spots encircle the area of the implanted pellet). Corneal neovascularization in spongistatin 1-treated animals was markedly reduced compared to vehicle-treated control animals. (B) Angiogenic responses were measured as clock hours and vessel length of neovascularization. Bars, the mean ± S.D.M., * $p < 0.05$, student's *t*-test.

10 The Influence of Spongistatin 1 on Endothelial Signaling

10.1 Kinome Array (PepChip)

PepChip analysis was performed with spongistatin 1-, vinblastine-, and CA4P-treated HUVECs, to investigate specific spongistatin 1-induced and 'general microtubules' effects of tubulin antagonists on overall signaling in a cellular context. All kinases, which showed significantly reduced activity in spongistatin 1-treated cells, are summarized in Table V.2. The table also shows the kinases inhibited by vinblastine and CA4P, but only those which have been inhibited by all three tubulin antagonists. The activities of kinases were expressed as percentage of the activity in untreated cells. Special attention was given to kinases of signal transduction pathways, which are prominent in cellular communication and survival. Interestingly, inhibition of c-src activity was only detected in PepChip-analysis of spongistatin 1-treated cells and not in vinblastine, or CA4P-stimulated HUVEC. Thus, effects on c-src phosphorylation activity might be specific for spongistatin 1. In contrast, the phosphorylation of AKT, PKC isoforms, and CK2 downstream targets was reduced by all investigated tubulin antagonists, arguing for an effect occurring whenever microtubules are inhibited. CK2 is a protein involved in cell survival. Effects on this kinase may be therefore unspecific response to the exposure to cytotoxic compounds (88). The inhibition of AKT phosphorylation activity by spongistatin 1 in PepChip analysis may confirm the previous findings of reduced AKT phosphorylation induced by spongistatin 1 (III 6.2 Proliferative Signaling: Spongistatin 1 Inhibits AKT-Phosphorylation). The activity of PKC isoforms under treatment with spongistatin 1 were investigated in more detail, since the importance of PKC isoforms PKC α , δ , and ϵ , in angiogenesis has been described previously (64-66).

Table V.2 Impact of spongistatin 1, vinblastine, and CA4P on kinases.

The table shows kinases (first column) with significantly reduced activity in HUVECs which were treated with the respective compound in comparison to control cells (second column, values are percentage of the activity of the respective kinase in untreated cells) and the standard error of the measurement (third column). The protein identification number of the phosphorylated substrate is given in the column entitled 'Substrate protein'. Further the cellular context of the phosphorylation event is given in the last column. The data of vinblastine and CA4P-treated HUVECs show only the kinases, which are inhibited by all three tubulin antagonists.

Kinase	Spongistatin 1	S.E.M.	Substrate protein	Cellular context
AKT1	0.0	0.03	NP_005195	Signaling
CK2	0.1	0.03	NP_002961	Metabolism
EGFR, c-src	0.3	0.03	NP_008819	Signaling
c-src	0.4	0.05	NP_001703	Immunity
CK2 α	0.5	0.02	NP_003753	Transport
PKC	0.6	0.03	NP_000015	Signaling
PAK1	0.6	0.01	NP_000116	Transcription
Kinase	Vinblastine	S.E.M.	Substrate protein	Cellular context
PKC ζ	0.3	0.03	NP_003395	Signaling
PKC	0.4	0.02	NP_004753	Signaling
PKC	0.4	0.03	NP_001984	Signaling
CK2 α _1	0.4	0.01	NP_005339	Transcription
PKA; PKC α	0.4	0.03	NP_004812	Protein synthesis
AKT1	0.4	0.04	NP_003001	Protein synthesis
CK2	0.5	0.03	NP_008819	Signaling
PKC	0.7	0.04	NP_001610	Signaling
Kinase	CA4P	S.E.M.	Substrate protein	Cellular context
AKT1	0.0	0.00	NP_001220	Apoptosis
PKC	0.5	0.04	NP_004753	Signaling
PKA; PKC α	0.5	0.04	NP_004812	Transcription
CK2	0.5	0.04	NP_009028	Signaling

10.2 The Influence of Spongistatin 1 on PKC Activity

10.2.1 Spongistatin 1 Inhibits the Phosphorylation of Distinct PKC Substrates

To validate the PepChip findings of reduced PKC activity by spongistatin 1, Western blot analysis on the phosphorylation of serine residues of PKC-substrates was performed. PKC are serine/threonine-specific kinases, however the majority of PKC substrates are serine

residues (89). The phosphorylation motifs of PKC phosphorylation substrates are very similar, thus it was possible to develop an antibody, detecting many different PKC substrates independent of the upstream PKC isoform (90). Employing this antibody in Western blot analysis is supposed to provide information on overall PKC activity.

In control cells, different bands of PKC substrates, which were phosphorylated at their serine residues, could be detected. Incubation with the well established kinase inhibitor staurosporine (100 nM, 30 minutes), which is known to inhibit PKC activity by binding to the ATP-site, caused complete inhibition of PKC-substrate phosphorylation, whereas spongistatin 1 (5.0 nM, 30 minutes) reduced phosphorylation not of all, but of distinct PKC-substrates. This indicates that spongistatin 1 might inhibit a specific PKC isoform (Figure V.18).

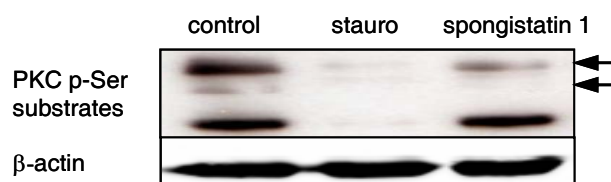


Figure V.18 Spongistatin 1 inhibits phosphorylation of distinct PKC substrates.

In Western blot analysis of untreated HUVECs (control), bands of phosphorylated PKC-substrates could be detected. Incubation with staurosporine (stauro), a strong kinase inhibitor, completely abolished phosphorylation of PKC-substrates. In contrast, treatment with spongistatin 1 caused reduced phosphorylation only of distinct PKC substrates (arrows). Detection of β -actin proved equality of protein amounts.

10.2.2 Spongistatin 1 Has no Impact on PKC Activity *In Vitro*

The catalytically active centers of PKC isoforms are structurally very similar and selective inhibition is therefore quite unlikely. In fact, employing spongistatin 1 in PKC *in vitro* activity assays revealed no direct inhibitory effect on analyzed PKC isoforms α , β_1 , β_{11} , δ , ϵ , or ζ (Figure V.19). Thus, there must be another mechanism, by which spongistatin 1 affects PKC activity. The PKC *in vitro* assay was performed by Dr. Johann Hofmann, Division of Medical Biochemistry, Innsbruck Medical University, Austria.

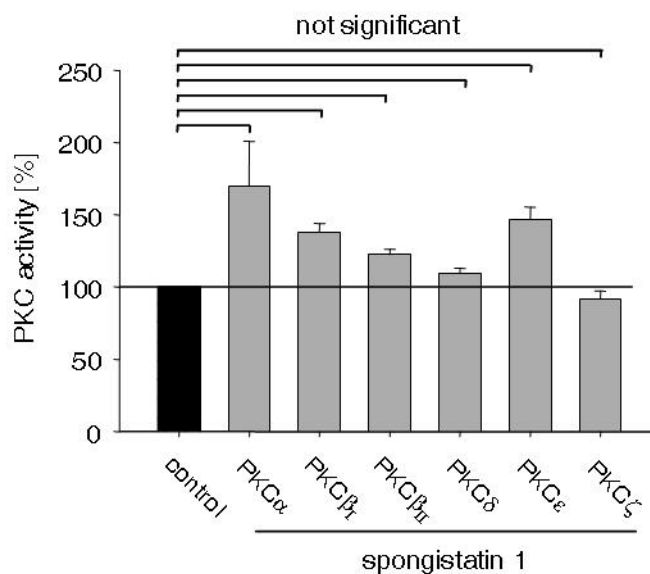


Figure V.19 Spongistatin 1 does not influence PKC activity *in vitro*.

PKC *in vitro* activity assay revealed that spongistatin 1 has no significant influence on the activity of PKC isoforms α , β_I , β_{II} , δ , ϵ , and ζ . For PKC isoforms α , β_I , δ , and ζ 100 nM spongistatin 1 were employed, whereas for PKC β_{II} and ϵ 50 nM spongistatin 1 were used. Bars, the mean \pm S.E.M., $p > 0.05$, Rank On Sum-test.

10.3 The Influence of Spongistatin 1 on PKC-Translocation

Since most of the PKC isoforms, conventional as well as novel, have to be translocated from the cytoplasm to membranes for activation, spongistatin 1 may inhibit the activity of specific PKC isoforms via disruption of its transport to membranes. Endothelial cell lysates were fractionated into a membranous fraction, containing the cytoplasmic membrane and all intracellular membranes, and a cytosolic fraction by ultracentrifugation. Detection and quantification of different PKC isoforms in both fractions was used to analyze translocation of these proteins.

10.3.1 PKC Expression in HUVECs

Prior to investigations on spongistatin 1 and its effects on PKC activity in endothelial cells, the expression of the several PKC isoforms in HUVECs was analyzed by Western blot of membrane/cytoplasm fractions. The PKC isoforms α , δ , ϵ , η , and ζ could be detected. Further it could be shown, that except of PKC ζ , the translocation of all these proteins to the membrane-site can be stimulated with PMA (10 nM, 2 hours).

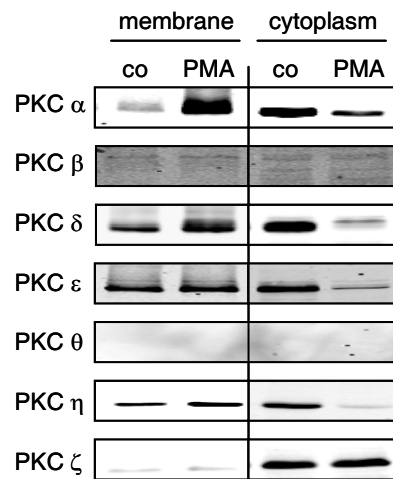


Figure V.20 Expression of PKC isoforms in endothelial cells.

The expression of diverse PKC isoforms in endothelial cells was investigated via Western blot analysis of membrane/cytoplasm fractions. PKC isoforms α , δ , ε , η , and ζ could be detected. Aside from PKC ζ , the translocation of all detectable PKC proteins to membrane was induced by PMA (10 nM, 2 hours).

10.3.2 The Translocation of PKC α is reduced by Spongistatin 1-Treatment

Since PKC α , δ , and ε are of particular importance for angiogenesis, the effects of spongistatin 1 on these three PKC isoforms were investigated in more detail. PKC translocation was induced with 10 nM PMA for 2 hours. Pre-incubation with spongistatin 1 (5.0 nM, 30 minutes) prior to PMA-stimulation resulted in reduced transport of PKC α to membranes. Accordingly, an enrichment of PKC α in the cytoplasm was observed. In contrast, the translocation of PKC δ and ε were not significantly affected by spongistatin 1 (Figure V.21 A). Quantitative analysis of Western blots of PKC isoforms after membrane/cytosol fractionation proved the visual impressions from Western blot analysis (Figure V.21 B).

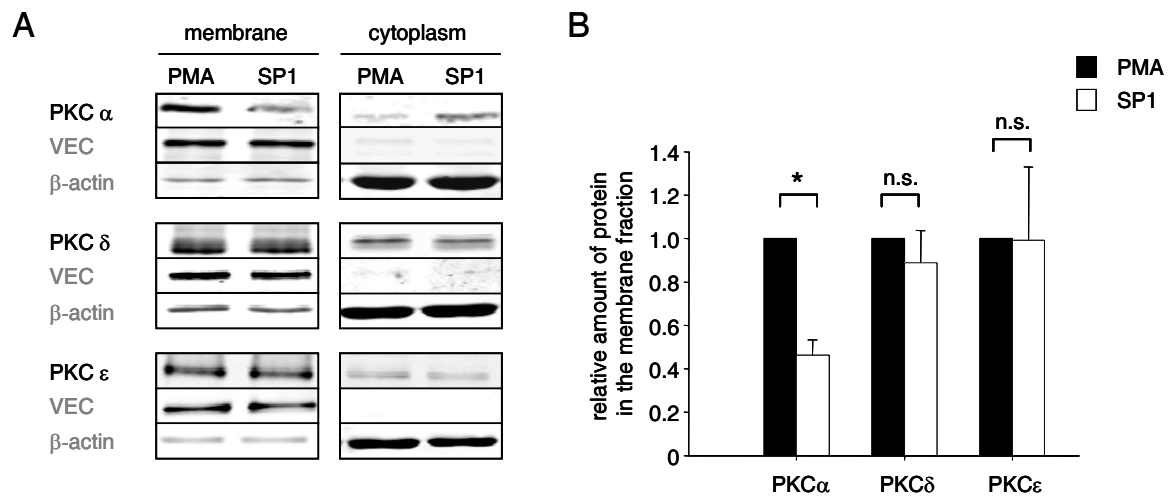


Figure V.21 Spongistatin 1 specifically inhibits the translocation of PKC α .

(A) Detection of the PKC-isoforms α , δ , and ϵ in membranous and cytoplasmic fractions of HUVECs that were either stimulated with 10 nM PMA for 2 hours (PMA), or pre-incubated with 5 nM spongistatin 1 prior to PMA-stimulus (SP1). Detection of VE-cadherin (VEC) and β -actin proved purity of the fractions, and the equality of protein amounts. (B) Quantification of PKC isoforms in the membrane fraction: the PKC-isoform α is specifically reduced to half by spongistatin 1, whereas PKC δ and PKC ϵ were not significantly affected. Bars, the mean \pm S.E.M., * p <0.05, n.s., not significant, Rank On Sum-test.

VI. DISCUSSION

1 Spongistatin 1 is a Powerful Experimental Compound against Pancreatic Tumor Progression and Metastasis

Pancreatic cancer is still a severe disease with poor prognosis, in respect of advanced tumor progression and metastasis at the time point of diagnosis. Thus, elucidation of new anticancer drugs is required to improve chemotherapy inoperable advanced cases (13-15). Intraperitoneal application of spongistatin 1 at the very low dose of 10 µg/kg body weight in an orthotopic *in vivo* model significantly reduced pancreatic tumor growth. Moreover, spongistatin 1 remarkably abrogated metastatic activity, which is in line with reduced activity of MMP-9 in tumor tissue of mice treated with spongistatin 1. The reduction of metastasis by spongistatin 1 is of particular importance, as 90% of all cancer death arise from the metastatic spread of primary tumors (91, 92). In contrast to other cytotoxic compounds examined in the same experimental model (93-95), spongistatin 1 seems to be tolerated quite well as no influence on the overall body weight of the mice has been observed. Thus, spongistatin 1 can be regarded as a powerful experimental agent to combat pancreatic tumors.

2 The Impact of Spongistatin 1 on Hypoxia Signaling

HIF-1 α expression has been detected in the majority of solid tumors, including brain, bladder, breast, colon, ovarian, renal, prostate, and pancreatic cancers. Clinically, HIF-1 α overexpression is a marker for the highly aggressive disease and has been associated with poor prognosis, whereas the loss of HIF-1 activity dramatically decreases tumor growth, vascularization, and energy metabolism. Thus, the inhibition of HIF-1/HIF-1 α has become a very promising approach in cancer therapy (83, 96, 97).

Since the inhibition of HIF-1 has gained clinical relevance and tubulin-inhibiting drugs, both the stabilizing as well as the disassembling types, have been shown to diminish HIF-1 α stabilization *in vitro* (98, 99), it seemed to be most promising to investigate effects of spongistatin 1 on HIF-1 in the pancreatic tumor model. Indeed, spongistatin 1 was able to reduce HIF-1 α -levels *in vitro* in L3.6pl pancreatic tumor cells. However, molecular analysis of tumor tissues revealed no impact of spongistatin 1 on HIF-1 activity *in vivo*. This finding is well corresponding with the fact that until now only specific HIF-1 inhibitors were able to reduce HIF-1-activity *in vivo* - although many cytotoxic compounds were described to inhibit HIF-1 α stability *in vitro* (83). Thus, the clinical relevance of anti-HIF-1 α effects of tubulin

antagonists *in vitro* is quite doubtful and seems to be a phenomenon of an unspecific stress response rather than of specific anti-HIF-1 activity.

3 Reduction of MMP-9 Levels by Spongistatin 1 *in Vivo*

3.1.1 The Relevance of MMP-9 in Pancreatic Cancer

MMP-dependent remodeling of the tumor microenvironment and ECM through lysis of matrix proteins is a necessary step in local invasion and metastasis (100-103). In pancreatic cancer, the up-regulation of MMPs, especially of the gelatinases MMP-2 and MMP-9, is shown to correlate with invasiveness and metastatic potential, and application of MMP-inhibitors has shown benefit for patients in clinical trials (104, 105). Additionally, the application of the MMP inhibitor BB-94 imparted a survival advantage in the treated animals in an orthotopic nude mouse model, similar to the model in the present study (106).

The highly metastatic L3.6pl carcinoma in the orthotopic tumor model strongly expressed MMP-9. Treatment with spongistatin 1 resulted in a significant reduction of MMP-9 mRNA and protein levels in comparison to control mice. In fact, MMP-2 is also expressed, but in marginal amounts and a compensatory up-regulation of MMP-2 in the spongistatin 1-treated group could not be observed. Thus, the reduction of MMP-9 may contribute to the inhibitory effects of spongistatin 1 on tumor growth and metastasis.

3.1.2 Reduction of MMP-9 mRNA Levels by Spongistatin 1

The secretion of MMPs into the extracellular space is a microtubule-dependent process and can be disrupted by microtubule-inhibiting compounds (107). However, a reduction of MMP mRNA levels by tubulin antagonists has not been described before. Spongistatin 1 reduced mRNA levels of MMP-9, but not of VEGF, suggesting selectivity for MMP-9 mRNA. Whether this reduction is a matter of a diminished transcription of the MMP-9 gene, or of a destabilization of MMP-9 mRNA is not clear.

Recently, it was described that destruction of microtubules leads to a reduced mRNA expression of VEGFR2. The authors have shown the tubulin antagonist nocodazole to inhibit the transcription factor Sp1, and thereby reducing the transcription of VEGFR2 (108). Since the MMP-9 promoter region contains consensus sequences for the transcription factors Sp1, Ap1, and NF κ B (109), spongistatin 1 may act in a similar way on the transcription of the MMP-9 gene. EMSA-studies revealed no differences in the DNA-binding activity of any of

these transcription factors in both treatment groups (data not shown). This may argue for spongistatin 1 acting on the stability of MMP-9 mRNA, rather than on its transcription. However, it must be regarded that the time point of investigation may be a crucial factor in this context, since tumors were in a very late progression state at necropsy, and DNA-binding activities of transcription factors may be no longer detectable. Further studies are necessary to uncover the mechanism by which spongistatin 1 acts on MMP-9 mRNA levels. These investigations would be of relevance, since findings may provide a new mechanism by which tubulin antagonist act on tumor progression and metastasis, but the fact that L3.6pl cells do not express MMP-9 *in vitro* (own observations) complicates continuative studies in the pancreatic tumor model.

4 Antiangiogenic Action of Spongistatin 1 and the Underlying Mechanisms

4.1 Spongistatin 1 Exerts strong Antiangiogenic Action *In Vitro* and *In Vivo*

Since the inhibition of angiogenesis gains more and more relevance in cancer therapy, there is an increasing demand for appropriate drugs. Microtubule-targeting drugs belong to the most potent antiangiogenic compounds, but they also suffer from toxic-side effects. Thus, new tubulin-binding compounds with fewer side effects are currently being sought after (18). Spongistatin 1 disrupts microtubules *via* binding to a specific site on β -tubulin. The uniqueness of this site may add therapeutic qualities to spongistatin 1, making it worthwhile to investigate the antiangiogenic potency of this compound.

Spongistatin 1 inhibited angiogenesis *in vitro* and *in vivo* at extremely low concentrations, far below toxic doses. Further, inhibition of angiogenesis by spongistatin 1 occurred at concentrations beneath that of the established tubulin antagonists including vinblastine, paclitaxel, and the new promising compound CA4P. Moreover, proliferating endothelial cells were particularly sensitive to spongistatin 1, since proliferation was inhibited at a concentration as low as 100 pM. In cytotoxicity measurements, non-proliferating HUVECs tolerated more than 10-fold higher concentrations of spongistatin 1 than proliferating cells, arguing for a specific action on newly developing vessels. Additionally, applied intraperitoneally, spongistatin 1 inhibited neovascularization *in vivo*. This indicates the drugability of spongistatin 1. Summing up, spongistatin 1 is a potent antiangiogenic compound exhibiting many qualities that support its use in therapeutic applications.

4.2 Inhibition of Endothelial Proliferation

4.2.1 Spongistatin 1 Particularly Affects Endothelial Proliferation

Spongistatin 1 exerted a particularly high impact on proliferating endothelial cells. It is not clear where the sensitivity of proliferating cells towards spongistatin 1 comes from and why the other tubulin-inhibiting drugs, vinblastine, paclitaxel, or CA4P were not that effective on proliferating cells. Potentially the strong effect of spongistatin 1 derives from its ability to bind to a unique site at β -tubulin. Furthermore, there might be significant differences in drug-uptake, leading to an enhanced incorporation of spongistatin 1 in proliferating cells. Interestingly, spongistatin 1 was the only tubulin antagonist inhibiting c-src and thereby reducing the activating phosphorylation of CEACAM-1 (NP_001703) in the kinome array. This receptor was recently shown to be involved in proliferation and to be expressed only on proliferating endothelial cells, especially during tumor angiogenesis. This selectivity for tumor-induced angiogenesis turned CEACAM-1 out to be a particular attractive target in antiangiogenic therapy and might be therefore an interesting aspect in antiangiogenic action of spongistatin 1 (110-112). However, further studies are necessary to reveal the influence of spongistatin 1 on c-src and CEACAM-1 activity, and its relevance for antiproliferative effects of spongistatin 1.

4.2.2 Mitotic and Non-Mitotic Actions of Spongistatin 1 on Proliferation

The mechanisms by which spongistatin 1 exerts its antiproliferative effects are not clear at all. Of course, the tubulin antagonist spongistatin 1 inhibits mitotic spindle formation as shown in the flow cytometric measurements. However, spindle-poisoning effects were detected at a concentration as low as 1.0 nM, a 10-fold higher concentration than that which inhibits proliferation. Thus, the effects observed have to be interpreted as different from simple antimitotic actions. Also acute cytotoxicity can be excluded as the reason for the strong impact of spongistatin 1, since significant reduction of cell viability in the CellTiter Blue™ assay occurred at concentrations beginning at 5.0 nM.

Interestingly, spongistatin 1 inhibited the activating phosphorylation of AKT. The AKT-dependent pathway is of vital importance in endothelial proliferation since the majority of growth factor-induced responses are mediated by the activation of the PI3K/AKT signaling cascade (58). Spongistatin 1 might influence proliferation by inhibiting AKT-mediated signaling. Thus, spongistatin 1 seems to act on proliferation by both the inhibition of mitotic spindle formation and by the disruption of the proliferative signaling pathways in the interphase.

4.3 Directed Migration

Intercellular coordination and cellular motility are associated with the microtubule-skeleton and are basic elements of directed migration and the formation of tubes. In line with these facts, spongistatin 1 inhibited both processes. Moreover, employing spongistatin 1 in migration and chemotaxis assays elucidated several aspects of the role of microtubules in directional migration in endothelial cells.

4.3.1 Microtubules Do Not Contribute to the Migration Force in Endothelial Cells

The influence of microtubules on migration is cell type-dependent. Migration is unaffected in fish keratocytes or even enhanced in neutrophils, when microtubules are disrupted (29, 30). However, in most cell types, including endothelial cells, the breakdown of the microtubule network correlates with motility impairments. Microtubules may be involved directly in the generation of protrusive forces, since the plus ends of growing microtubules generate a force of several pN, which is enough to deform lipid bilayers (37). Spongistatin 1-treated endothelial cells were not reduced in accumulative migration distance or velocity in the chemotaxis assay, suggesting that the tractive force of the cells is not affected by spongistatin 1-induced inhibition of the microtubules. Hence, the main force of cell movement seems to be generated by the actin-cytoskeleton, whereas the contribution of microtubules to traction in endothelial cells is negligible. Antimigratory effects in endothelial cells caused by the inhibition of the microtubules have been demonstrated before. However, this work clearly demonstrates that the microtubule-inhibiting compound spognistatin 1 does not act by inhibition of tractive forces.

4.3.2 Microtubules and the Intracellular Polarization

Given that microtubules do not contribute to tractional forces in endothelial cells, the inhibitory mechanism of spongistatin 1 on endothelial migration remains to be elucidated. The morphological changes endothelial cells are undergoing upon spongistatin 1 treatment, including cell rounding, dearrangement of mitochondria and the disorientation of F-actin arrangement suggest that spongistatin 1 inhibits polarization of the cell and thereby prohibits directed cell migration. These suggestions are well in line with findings that microtubules are essential for the generation and maintenance of cellular polarity in fibroblasts. Disassembly of microtubules in these cells results in loss of polarization and the ability of directional migration (40). However, the molecular processes underlying the affection of cellular polarity by tubulin antagonism are still unclear.

4.4 How Microtubules May Control Polarization

How does the disassembly of microtubules inhibit cellular polarization? The generation and maintenance of cellular polarity is an interplay of several factors including sensing and regulatory elements (PI3K, small RhoGTPases) and the cytoskeleton (actin-filaments, microtubules, motorproteins). These factors are generating a system of interlinked modules, which regulate each others functionality depending on negative and positive feedback loops. Thus, the inhibition of the module 'microtubules', is likely to interfere with the functionality of other modules in the polarization system. Investigation of the effects of spongistatin 1 on directional migration raised several evidences of which elements might be affected, as discussed in the following.

4.4.1 The Small RhoGTPases

During migration, highly coordinated processes between actin and microtubules are taking place and both affect each others dynamics through the regulation of the small Rho GTPases RhoA, Cdc42, and Rac1 (113-115). The linkage of microtubules and actin, as well as the fact that spongistatin 1-treatment affects F-actin arrangement indicates that the functionality of small RhoGTPases is influenced upon the disassembly of microtubules.

RhoA is regulating contractile forces during migration. Since the overall cellular movement was not inhibited by spongistatin 1, it seems to be unlikely that the activity of RhoA was affected. Further, the group of Omelchenko *et al.* shows that microtubular control of polarity is independent of RhoA-mediated contractility in fibroblasts (116).

Cdc42 is involved in microtubules plus end capture and their stabilization at the leading edge. Additionally, Cdc42 is responsible for MTOC orientation (48, 117). It has been discussed whether dynein is implicated in centering the MTOC, as it can pull the plus ends of cortically attached microtubules (118). The present study shows that the orientation of the MTOC was not inhibited upon spongistatin 1-treatment. Even when microtubules were completely depolymerized, the MTOC was still orientated to the leading edge and the cell moved into the direction provided by the MTOC. It has been reported that vinblastine inhibits Cdc42-activity in endothelial cells (119). Thus, either the Cdc42-function of orientating the MTOC is not affected by spongistatin 1, as it this function of Cdc42 is microtubule-independent or the MTOC-orientation in random-migration is independent of Cdc42.

Rac1 is localized at the leading edge of migrating cells and promotes the formation of the lamellipodium by inducing the polymerization of F-actin. Treatment with spongistatin 1 did not abrogate lamellipodia formation, but their number was reduced. It was shown that Rac1 and microtubules are activating each other in a reciprocal manner. Rac1-activating protein IQGAP1 binds to CLIP170 which in turn binds to the plus ends of the growing microtubules

(120). Further, the guanine nucleotide exchange factors Trio, GEF-H1, and Asef, which activates Rac1 by substituting GDP to GTP, are shown to be microtubule-associated (40, 121-123). Besides, the group of Bijman *et al.* could show vinblastine-mediated inhibition of Rac1 in endothelial cells (119). Thus, the inhibition of microtubules by spongistatin 1 may reduce Rac1 activation at the leading edge.

4.4.2 Effects on PI3K

The elementary importance of PI3K for chemotactic migration has been elucidated in very recent works. In this context, it was shown that the PI3K/AKT pathway promotes microtubules stabilization in migrating fibroblasts and endothelial cells, which in turn might promote Rac1 activity. Further, it has been shown that the activity of Rac1 and AKT are interlinked by a positive feedback loop, although it is not yet clear, whether Rac1 is activated by AKT downstream of PI3K or vice versa (124-127). The inhibition of AKT-phosphorylation by spongistatin 1 may be symptomatic for effects of microtubule-disassembly on PI3K-dependent signaling. The interference with PI3K/AKT-signaling and the reduction in directionality and formation of lamellipodia upon spongistatin 1-treatment implicates that microtubules are the connection between PI3K/AKT and Rac1-dependent actin organization and breaking this linkage by tubulin-inhibiting drugs abrogates directional migration.

5 Microtubules in Endothelial Signaling

5.1 Tubulin Antagonists Inhibit AKT, CK2, and PKC isoforms

To gain more insights on the global effects of spongistatin 1 on cellular signaling in special and microtubule-inhibiting drugs in general, a kinome array with tubulin antagonist-treated HUVECs was performed. The advantage of this array in comparison to conventional *in vitro* kinase activity screenings is that the impact of a compound can be investigated on the overall kinase activity in the cellular context, and therefore both the direct and indirect actions of the respective compound on kinase activity can be detected (cf. PepChip data and PKC *in vitro* assay). The array was supposed to reveal influences of tubulin antagonism on signaling pathways with relevance in angiogenesis and thereby identify new mechanisms by which tubulin antagonists act.

In the kinome array, three kinases were affected in their activity by all three tested tubulin antagonists: CK2, AKT, and PKC isoforms. CK2 is mainly involved in cell survival and may be unspecifically affected by cytotoxic drugs (88). However, CK2 seems also to be a

microtubules-associated protein, promoting the stabilization of microtubules (128). This might explain why all three tubulin binding-drugs affect CK2.

The importance of AKT-signaling in angiogenesis has been discussed in forgoing sections of this work. Tubulin antagonist-induced reduction of AKT-activity in the kinome array is well corresponding with reduced phosphorylation of AKT by spongistatin 1, and previous reports of tubulin-targeting drugs inhibiting AKT phosphorylation in endothelial cells (129, 130). Further studies on the underlying mechanisms of tubulin antagonist-mediated inhibition of AKT might be quite interesting. However such studies would not provide the discovery of a new, unknown mechanism of tubulin antagonism.

Thus, ongoing investigations of the impact of spongistatin 1 on PKC activity were most promising, since the close relationship of PKC signaling and angiogenesis has been described previously. The repeated appearance of reduced PKC activity upon incubation with spongistatin 1, vinblastine, and CA4P, indicates that effects on PKC-signaling may provide a general mechanism by which tubulin antagonists act on angiogenesis.

5.2 PKC α Translocation Depends on Functional Microtubules in Endothelial Cells

Analysis of spongistatin 1 on PKC activity has shown a rapid and selective impact on PKC isoform α . However, spongistatin 1 does not inhibit PKC α directly, since PKC α activity was not inhibited in the PKC *in vitro* assay. Rather, the translocation and therefore the activation of PKC α is disrupted by spongistatin 1. Similar effects could be observed when treating cells with vinblastine (data not shown). Thus, it can be assumed that inhibition of PKC α -translocation is not a spongistatin 1-specific phenomenon but relies on the disassembly of microtubules. These findings are well in line with findings of microtubule-dependent PKC α -translocation in neurons and smooth muscle cells (131, 132). However, the present study shows for the very first time the microtubule-dependency of PKC α -translocation in endothelial cells.

Previous work on knock-down and over-expression of PKC α in endothelial cells has clearly shown that PKC α is essential for angiogenesis: migration and cord formation are inhibited by PKC α knock-down, whereas PKC α over-expression results in increased proliferation, migration, and tube formation (133-135). Anti-sense RNA-studies on PKC α revealed that endothelial cells are not able to adhere to an extracellular matrix (134). Further, it is known that VEGF-induced proliferation requires PKC α (133), and it has been shown that PMA-induced angiogenesis is depending on PKC α activity (136).

All these studies have demonstrated the elementary importance of PKC α in angiogenesis. Hence, inhibition of interphase microtubules by tubulin antagonists and subsequently

reduced PKC α -translocation may provide a new mechanism by which tubulin antagonists act on angiogenesis.

5.3 Microtubule-Inhibiting Drugs Disrupt Translocation Processes

Spongistatin 1 inhibits the translocation of PKC α to the membrane. Furthermore, the activating phosphorylation of AKT, which is also a process depending on translocation to membrane, is reduced by spongistatin 1. Additionally, the activity of c-src has been shown to be microtubule-associated and to depend on translocation (137) and is inhibited by spongistatin 1 in the kinome array. In contrast, spongistatin 1 has no inhibitory effects on ERK1/2 phosphorylation. ERK and other MAPK are organized in huge protein complexes which are assembled by scaffold proteins. Thus, kinases of the cascade are in spatial closeness which makes translocation processes unnecessary. This might explain why spongistatin 1 had no impact. However, this finding also confirms the suggestion that the inhibition of microtubules disrupts several signaling pathways in endothelial cells by inhibition of translocation processes.

6 Conclusions

6.1 Anticancer Activities of Spongistatin 1

This work presents the marine compound spongistatin 1 as a promising agent in the combat against cancer, since spongistatin 1 inhibits pancreatic tumor progression and metastasis *in vivo*. The reduction of MMP-9 levels by spongistatin 1 might be involved in antimetastatic effects and more over, potentially presents a novel mechanism by which tubulin antagonists inhibit tumor progression and metastasis.

Investigations of tumor tissues and of spongistatin 1 effects on pancreatic cancer cells *in vitro* also exhibited the difficulties of the transference of *in vitro* effects to *in vivo* models and vica verse. Thus, inhibitory effects of HIF-1 α *in vitro* could not be observed in the tumor model. In contrast, underlying mechanisms of the reduction of MMP-9 levels by spongistatin 1 *in vivo* could not be further investigated, since the cancer cell line does not express MMP-9 *in vitro*.

6.2 Non-Mitotic Action of Tubulin Antagonist on Angiogenesis

Spongistatin 1 exerts strong antiangiogenic effects both *in vitro* and *in vivo*. Importantly, spongistatin 1 was even more potent in angiogenic *in vitro* assays than the established tubulin antagonists vinblastine, CA4P, and paclitaxel. Moreover, molecular analysis of the mechanisms of spongistatin 1 shed light on the still poorly understood antiangiogenic action of tubulin antagonism. Detailed analysis of spongistatin 1 effects on endothelial cell morphology, organelle arrangement, directionality, cytoskeleton, and signaling pathways facilitates the creation of a model of the non-mitotic effects of tubulin antagonists on angiogenesis.

6.2.1 The Importance of Cellular Polarization in Vessel Formation

Treatment with spongistatin 1 abrogates directed migration by inhibition of the intrinsic polarity in endothelial cells. Spongistatin 1 most likely acts by interrupting the connection between the chemo-attractive sensing elements (PI3K/AKT) and the migratory apparatus (F-actin). Polarization of the cell is not only the first step in the process of directed migration, but a fundamental process throughout the whole vessel formation. First, the tip cell has to establish an intrinsic polarization to form filopodia for sensing chemo-attractive signals and to form one leading edge to guide the trailing stalk cells. Secondly, the stalk cells need to polarize to distinguish between the direction of the tip cell (front), and the direction of the parent vessel (back). Finally, the completed vessel develops an apical (towards the vessel lumen) and a basal face (towards the vessel wall) of the endothelium depending on an intrinsic polarity (59, 138). Thus, inhibition of cellular polarization by the depolymerization of the microtubules has a global impact on vessel formation.

6.2.2 Microtubule-Inhibiting Drugs Affect Multiple Signaling Pathways

The impact of functional microtubules on endothelial signaling is not very well characterized, since the contribution of microtubules to cell signaling is extremely cell type-specific: signaling pathways vary in different cell types and translocation processes also occur along actin filaments. Additionally, due to the cellular morphology or intracellular organization, translocation processes are not always necessary. Endothelial cells are very large and flat cells, and are therefore depending on bridging long distances in signaling transduction. Thus, it can be assumed that in endothelial cells several signaling pathways require translocation processes. As it was shown for PKC α , many of these translocation processes most likely depend on functional microtubules. Consequently, the disassembly of microtubules affects

not only one but several signaling pathways. Moreover, translocation-dependent kinases like AKT and PKC α present central signaling nodes with a great number of downstream signaling pathways. For instance, AKT is able to phosphorylate more than 9000 proteins (139).

Thus, the impact of microtubule-inhibiting compounds like spongistatin 1 on cellular signaling resembles the effects of multiple kinase inhibitors. Recent investigations indicate that targeting multiple signaling pathways by respective kinase inhibitors, e.g. sunitinib malate or sorafenib, improve efficacy of tumor therapies. Especially MAPK, PI3K/AKT, and PKC are in the focus of interest, since these kinases represent integrative nodes of growth factor signaling (140, 141). Thus, multi kinase inhibiting qualities are most likely to be involved in the strong antiangiogenic action of tubulin antagonists.

VII. SUMMARY

SUMMARY

A *In Vivo* Effects of the Anticancer Compound Spongistatin 1

The marine compound spongistatin 1 disrupts microtubules by binding to a specific site at β -tubulin. Microtubule-inhibiting drugs belong to a very successful class of anticancer compounds, and also spongistatin 1 has shown strong anticancer properties in previous *in vitro* studies. Based on this pronounced antitumor efficacy, we investigated the chemotherapeutic potential of spongistatin 1 *in vivo* in an orthotopic pancreatic tumor model. Spongistatin 1 strongly inhibited tumor progression, as judged by tumor volume and tumor weight. Moreover, incidences of metastases in liver, regional lymph nodes and peritoneum were dramatically reduced by spongistatin 1. Molecular analysis of tumor tissues revealed the mRNA and protein levels of matrix metalloproteinase 9 to be significantly lower in spongistatin 1-treated mice than in control animals, which is well in line with inhibition of tumor progression and metastasis. Thus, spongistatin 1 seems to be a powerful experimental drug in combating cancer.

B The Antiangiogenic Potential of Spongistatin 1

Besides their application as classical chemotherapeutics, microtubule-inhibiting drugs have been shown to be very potent in antiangiogenic therapy, which prompted us to investigate the antiangiogenic potential of spongistatin 1. In angiogenic *in vitro* assays, spongistatin 1 inhibited endothelial proliferation, migration and tube formation at non-toxic concentrations. Most importantly, spongistatin 1 was even more potent than the well-known tubulin antagonists vinblastine, CA4P, and paclitaxel. In the mouse cornea pocket assay, the antiangiogenic effects of spongistatin 1 were investigated *in vivo*. Application of spongistatin 1 into the intraperitoneum significantly reduced growth factor-induced neovascularization of mouse corneas. Thus, spongistatin 1 has been demonstrated to effectively inhibit angiogenesis *in vitro* and *in vivo*.

Since it has been reported that the affection of interphase microtubules plays an important role in the antiangiogenic action of tubulin antagonists, non-mitotic effects of spongistatin 1 were investigated in order to elucidate the underlying mechanisms of its antiangiogenic effects. Employing spongistatin 1 in a chemotaxis assay has shown that endothelial migration is not inhibited by affection of the cellular motility itself, but rather by reduction of the directionality of endothelial cells. Life-cell imaging of GFP-tubulin transfected cells demonstrated that spongistatin 1 has no effect on the orientation of the MTOC towards the

leading edge, which is a crucial factor in directed migration. In contrast, spongistatin 1-induced de-arrangement of F-actin seems to be involved in the inhibition of endothelial directionality.

To get further insights into the effects of spongistatin 1 on angiogenic cell signaling, a kinome array with spongistatin 1-treated HUVECs was performed. Interestingly, spongistatin 1 reduced the activity of PKC. Continuative investigations have further shown that spongistatin 1 affects the phosphorylation of certain PKC substrates, indicating that the impact of spongistatin 1 might be PKC isoform-specific. PKC *in vitro* assay did not reveal any direct inhibition of PKC isoforms α , β_I , β_{II} , δ , ϵ , or ζ by spongistatin 1, but we could show that the translocation of PKC α from the cytosol to the membrane is reduced. Since the translocation of PKC α to the membrane is essential for its activation, and PKC α is an important factor in angiogenesis, the reduction of its translocation is likely to contribute to antiangiogenic effects of spongistatin 1. Moreover, this might provide a new general mechanism of tubulin antagonism in angiogenesis, since the activity of PKC isoforms in the kinome array was also reduced in vinblastine and CA4P-treated cells.

In summary, this work presents the marine compound spongistatin 1 as a promising agent in the combat against cancer, since it inhibited pancreatic tumor progression and metastasis *in vivo* and exerted strong antiangiogenic effects *in vitro* and *in vivo*. Moreover, the characterization of underlying mechanisms of the antiangiogenic action of spongistatin 1 might be prototypic for general tubulin antagonism in angiogenesis.

VIII. REFERENCES

- 1 Amador,M.L., Jimeno,J., Paz-Ares,L., Cortes-Funes,H. and Hidalgo,M. Progress in the development and acquisition of anticancer agents from marine sources, *Ann.Oncol.*, *14*: 1607-1615, 2003.
- 2 Haygood,M.G., Schmidt,E.W., Davidson,S.K. and Faulkner,D.J. Microbial symbionts of marine invertebrates: opportunities for microbial biotechnology, *J Mol Microbiol.Biotechnol.*, *1*: 33-43, 1999.
- 3 Diwan S.Rawat, Mukesh C.Joshi, Penny Joshi and Himanshu Atheaya Marine Peptides and Related Compounds in Clinical Trial, *Anti-Cancer Agents - Med.Chem.*, *6*: 1-8, 2006.
- 4 Jimeno,J., Lopez-Martin,J.A., Ruiz-Casado,A., Izquierdo,M.A., Scheuer,P.J. and Rinehart,K. Progress in the clinical development of new marine-derived anticancer compounds, *Anticancer Drugs*, *15*: 321-329, 2004.
- 5 Pettit,G.R., Cichacz,Z.A., Gao,F., Herald,C.L., Boyd,M.R., Schmidt,J.M. and Hooper,J.N.A. Isolation and Structure of Spongistatin-1, *Journal of Organic Chemistry*, *58*: 1302-1304, 1993.
- 6 Kobayashi,M., Aoki,S., Sakai,H., awazoe,K., ihara,N., asaki,T. and itagawa,I. Althohyrin A, a potent anti-tumor macrolide from the Okinawan marine sponge *Hyrtios altum*, *Tetrahedron letters*, *34*: 2795-2798, 1993.
- 7 Ball,M., Gaunt,M.J., Hook,D.F., Jessiman,A.S., Kawahara,S., Orsini,P., Scolaro,A., Talbot,A.C., Tanner,H.R., Yamanoi,S. and Ley,S.V. Total synthesis of spongistatin 1: a synthetic strategy exploiting its latent pseudo-symmetry 1, *Angew.Chem.Int.Ed Engl.*, *44*: 5433-5438, 2005.
- 8 Bai,R.L., Taylor,G.F., Cichacz,Z.A., Herald,C.L., Kepler,J.A., Pettit,G.R. and Hamel,E. The Spongistatins, Potently Cytotoxic Inhibitors of Tubulin Polymerization, Bind in A Distinct Region of the Vinca Domain, *Biochemistry*, *34*: 9714-9721, 1995.
- 9 Bai,R.L., Cichacz,Z.A., Herald,C.L., Pettit,G.R. and Hamel,E. Spongistatin-1, A Highly Cytotoxic, Sponge-Derived, Marine Natural Product That Inhibits Mitosis, Microtubule Assembly, and the Binding of Vinblastine to Tubulin, *Molecular Pharmacology*, *44*: 757-766, 1993.
- 10 Schyschka,L., Rudy,A., Jeremias,I., Barth,N., Pettit,G.R. and Vollmar,A.M. Spongistatin 1: a new chemosensitizing marine compound that degrades XIAP, *Leukemia*, 2008.
- 11 world health organization cancer fact sheet. *In*: Anonymous2007.
- 12 Westphal,S. and Kalthoff,H. Apoptosis: targets in pancreatic cancer, *Mol.Cancer*, *2*: 6, 2003.
- 13 Parker,S.L., Tong,T., Bolden,S. and Wingo,P.A. Cancer statistics, 1997, *CA Cancer J.Clin.*, *47*: 5-27, 1997.

- 14 Brand,R.E. and Tempero,M.A. Pancreatic cancer, *Curr.Opin.Oncol.*, *10*: 362-366, 1998.
- 15 Ries,L.A.G., Krapcho,M., Howlader,N., Horner,M.J., Mariotto,A., Miller,B.A., Feuer,E.J., Altekruse,S.F., Lewis,D.R., Clegg,L., Eisner,M.P., Reichman,M., Edwards,B.K. and Melbert,D., SEER cancer statistics review 1975-2005, Bethesda (MD): National Cancer Institute, 2008 (Abstract)
- 16 Jordan,M.A. and Wilson,L. Microtubules as a target for anticancer drugs, *Nat.Rev Cancer*, *4*: 253-265, 2004.
- 17 Dumontet,C. and Sikic,B.I. Mechanisms of action of and resistance to antitubulin agents: microtubule dynamics, drug transport, and cell death, *J Clin Oncol.*, *17*: 1061-1070, 1999.
- 18 Attard,G., Greystoke,A., Kaye,S. and De Bono,J. Update on tubulin-binding agents, *Pathologie Biologie*, *54*: 72-84, 2006.
- 19 Folkman,J., Bach,M., Rowe,J.W., Davidoff,F., Lambert,P., Hirsch,C., Goldberg,A., Hiatt,H.H., Glass,J. and Henshaw,E. Tumor Angiogenesis - Therapeutic Implications, *New England Journal of Medicine*, *285*: 1182-&, 1971.
- 20 Folkman,J. Angiogenesis in Cancer, Vascular, Rheumatoid and Other Disease, *Nature Medicine*, *1*: 27-31, 1995.
- 21 Cristofanilli,M., Charnsangavej,C. and Hortobagyi,G.N. Angiogenesis modulation in cancer research: novel clinical approaches, *Nat.Rev Drug Discov.*, *1*: 415-426, 2002.
- 22 Longo,R., Sarmiento,R., Fanelli,M., Capaccetti,B., Gattuso,D. and Gasparini,G. Anti-angiogenic therapy: rationale, challenges and clinical studies, *Angiogenesis.*, *5*: 237-256, 2002.
- 23 Miller,K.D., Sweeney,C.J. and Sledge,G.W. Redefining the target: Chemotherapeutics as antiangiogenics, *Journal of Clinical Oncology*, *19*: 1195-1206, 2001.
- 24 Tozer,G.M., Kanthou,C. and Baguley,B.C. Disrupting tumour blood vessels, *Nat.Rev Cancer*, *5*: 423-435, 2005.
- 25 Hinnen,P. and Eskens,F.A.L.M. Vascular disrupting agents in clinical development, *British Journal of Cancer*, *96*: 1159-1165, 2007.
- 26 Pasquier,E., Honore,S. and Braguer,D. Microtubule-targeting agents in angiogenesis: Where do we stand?, *Drug Resistance Updates*, *9*: 74-86, 2006.
- 27 Broxterman,H.J. and Georgopapadakou,N.H. Anticancer therapeutics: "Addictive" targets, multi-targeted drugs, new drug combinations, *Drug Resistance Updates*, *8*: 183-197, 2005.

- 28 Pasquier,E., Andre,N. and Braguer,D. Targeting microtubules to inhibit angiogenesis and disrupt tumour vasculature: implications for cancer treatment, *Curr.Cancer Drug Targets.*, 7: 566-581, 2007.
- 29 Euteneuer,U. and Schliwa,M. Persistent, Directional Motility of Cells and Cytoplasmic Fragments in the Absence of Microtubules, *Nature*, 310: 58-61, 1984.
- 30 Keller,H.U., Naef,A. and Zimmermann,A. Effects of Colchicine, Vinblastine and Nocodazole on Polarity, Motility, Chemotaxis and Camp Levels of Human Polymorphonuclear Leukocytes, *Experimental Cell Research*, 153: 173-185, 1984.
- 31 Campbell,N.A. and Reece,J.B. *Biology*, 7th edn, Benjamin Cummings, San Francisco: 2005.
- 32 Lodish,H., Berk,A., Zipursky,S.L., Matsudaira,P., Baltimore,D. and Darnell,E.J. *Molecular Cell Biology*, 5th edn, W. H. Freeman and Company, New York: 2000.
- 33 McKean,P.G., Vaughan,S. and Gull,K. The extended tubulin superfamily, *J Cell Sci.*, 114: 2723-2733, 2001.
- 34 Erickson,H.P. Atomic structures of tubulin and FtsZ, *Trends Cell Biol.*, 8: 133-137, 1998.
- 35 Desai,A. and Mitchison,T.J. Microtubule polymerization dynamics, *Annu.Rev.Cell Dev.Biol.*, 13: 83-117, 1997.
- 36 Satir,P. and Christensen,S.T. Overview of structure and function of mammalian cilia, *Annu.Rev.Physiol*, 69: 377-400, 2007.
- 37 Howard,J. and Hyman,A.A. Dynamics and mechanics of the microtubule plus end, *Nature*, 422: 753-758, 2003.
- 38 Lippincott-Schwartz,J., Cole,N.B., Marotta,A., Conrad,P.A. and Bloom,G.S. Kinesin is the motor for microtubule-mediated Golgi-to-ER membrane traffic, *J.Cell Biol.*, 128: 293-306, 1995.
- 39 Akhmanova,A. and Steinmetz,M.O. Tracking the ends: a dynamic protein network controls the fate of microtubule tips, *Nat.Rev Mol Cell Biol.*, 9: 309-322, 2008.
- 40 Siegrist,S.E. and Doe,C.Q. Microtubule-induced cortical cell polarity, *Genes Dev.*, 21: 483-496, 2007.
- 41 Galjart,N. CLIPs and CLASPs and cellular dynamics, *Nat.Rev Mol Cell Biol.*, 6: 487-498, 2005.
- 42 Doxsey,S., Zimmerman,W. and Mikule,K. Centrosome control of the cell cycle, *Trends Cell Biol.*, 15: 303-311, 2005.

-
- 43 Musacchio,A. and Salmon,E.D. The spindle-assembly checkpoint in space and time, *Nat.Rev Mol Cell Biol.*, *8*: 379-393, 2007.
- 44 Mallik,R. and Gross,S.P. Molecular motors: strategies to get along, *Curr.Biol.*, *14*: R971-R982, 2004.
- 45 Murray,J.W. and Wolkoff,A.W. Roles of the cytoskeleton and motor proteins in endocytic sorting, *Adv.Drug Deliv.Rev.*, *55*: 1385-1403, 2003.
- 46 Mallik,R., Carter,B.C., Lex,S.A., King,S.J. and Gross,S.P. Cytoplasmic dynein functions as a gear in response to load, *Nature*, *427*: 649-652, 2004.
- 47 Caviston,J.P. and Holzbaur,E.L. Microtubule motors at the intersection of trafficking and transport, *Trends Cell Biol.*, *16*: 530-537, 2006.
- 48 Cau,J.L. and Hall,A. Cdc42 controls the polarity of the actin and microtubule cytoskeletons through two distinct signal transduction pathways, *Journal of Cell Science*, *118*: 2579-2587, 2005.
- 49 Jordan,A., Hadfield,J.A., Lawrence,N.J. and Mcgown,A.T. Tubulin as a target for anticancer drugs: Agents which interact with the mitotic spindle, *Medicinal Research Reviews*, *18*: 259-296, 1998.
- 50 Sengupta,S. and Thomas,S.A. Drug target interaction of tubulin-binding drugs in cancer therapy, *Expert.Rev Anticancer Ther.*, *6*: 1433-1447, 2006.
- 51 Adams,R.H. and Alitalo,K. Molecular regulation of angiogenesis and lymphangiogenesis, *Nat.Rev Mol Cell Biol.*, *8*: 464-478, 2007.
- 52 Carmeliet,P. Mechanisms of angiogenesis and arteriogenesis, *Nature Medicine*, *6*: 389-395, 2000.
- 53 Semenza,G.L. Vasculogenesis, angiogenesis, and arteriogenesis: mechanisms of blood vessel formation and remodeling, *J.Cell Biochem.*, *102*: 840-847, 2007.
- 54 Du,K. and Tschlis,P.N. Regulation of the Akt kinase by interacting proteins, *Oncogene*, *24*: 7401-7409, 2005.
- 55 Manning,B.D. and Cantley,L.C. AKT/PKB signaling: Navigating downstream, *Cell*, *129*: 1261-1274, 2007.
- 56 Jiang,B.H. and Liu,L.Z. PI3K/PTEN signaling in tumorigenesis and angiogenesis, *Biochim.Biophys.Acta*, *1784*: 150-158, 2008.
- 57 Ackah,E., Yu,J., Zoellner,S., Iwakiri,Y., Skurk,C., Shibata,R., Ouchi,N., Easton,R.M., Galasso,G., Birnbaum,M.J., Walsh,K. and Sessa,W.C. Akt1/protein kinase Balpha is critical for ischemic and VEGF-mediated angiogenesis, *J Clin Invest*, *115*: 2119-2127, 2005.

-
- 58 Somanath,P.R., Razorenova,O.V., Chen,J. and Byzova,T.V. Akt1 in endothelial cell and angiogenesis, *Cell Cycle*, 5: 512-518, 2006.
- 59 Kolch,W. Coordinating ERK/MAPK signalling through scaffolds and inhibitors, *Nat.Rev.Mol.Cell Biol.*, 6: 827-837, 2005.
- 60 Berra,E., Milanini,J., Richard,D.E., Le,G.M., Vinals,F., Gothie,E., Roux,D., Pages,G. and Pouyssegur,J. Signaling angiogenesis via p42/p44 MAP kinase and hypoxia, *Biochem.Pharmacol*, 60: 1171-1178, 2000.
- 61 Seger,R. and Krebs,E.G. The MAPK signaling cascade, *FASEB J*, 9: 726-735, 1995.
- 62 Newton,A.C. Protein-Kinase-C - Structure, Function, and Regulation, *Journal of Biological Chemistry*, 270: 28495-28498, 1995.
- 63 Nishizuka,Y. Intracellular Signaling by Hydrolysis of Phospholipids and Activation of Protein-Kinase-C, *Science*, 258: 607-614, 1992.
- 64 Gliki,G., Wheeler-Jones,C. and Zachary,I. Vascular endothelial growth factor induces protein kinase C (PKC)-dependent Akt/PKB activation and phosphatidylinositol 3'-kinase-mediated PKC delta phosphorylation: Role of PKC in angiogenesis, *Cell Biology International*, 26: 751-759, 2002.
- 65 Rask-Madsen,C. and King,G.L. Differential regulation of VEGF signaling by PKC-alpha and PKC-epsilon in endothelial cells, *Arterioscler.Thromb.Vasc.Biol.*, 28: 919-924, 2008.
- 66 Xu,H., Czerwinski,P., Hortmann,M., Sohn,H.Y., Forstermann,U. and Li,H. Protein kinase C {alpha} promotes angiogenic activity of human endothelial cells via induction of vascular endothelial growth factor, *Cardiovasc.Res.*, 78: 349-355, 2008.
- 67 Clark,I.M., Swingler,T.E., Sampieri,C.L. and Edwards,D.R. The regulation of matrix metalloproteinases and their inhibitors, *Int.J Biochem.Cell Biol.*, 40: 1362-1378, 2008.
- 68 Rundhaug,J.E. Matrix metalloproteinases and angiogenesis, *J Cell Mol Med.*, 9: 267-285, 2005.
- 69 van,H., V and Koolwijk,P. Endothelial sprouting and angiogenesis: matrix metalloproteinases in the lead, *Cardiovasc.Res*, 78: 203-212, 2008.
- 70 Hellstrom,M., Phng,L.K., Hofmann,J.J., Wallgard,E., Coultas,L., Lindblom,P., Alva,J., Nilsson,A.K., Karlsson,L., Gaiano,N., Yoon,K., Rossant,J., Iruela-Arispe,M.L., Kalen,M., Gerhardt,H. and Betsholtz,C. Dll4 signalling through Notch1 regulates formation of tip cells during angiogenesis, *Nature*, 445: 776-780, 2007.
- 71 Suchting,S., Freitas,C., le,N.F., Benedito,R., Breant,C., Duarte,A. and Eichmann,A. The Notch ligand Delta-like 4 negatively regulates endothelial tip cell formation and vessel branching, *Proc.Natl.Acad.Sci.U.S.A*, 104: 3225-3230, 2007.

-
- 72 Ridley,A.J., Schwartz,M.A., Burridge,K., Firtel,R.A., Ginsberg,M.H., Borisy,G., Parsons,J.T. and Horwitz,A.R. Cell migration: integrating signals from front to back, *Science*, *302*: 1704-1709, 2003.
- 73 Wittmann,T. and Waterman-Storer,C.M. Cell motility: can Rho GTPases and microtubules point the way?, *Journal of Cell Science*, *114*: 3795-3803, 2001.
- 74 Jaffe,E.A., Nachman,R.L., Becker,C.G. and Minick,C.R. Culture of Human Endothelial Cells Derived from Umbilical Veins - Identification by Morphologic and Immunological Criteria, *Journal of Clinical Investigation*, *52*: 2745-2756, 1973.
- 75 Li,H., Wallerath,T., Ihrig-Biedert,I., Oehrlein,S.A., Herget,T., Kleinert,H. and Forstermann,U. Activation of protein kinase C alpha and/or epsilon enhances transcription of the human endothelial NO synthase gene, *Naunyn-Schmiedebergs Archives of Pharmacology*, *357*: R42, 1998.
- 76 Bradford,M.M. A rapid and sensitive method for the quantitation of microgram quantities of protein utilizing the principle of protein-dye binding, *Anal.Biochem.*, *72*: 248-254, 1976.
- 77 Laemmli,U.K. Cleavage of structural proteins during the assembly of the head of bacteriophage T4, *Nature*, *227*: 680-685, 1970.
- 78 van Baal,J.W., Diks,S.H., Wanders,R.J., Rygiel,A.M., Milano,F., Joore,J., Bergman,J.J., Peppelenbosch,M.P. and Krishnadath,K.K. Comparison of kinome profiles of Barrett's esophagus with normal squamous esophagus and normal gastric cardia, *Cancer Res.*, *66*: 11605-11612, 2006.
- 79 Mwanjewe,J., Spitaler,M., Ebner,M., Windegger,M., Geiger,M., Kampfer,S., Hofmann,J., Uberall,F. and Grunicke,H.H. Regulation of phospholipase D isoenzymes by transforming Ras and atypical protein kinase C-iota, *Biochem.J.*, *359*: 211-217, 2001.
- 80 Kenyon,B.M., Voest,E.E., Chen,C.C., Flynn,E., Folkman,J. and Damato,R.J. A model of angiogenesis in the mouse cornea, *Investigative Ophthalmology & Visual Science*, *37*: 1625-1632, 1996.
- 81 Bruns,C.J., Harbison,M.T., Kuniyasu,H., Eue,I. and Fidler,I.J. In vivo selection and characterization of metastatic variants from human pancreatic adenocarcinoma by using orthotopic implantation in nude mice, *Neoplasia.*, *1*: 50-62, 1999.
- 82 Pfaffl,M.W. A new mathematical model for relative quantification in real-time RT-PCR, *Nucleic Acids Res.*, *29*: e45, 2001.
- 83 Powis,G. and Kirkpatrick,L. Hypoxia inducible factor-1alpha as a cancer drug target, *Mol Cancer Ther.*, *3*: 647-654, 2004.
- 84 Wang,G.L. and Semenza,G.L. General involvement of hypoxia-inducible factor 1 in transcriptional response to hypoxia, *Proc.Natl.Acad.Sci.U.S.A.*, *90*: 4304-4308, 1993.

-
- 85 Rudd,P.M., Mattu,T.S., Masure,S., Bratt,T., Van den Steen,P.E., Wormald,M.R., Kuster,B., Harvey,D.J., Borregaard,N., Van,D.J., Dwek,R.A. and Opdenakker,G. Glycosylation of natural human neutrophil gelatinase B and neutrophil gelatinase B-associated lipocalin, *Biochemistry*, **38**: 13937-13950, 1999.
- 86 Rubinfeld,H. and Seger,R. The ERK cascade: a prototype of MAPK signaling, *Mol Biotechnol.*, **31**: 151-174, 2005.
- 87 Alessi,D.R., Andjelkovic,M., Caudwell,B., Cron,P., Morrice,N., Cohen,P. and Hemmings,B.A. Mechanism of activation of protein kinase B by insulin and IGF-1, *EMBO J*, **15**: 6541-6551, 1996.
- 88 Litchfield,D.W. Protein kinase CK2: structure, regulation and role in cellular decisions of life and death, *Biochem.J*, **369**: 1-15, 2003.
- 89 Hofmann,J. The potential for isoenzyme-selective modulation of protein kinase C, *FASEB J*, **11**: 649-669, 1997.
- 90 Nishikawa,K., Toker,A., Johannes,F.J., Songyang,Z. and Cantley,L.C. Determination of the specific substrate sequence motifs of protein kinase C isozymes, *J Biol.Chem*, **272**: 952-960, 1997.
- 91 Christofori,G. New signals from the invasive front, *Nature*, **441**: 444-450, 2006.
- 92 Steeg,P.S. Tumor metastasis: mechanistic insights and clinical challenges, *Nat.Med.*, **12**: 895-904, 2006.
- 93 Conrad,C., Ischenko,I., Kohl,G., Wiegand,U., Guba,M., Yezhelyev,M., Ryan,A.J., Barge,A., Geissler,E.K., Wedge,S.R., Jauch,K.W. and Bruns,C.J. Antiangiogenic and antitumor activity of a novel vascular endothelial growth factor receptor-2 tyrosine kinase inhibitor ZD6474 in a metastatic human pancreatic tumor model, *Anti-Cancer Drug*, **18**: 569-579, 2007.
- 94 Kleespies,A., Kohl,G., Friedrich,M., Ryan,A.J., Barge,A., Jauch,K.W. and Bruns,C.J. Vascular targeting in pancreatic cancer: the novel tubulin-binding agent ZD6126 reveals antitumor activity in primary and metastatic tumor models, *Neoplasia.*, **7**: 957-966, 2005.
- 95 Yezhelyev,M.V., Koehl,G., Guba,M., Brabletz,T., Jauch,K.W., Ryan,A., Barge,A., Green,T., Fennell,M. and Bruns,C.J. Inhibition of Src tyrosine kinase as treatment for human pancreatic cancer growing orthotopically in nude mice, *Clinical Cancer Research*, **10**: 8028-8036, 2004.
- 96 Bardos,J.I. and Ashcroft,M. Negative and positive regulation of HIF-1: a complex network, *Biochim.Biophys.Acta*, **1755**: 107-120, 2005.
- 97 Chau,N.M., Rogers,P., Aherne,W., Carroll,V., Collins,I., McDonald,E., Workman,P. and Ashcroft,M. Identification of novel small molecule inhibitors of hypoxia-inducible factor-1 that differentially block hypoxia-inducible factor-1 activity and hypoxia-inducible factor-1alpha induction in response to hypoxic stress and growth factors, *Cancer Res*, **65**: 4918-4928, 2005.

-
- 98 Dachs,G.U., Steele,A.J., Coralli,C., Kanthou,C., Brooks,A.C., Gunningham,S.P., Currie,M.J., Watson,A.I., Robinson,B.A. and Tozer,G.M. Anti-vascular agent Combretastatin A-4-P modulates hypoxia inducible factor-1 and gene expression, *BMC.Cancer*, 6: 280, 2006.
- 99 Escuin,D., Kline,E.R. and Giannakakou,P. Both microtubule-stabilizing and microtubule-destabilizing drugs inhibit hypoxia-inducible factor-1alpha accumulation and activity by disrupting microtubule function, *Cancer Res*, 65: 9021-9028, 2005.
- 100 Deryugina,E.I. and Quigley,J.P. Matrix metalloproteinases and tumor metastasis, *Cancer and Metastasis Reviews*, 25: 9-34, 2006.
- 101 Geho,D.H., Bandle,R.W., Clair,T. and Liotta,L.A. Physiological mechanisms of tumor-cell invasion and migration, *Physiology*, 20: 194-200, 2005.
- 102 Fingleton,B. Matrix metalloproteinases: roles in cancer and metastasis, *Frontiers in Bioscience*, 11: 479-491, 2006.
- 103 Liotta,L.A., Tryggvason,K., Garbisa,S., Hart,I., Foltz,C.M. and Shafie,S. Metastatic Potential Correlates with Enzymatic Degradation of Basement-Membrane Collagen, *Nature*, 284: 67-68, 1980.
- 104 Bloomston,M., Zervos,E.E. and Rosemurgy,A.S. Matrix metalloproteinases and their role in pancreatic cancer: a review of preclinical studies and clinical trials, *Ann.Surg.Oncol.*, 9: 668-674, 2002.
- 105 Jimenez,R.E., Hartwig,W., Antoniu,B.A., Compton,C.C., Warshaw,A.L. and Fernandez-Del,C.C. Effect of matrix metalloproteinase inhibition on pancreatic cancer invasion and metastasis: an additive strategy for cancer control, *Ann.Surg*, 231: 644-654, 2000.
- 106 Zervos,E.E., Franz,M.G., Salhab,K.F., Shafii,A.E., Menendez,J., Gower,W.R. and Rosemurgy,A.S. Matrix metalloproteinase inhibition improves survival in an orthotopic model of human pancreatic cancer, *J Gastrointest Surg*, 4: 614-619, 2000.
- 107 Schnaeker,E.M., Ossig,R., Ludwig,T., Dreier,R., Oberleithner,H., Wilhelmi,M. and Schneider,S.W. Microtubule-dependent matrix metalloproteinase-2/matrix metalloproteinase-9 exocytosis: prerequisite in human melanoma cell invasion, *Cancer Res*, 64: 8924-8931, 2004.
- 108 Meissner,M., Pinter,A., Michailidou,D., Hrgovic,I., Kaprolat,N., Stein,M., Holtmeier,W., Kaufmann,R. and Gille,J. Microtubule-targeted drugs inhibit VEGF receptor-2 expression by both transcriptional and post-transcriptional mechanisms, *J Invest Dermatol.*, 128: 2084-2091, 2008.
- 109 Yoshizaki,T., Sato,H., Furukawa,M. and Pagano,J.S. The expression of matrix metalloproteinase 9 is enhanced by Epstein-Barr virus latent membrane protein 1, *Proc.Natl.Acad.Sci.U.S.A*, 95: 3621-3626, 1998.

-
- 110 Kilic,N., Oliveira-Ferrer,L., Wurmbach,J.H., Loges,S., Chalajour,F., Neshat-Vahid,S., Weil,J., Fernando,M. and Ergun,S. Pro-angiogenic signaling by the endothelial presence of CEACAM1, *J Biol.Chem*, *280*: 2361-2369, 2005.
- 111 Oliveira-Ferrer,L., Tilki,D., Ziegeler,G., Hauschild,J., Loges,S., Irmak,S., Kilic,E., Huland,H., Friedrich,M. and Ergun,S. Dual role of carcinoembryonic antigen-related cell adhesion molecule 1 in angiogenesis and invasion of human urinary bladder cancer, *Cancer Res*, *64*: 8932-8938, 2004.
- 112 Tilki,D., Irmak,S., Oliveira-Ferrer,L., Hauschild,J., Miethe,K., Atakaya,H., Hammerer,P., Friedrich,M.G., Schuch,G., Galalae,R., Stief,C.G., Kilic,E., Huland,H. and Ergun,S. CEA-related cell adhesion molecule-1 is involved in angiogenic switch in prostate cancer, *Oncogene*, *25*: 4965-4974, 2006.
- 113 Etienne-Manneville,S. Actin and microtubules in cell motility: Which one is in control?, *Traffic*, *5*: 470-477, 2004.
- 114 Etienne-Manneville,S. and Hall,A. Rho GTPases in cell biology, *Nature*, *420*: 629-635, 2002.
- 115 Wittmann,T. and Waterman-Storer,C.M. Cell motility: can Rho GTPases and microtubules point the way?, *Journal of Cell Science*, *114*: 3795-3803, 2001.
- 116 Omelchenko,T., Vasiliev,J.M., Gelfand,I.M., Feder,H.H. and Bonder,E.M. Mechanisms of polarization of the shape of fibroblasts and epitheliocytes: Separation of the roles of microtubules and Rho-dependent actin-myosin contractility, *Proceedings of the National Academy of Sciences of the United States of America*, *99*: 10452-10457, 2002.
- 117 Gomes,E.R., Jani,S. and Gundersen,G.G. Nuclear movement regulated by Cdc42, MRCK, myosin, and actin flow establishes MTOC polarization in migrating cells, *Cell*, *121*: 451-463, 2005.
- 118 Lansbergen,G. and Akhmanova,A. Microtubule plus end: A hub of cellular activities, *Traffic*, *7*: 499-507, 2006.
- 119 Bijman,M.N., van Nieuw Amerongen,G.P., Laurens,N., van,H., V and Boven,E. Microtubule-targeting agents inhibit angiogenesis at subtoxic concentrations, a process associated with inhibition of Rac1 and Cdc42 activity and changes in the endothelial cytoskeleton, *Mol Cancer Ther.*, *5*: 2348-2357, 2006.
- 120 Noritake,J., Watanabe,T., Sato,K., Wang,S. and Kaibuchi,K. IQGAP1: a key regulator of adhesion and migration, *J Cell Sci.*, *118*: 2085-2092, 2005.
- 121 Krendel,M., Zenke,F.T. and Bokoch,G.M. Nucleotide exchange factor GEF-H1 mediates cross-talk between microtubules and the actin cytoskeleton, *Nature Cell Biology*, *4*: 294-301, 2002.
- 122 Ren,Y., Li,R., Zheng,Y. and Busch,H. Cloning and characterization of GEF-H1, a microtubule-associated guanine nucleotide exchange factor for Rac and Rho GTPases, *J Biol.Chem*, *273*: 34954-34960, 1998.

- 123 Kawasaki,Y., Sato,R. and Akiyama,T. Mutated APC and Asef are involved in the migration of colorectal tumour cells, *Nature Cell Biology*, 5: 211-215, 2003.
- 124 Barber,M.A. and Welch,H.C. PI3K and RAC signalling in leukocyte and cancer cell migration, *Bull.Cancer*, 93: E44-E52, 2006.
- 125 Graupera,M., Guillermet-Guibert,J., Foukas,L.C., Phng,L.K., Cain,R.J., Salpekar,A., Pearce,W., Meek,S., Millan,J., Cutillas,P.R., Smith,A.J., Ridley,A.J., Ruhrberg,C., Gerhardt,H. and Vanhaesebroeck,B. Angiogenesis selectively requires the p110alpha isoform of PI3K to control endothelial cell migration, *Nature*, 2008.
- 126 Onishi,K., Higuchi,M., Asakura,T., Masuyama,N. and Gotoh,Y. The PI3K-Akt pathway promotes microtubule stabilization in migrating fibroblasts, *Genes to Cells*, 12: 535-546, 2007.
- 127 Shiojima,I. and Walsh,K. Role of Akt signaling in vascular homeostasis and angiogenesis, *Circ.Res*, 90: 1243-1250, 2002.
- 128 Canton,D.A. and Litchfield,D.W. The shape of things to come: an emerging role for protein kinase CK2 in the regulation of cell morphology and the cytoskeleton, *Cell Signal.*, 18: 267-275, 2006.
- 129 Eyster,C.A., Duggins,Q.S., Gorbisky,G.J. and Olson,A.L. Microtubule network is required for insulin signaling through activation of Akt/protein kinase B - Evidence that insulin stimulates vesicle docking/fusion but not intracellular mobility, *Journal of Biological Chemistry*, 281: 39719-39727, 2006.
- 130 Murtagh,J., Lu,H.Y. and Schwartz,E.L. Taxotere-induced inhibition of human endothelial cell migration is a result of heat shock protein 90 degradation, *Cancer Research*, 66: 8192-8199, 2006.
- 131 Battistella-Patterson,A.S., Fultz,M.E., Li,C., Geng,W., Norton,M. and Wright,G.L. PKC alpha translocation is microtubule-dependent in passaged smooth muscle cells, *Acta Physiologica Scandinavica*, 170: 87-97, 2000.
- 132 Nakhost,A., Kabir,N., Forscher,P. and Sossin,W.S. Protein kinase C isoforms are translocated to microtubules in neurons, *Journal of Biological Chemistry*, 277: 40633-40639, 2002.
- 133 Wellner,M., Maasch,C., Kupprion,C., Lindschau,C., Luft,F.C. and Haller,H. The proliferative effect of vascular endothelial growth factor requires protein kinase C-alpha and protein kinase C-zeta, *Arteriosclerosis Thrombosis and Vascular Biology*, 19: 178-185, 1999.
- 134 Wang,A., Nomura,M., Patan,S. and Ware,J.A. Inhibition of protein kinase Calpha prevents endothelial cell migration and vascular tube formation in vitro and myocardial neovascularization in vivo, *Circ.Res.*, 90: 609-616, 2002.

- 135 Harrington,E.O., Loffler,J., Nelson,P.R., Kent,K.C., Simons,M. and Ware,J.A. Enhancement of migration by protein kinase C alpha and inhibition of proliferation and cell cycle progression by protein kinase C delta in capillary endothelial cells, *Journal of Biological Chemistry*, *272*: 7390-7397, 1997.
- 136 Taylor,C.J., Motamed,K. and Lilly,B. Protein kinase C and downstream signaling pathways in a three-dimensional model of phorbol ester-induced angiogenesis, *Angiogenesis.*, *9*: 39-51, 2006.
- 137 bu-Amer,Y., Ross,F.P., Schlesinger,P., Tondravi,M.M. and Teitelbaum,S.L. Substrate recognition by osteoclast precursors induces C-src/microtubule association, *J Cell Biol.*, *137*: 247-258, 1997.
- 138 Holderfield,M.T. and Hughes,C.C. Crosstalk between vascular endothelial growth factor, notch, and transforming growth factor-beta in vascular morphogenesis, *Circ.Res.*, *102*: 637-652, 2008.
- 139 Lawlor,M.A. and Alessi,D.R. PKB/Akt: a key mediator of cell proliferation, survival and insulin responses?, *J Cell Sci.*, *114*: 2903-2910, 2001.
- 140 Faivre,S., Djelloul,S. and Raymond,E. New paradigms in anticancer therapy: targeting multiple signaling pathways with kinase inhibitors, *Semin.Oncol.*, *33*: 407-420, 2006.
- 141 Faivre,S., Demetri,G., Sargent,W. and Raymond,E. Molecular basis for sunitinib efficacy and future clinical development, *Nat.Rev.Drug Discov.*, *6*: 734-745, 2007.

IX. APPENDIX

1 PUBLICATIONS

1.1 Abstracts

Rothmeier AS., Ischenko I, Joore J, Hofmann J, Bruns CJ, Vollmar AM, Zahler S

The marine compound Spongistatin 1 inhibits angiogenesis by multiple mechanisms.

(Poster)

15th International Vascular Biology Meeting, June 1.-5., 2008, Sydney, Australia

Rothmeier AS, Ischenko I, Bruns CJ, Vollmar AM, Zahler S

The marine compound Spongistatin 1 inhibits angiogenesis *in vitro* and *in vivo*. (Talk)

>interact2007 PhD Symposium, December 7., 2007, Martinsried, Germany

Rothmeier AS, Ischenko I, Bruns CJ, Vollmar AM, Zahler S

The marine compound Spongistatin 1 inhibits angiogenesis *in vitro* and *in vivo*. (Poster)

Joint Meeting: Annual Meeting of the Society for Microcirculation and Vascular Biology and

6th International Symposium on the Biology of Endothelial Cells, October 4.-6., 2007,

Heidelberg, Germany

Rothmeier AS, Vollmar AM, Zahler S

The novel tubulin-antagonist Spongistatin 1 is an extremely potent anti-angiogenic agent.

(Poster)

48th Spring Meeting of the Deutsche Gesellschaft für experimentelle klinische Pharmakologie und Toxikologie, March 13.-15., 2007, Mainz, Germany

Rothmeier AS, Vollmar AM, Zahler S

Spongistatin 1: a novel powerful anti-angiogenic agent. (Poster)

Annual Meeting of the Society for Microcirculation and Vascular Biology, October 12.-14.,

2006, Munich, Germany

1.2 Original Publications

Rothmeier AS, Ischenko I, Joore J, Garczarczyk D, Fürst R, Bruns CJ, Vollmar AM, Zahler S

Investigation of the Marine Compound Spongistatin 1 Links the Inhibition of PKC α -Translocation to Non-Mitotic Effects of Tubulin Antagonism in Angiogenesis

The FASEB Journal (2008), in print

Rothmeier AS*, Schneiders UM*, Ischenko I, Bruns CJ, Rudy A, Zahler S, Vollmar AM

Spongistatin 1, a promising experimental drug, targets pancreatic tumor progression and metastasis

(2008) Submitted

*These authors contributed equally to this work

2 Grants and Awards

DFG Travel Grant

Convention Travel to the 15th IVBM, June 2008, Sydney, Australia

LMUexcellent Mentoring

October 2007 – recent, Ludwig-Maximilians-University Munich, Germany

Sanofi-Aventis Poster Award, Section Toxicology

48th Spring Meeting of the DGPT, March 2007, Mainz, Germany

3 Curriculum Vitae

Personal Data

Name	Andrea Silvia Rothmeier
Date of Birth	July 18 th , 1981
Place of Birth	Munich, Germany
Nationality	German

Academic Education

July 2005 - October 2008	Ph.D. Thesis at the department of Pharmaceutical Biology, LMU Munich, Chair Prof. Dr. A. M. Vollmar
October 2004 - May 2005	Diploma Thesis 'Functional and Biochemical Analysis of GRAS-Proteins' at the department of Biology I - Physiological Botany, LMU Munich, Chair Prof. Dr. R. G. Herrmann
September 2000 - May 2005	Study of biology at the LMU Munich, Diploma

School Education

September 1992 - July 2000	Käthe-Kollwitz-Gymnasium in Munich, Abitur
September 1988 – July 1992	Hirschbergschule in Munich, Primary school

4 Acknowledgements

First and foremost, I would like to thank PD Dr. Stefan Zahler and Prof. Dr. Angelika M. Vollmar. Herr Zahler, you have been a wonderful supervisor, supporting this work with your fundamental experience and great personal commitment. Frau Vollmar, I thank you so much for giving me the opportunity to perform my Ph.D.-studies in your labs. Moreover, you have been a real mentor to me. Your support and your encouragement motivated me to head for a scientific career.

My sincere thanks go to Prof. Dr. Christian Wahl-Schott for his time and effort to appraise this thesis. Further I would like to thank all members of the thesis committee, Prof. Dr. Franz Bracher, Prof. Dr. Wolfgang Frieß and PD Dr. Franz Paintner for their attendance.

Special thanks go to PD Dr. Christiane J. Bruns and Dr. Ivan Ischenko for their collaboration in the mouse *in vivo* studies, to Dr. Johann Hofmann and Dr. Dorota Garczarczyk for their support in PKC analysis, and to Dr. Jos Joore for performing PepChip analysis.

Further, I would like to thank Dr. Robert Fürst for his advice in plenty meetings, Dr. Andreas Hartkorn for his support in tissue preparations and Dr. Anja Koltermann for her help in qRT-PCR performance.

To all my lab members, the former as well as the current ones, I thank you so much for the warm and friendly atmosphere and the good times we have spent. It will be hard to find a team like you and I will remember you for long.

Finally, I deeply thank all my dears, my family and my friends. My beloved parents, it was your love and your never-ending support which gave me the courage and the power to go my way. My dearest Roland, my companion, my consultant, my listener, my friend, my love, thank you!